

AD 680280

AD

**USAAVLABS TECHNICAL REPORT 68-68**

**EVALUATION OF  
HELICOPTER FLIGHT SPECTRUM DATA**

By

John D. Porterfield

Paul F. Maloney

October 1968

**U. S. ARMY AVIATION MATERIEL LABORATORIES  
FORT EUSTIS, VIRGINIA**

**CONTRACT DAAJ02-67-C-0055  
KAMAN AIRCRAFT DIVISION, KAMAN CORPORATION  
BLOOMFIELD, CONNECTICUT**

*This document has been approved  
for public release and sale; its  
distribution is unlimited.*



D D C  
RECEIVED  
DEC 23 1968  
RECEIVED



DEPARTMENT OF THE ARMY  
U. S. ARMY AVIATION MATERIEL LABORATORIES  
FORT EUSTIS, VIRGINIA 23604

This report has been reviewed by the U. S. Army  
Aviation Materiel Laboratories and is considered  
to be technically sound. The report is published  
for the exchange of information and the stimulation  
of ideas.

Task 1F162204A14601  
Contract DAAJ02-67-C-0055  
USAAVLABS Technical Report 68-68  
October 1968

EVALUATION OF  
HELICOPTER FLIGHT SPECTRUM DATA

Kaman Aircraft Report Number R-739

By

John D. Porterfield  
Paul F. Maloney

Prepared by

Kaman Aircraft Division, Kaman Corporation  
Bloomfield, Connecticut

for

U. S. ARMY AVIATION MATERIEL LABORATORIES  
FORT EUSTIS, VIRGINIA

This document has been approved  
for public release and sale; its  
distribution is unlimited.

## SUMMARY

This report evaluates helicopter flight spectrum data previously recorded and published in other reports, with emphasis on the UH-1B utility, CH-47A cargo, and CH-54A load lifting helicopters as used in the Army environment. A limited statistical analysis of the data is presented for those parameters for which sufficient data were available. The report includes a comparison of the flight-measured data with the spectrum appearing in Appendix A of Civil Aeronautics Manual 6, and with the assumed fatigue substantiation spectrum, where this was available. Discussion and evaluation of the spectrum variations that do occur, particularly as they might affect component fatigue lives, are also included.

A method for deriving an operational spectrum for the classes of helicopters evaluated is presented along with discussion of some of the considerations and judgment which play a part in the establishment of a rational, conservative spectrum for the critical components.

## FOREWORD

This report, "Evaluation of Helicopter Flight Spectrum Data", was prepared by Kaman Aircraft Division, Kaman Corporation of Bloomfield, Connecticut, for the U. S. Army Aviation Materiel Laboratories, Fort Eustis, Virginia, under Contract DAAJ02-67-C-0055. Mr. William Alexander was the contract monitor.

In the past, many helicopter flight spectrum surveys have been conducted for the purpose of improving the accuracy of this portion of the general helicopter fatigue life problem. These surveys compiled data for particular aircraft and missions. However, no general review of results has heretofore been available. This report presents the results of a correlation and statistical analysis of data from 12 sources, with emphasis on extensive data recently recorded for the UH-1B, CH-47A, and CH-54A as they are used in the Army environment. An attempt was made to assimilate pertinent data, to present them in a form that would facilitate comparison with present and future data, and to extract trends and characteristics that would be useful for predicting fatigue lives of current helicopter components.

TABLE OF CONTENTS

	<u>Page</u>
SUMMARY . . . . .	iii
FOREWORD . . . . .	v
LIST OF ILLUSTRATIONS . . . . .	viii
LIST OF TABLES . . . . .	xi
INTRODUCTION . . . . .	1
PROGRAM OBJECTIVES . . . . .	2
DATA SOURCES . . . . .	3
MISSION SEGMENTS . . . . .	5
AIRSPEED . . . . .	16
GROSS WEIGHT . . . . .	27
RATE OF CLIMB . . . . .	31
NORMAL LOAD FACTORS . . . . .	36
ESTABLISHING A FLIGHT SPECTRUM . . . . .	45
CONCLUSIONS . . . . .	49
RECOMMENDATIONS . . . . .	50
REFERENCES CITED . . . . .	105
DISTRIBUTION . . . . .	107

LIST OF ILLUSTRATIONS

<u>Figure</u>		<u>Page</u>
1	Percent of Total Time Spent in the Ascent, Enroute, and Descent Mission Segments for Several Helicopters . . . . .	54
2	Percent of Total Time for the CH-47A, UH-1B, and CH-54A Helicopters Based on Two Different Mission Segment Breakdowns Including a Comparison of Flight-Measured Data With Fatigue and CAM-6 Spectrums . . . . .	55
3	Mission Segment Probability Curves Based on Median Rank - Three-Segment Breakdown . . . .	56
4	Percent Time Spent in Each Mission Segment for the Standard Mission and for the Non-standard Mission . . . . .	57
5	Standard Mission Scatter Band Determination for Plus and Minus One Standard Deviation Based on Median Rank . . . . .	58
6	Nonstandard Mission Scatter Band Determination for Plus and Minus One Standard Deviation Based on Median Rank . . . . .	59
7	Example Showing the Conversion of Tabular Airspeed Frequency Data and a Frequency Histogram into a Cumulative Airspeed Frequency Distribution . . . . .	60
8	Cumulative Airspeed Frequency Distributions	61
9	Comparison of Cumulative Airspeed Frequency Distributions . . . . .	65
10	Cumulative Airspeed Frequency Distributions for the CH-47A, UH-1B, and CH-54A helicopters	69

<u>Figure</u>		<u>Page</u>
11	Comparison of Flight-Measured Cumulative Airspeed Frequency Distributions With Fatigue and CAM-6 Spectrums . . . . .	70
12	Cumulative Airspeed Frequency Distribution by Altitude . . . . .	73
13	Cumulative Gross Weight Frequency Distribution for Turbine-Powered Helicopters Having a Design Normal Gross Weight of Greater Than 15,000 Pounds . . . . .	76
14	Cumulative Gross Weight Frequency Distribution by Mission Segment . . . . .	77
15	Cumulative Rate-of-Climb Frequency Distribution . . . . .	80
16	Composite Cumulative Rate-of-Climb Frequency Distributions . . . . .	83
17	Cumulative Rate-of-Climb Frequency Distributions for the CH-47A, UH-1B, and CH-54A Helicopters . . . . .	84
18	Vertical Load Factor Exceedance Curves . . . . .	85
19	Composite Vertical Load Factor Exceedance Curves . . . . .	88
20	Vertical Load Factor Exceedance Curves by Mission Segment for Reciprocating Engine- Powered Helicopters Having a Design Normal Gross Weight of Less Than 12,000 pounds. . . . .	89
21	Composite Vertical Load Factor Exceedance Curves by Mission Segment for Reciprocating Engine-Powered Helicopters Having a Design Normal Gross Weight of Less Than 12,000 Pounds . . . . .	92

<u>Figure</u>		<u>Page</u>
22	Vertical Load Factor Exceedance Curves by Mission Segment for Turbine-Powered Helicopters Having a Design Normal Gross Weight of Less Than 10,000 Pounds . .	93
23	Composite Vertical Load Factor Exceedance Curves by Mission Segment for Turbine- Powered Helicopters Having a Design Normal Gross Weight of Less Than 10,000 Pounds . . . . .	96
24	Vertical Load Factor Exceedance Curves for the CH-47A, UH-1B, and CH-54A Helicopters . . . . .	97
25	Vertical Load Factor Exceedance Curves for the CH-47A, UH-1B, and CH-54A by Mission Segment . . . . .	98
26	Vertical Load Factor Exceedance Curves by Source . . . . .	102
27	Composite Vertical Load Factor Exceedance Curves by Source . . . . .	104

LIST OF TABLES

<u>Table</u>		<u>Page</u>
I	Helicopter Characteristics . . . . .	51
II	Comparison of Flight Time and Mission Segments for Several Helicopters . . . . .	52
III	Mission Segment and Airspeed Spectrums Based on CAM-6 Used for Comparison With Flight-Measured Spectrums . . . . .	53

**BLANK PAGE**

## INTRODUCTION

In the fatigue substantiation of helicopter dynamic components, it is necessary to know the loadings to which the component will be subjected (flight loadings), the frequency of occurrence of those loads (flight spectrum), and the ability of the component to withstand those loads (fatigue strength). These three elements, in combination, determine the fatigue life of the components, and all are equally important. During the development phase on a new model helicopter, the flight spectrum is established based upon the manufacturer's experience or upon a previously stipulated schedule, such as Civil Aeronautics Manual 6. It is not possible to make an accurate determination of the actual flight spectrum until the helicopter has been in service for a period of time.

Although many service load surveys have been conducted in the past, they have, generally, been performed for limited reasons and, consequently, with limited results. Helicopter flight loads are affected by many factors, such as pilot control and flight environment. The total number of measurements required to completely define flight loads is, therefore, substantial. Recent operational flight load programs for the UH-1B, CH-47A, and CH-54A do contain adequate information to give good definition to the flight spectrum for each aircraft, and these data have been utilized to conduct a thorough comparative study of spectrums for modern helicopters. Some earlier studies, though not as complete, have been included to broaden the data base and to provide a general review. This study was undertaken so that the flight spectrum portion of the fatigue substantiation picture could be placed on a firmer basis than has heretofore been possible.

The subject report has been divided into five sections, namely, mission segments, airspeed, gross weight, rate of climb, and normal load factors, to permit a systematic approach for comparing available flight spectrum data obtained for the several helicopters noted herein. This organization is intended to facilitate access to specific parameters that have been shown to have an effect on helicopter component fatigue lives.

## PROGRAM OBJECTIVES

The purpose of this program was to assimilate and evaluate helicopter flight spectrum data from various sources with a view toward the determination of a usage schedule for particular helicopter types or for helicopters in general. Specifically, data for the UH-1B, CH-47A, and CH-54A were evaluated and correlated with each other and with published spectrums. To broaden the data base and to improve statistical evaluation, the results of a number of earlier flight surveys have been included in this study.

Discussion and evaluation of the various spectrums, and their relation to each other and to published spectrums, form an important part of this study program. The significance of variations as they occur is discussed, with the probable effect on component fatigue lives being a primary consideration.

## DATA SOURCES

The primary data used in this study are those collected by the Army on the UH-1B, CH-47A, and CH-54A during simulated combat air assault missions (References 1, 2, and 3). In addition to these primary sources of data, a literature survey of flight loads provided additional data that were extracted from References 4 through 12 and documented herein. The relatively large amount of data and the uniformity of data handling presented in References 1, 2, and 3 provide a substantial base for the study of helicopter operations in the Army environment. The remaining reports have been used to aid in the evaluation of flight spectrums for helicopters in general, covering a variety of civil and military missions. It should be noted that the listed data sources represent efforts in this area by three military services, NASA, and the FAA, attesting to the broad recognition of the importance of the flight spectrum in fatigue evaluation of helicopters. The complexity of the subject is evidenced by the fact that the more recent surveys provide substantially more data and break them down to give the occurrences of particular combinations of parameters which are of interest in fatigue evaluation. This continuing refinement is required to eliminate the necessity of making assumptions which are grossly conservative when evaluating the useful life of critical and expensive rotor components.

Table I presents the pertinent characteristics of the helicopters that were surveyed. In some instances, neither aircraft model identification nor pertinent characteristics were provided by the referenced documents; consequently, it was necessary to acquire this information directly from the reporting agency. For the purposes of this study, the important aircraft characteristics are those which tend to set the pattern of operation for the pilot. For instance, in the case of forward velocity, the attainable airspeed could be set by limitations of power, blade stall, structural loads, or transmission capacity. The limitation may be presented to the pilot in the form of a red line on a dial which displays airspeed, power, or torque information, and which provides a continuous indication of the relation of the critical parameter to its limit.

Under these conditions it is natural to expect that missions which involve traveling any significant distance will accrue a majority of flight time at airspeeds just below the limitation. On shorter missions, a higher percentage of flight time may be spent at lower airspeeds; during very urgent missions, it is probable that red-line limits which are below

the true capability of the aircraft will be exceeded in the critical flight phases. To examine helicopter airspeed spectrum on a uniform basis and to obtain data for the various aircraft that could logically be compared, it was necessary to determine the attainable level flight speed, which is designated as  $V_A$  in Table I. In general, the airspeeds shown are those considered to be representative of the helicopters' level flight capabilities at the usable power and gross weight values listed in Table I. Minor adjustments are made in some cases to improve the uniformity of approach. For example, consider the data for three H-34 helicopters reported in References 4, 8, and 9. Operating gross weights for the UH-34D (Reference 4) and the H-34 (Reference 8) were approximately 11,400 and 12,000 pounds respectively. As no operating gross weight was given for the H-34A of Reference 9, the 11,867-pound design normal gross weight listed in Reference 9 was used. Although the attainable level flight airspeed,  $V_A$ , varies with gross weight and, therefore, should be slightly different for each of these three ships, it was assumed that a single value of  $V_A$  could be used without injecting any appreciable error. Thus, based on a usable power of 1400 horsepower and a design normal gross weight of 11,867 pounds, the attainable level flight airspeed of 135 knots was established from the flight manual for the three H-34 helicopters. The airspeed spectrums for each aircraft listed in Table I were put in terms of  $V_A$  for the purpose of comparison and study. Table I also contains tabular data which aid in the description of the aircraft and missions.

Table II shows the depth of the data base for each of the studies in terms of flight hours, number of flights, and hours per flight for the sources that provided these data. It will be noted that the sampling varied over a broad range, from a minimum of 35 hours to a maximum of 982 hours, and that many types of missions were involved.

Table II also presents the general results of the surveys in terms of mission segments. A broad time distribution among ascent, enroute, and descent is shown, and it may be seen that the variations among aircraft that do occur are not of large magnitude.

The following sections of this report present a detailed study of the data from the referenced reports, commencing with an analysis of the mission segment distribution and proceeding through each of the important flight parameters.

## MISSION SEGMENTS

### DATA REDUCTION

Flight profile data obtained from flight load surveys, References 1 through 12 excluding 9, are categorized into various mission segments that reflect the differences in data reduction criteria. Essentially, there are three groups of mission segment definitions adopted in these reports; they are defined in the following subsections.

#### Four-Segment Breakdown

References 1, 2, and 3 divide the total flight time into four basic segments: (1) takeoff and ascent; (2) maneuvering; (3) descent, flare, and landing; and (4) steady state. Typically, these mission segments are as defined in Reference 1:

"During the first three mission segments which comprise the transient part of flight, the stick position traces show no steady values about which the stick traces seem to deviate, while the airspeed and altitude traces manifest frequent changes. Mission Segment 1 (takeoff and ascent) includes not only the takeoff and climb to the initial steady-flight altitude but also the unsteady ascents to other steady-flight altitudes. Mission Segment 2 (maneuvering) consists of any transient parts of flight which are not characteristic of Mission Segments 1 and 3. During maneuvering, the normal acceleration trace is usually very active. In addition to the unsteady part of flare and landing, Mission Segment 3 (descent, flare, and landing) includes the unsteady part of any descent whether intended for a new steady-flight altitude or for landing. Mission Segment 4 (steady state) includes those parts of the flight where the stick traces are relatively steady and where the airspeed and altitude traces are steady or changing smoothly. Such characteristics prevailed during cruise, hover, and steady ascent and descent."

### Three-Segment Breakdown

References 5 through 8 and 10 divide the total flight time into three basic segments: climb, enroute, and descent. Enroute time is defined as the time spent at rates of climb between  $\pm 300$  feet per minute (positive rates of climb represent ascent and negative rates of climb represent descent). Climb or ascent would include all the time spent at a rate of climb in excess of  $+300$  feet per minute, and descent would include all the time spent at a rate of descent faster than  $-300$  feet per minute.

Mission segment data presented in Reference 4 include the above segments as well as a hover segment. Since no mission segment definitions were presented in Reference 4, it was assumed that they were similar to the three-segment breakdown. Since hover usually has the same characteristics as steady-state or enroute segments, the hover time was incorporated into the level or enroute segment to reduce the number of mission segment groups to three.

### Five-Segment Breakdown

References 11 and 12 divide the total flight time into five segments, defined as follows by Reference 11:

- "1. Takeoff and Ascent (Flight Segment 1): Includes takeoff and climb to steady flight and all ascents during flight.
2. Cruise (Flight Segment 2): Includes portions characterized by steady airspeed and rate of climb generally within  $\pm 400$  feet per minute.
3. Descent (Flight Segment 3): Includes all descents during the flight as identified by decreasing altitude, decreasing airspeed, and generally decreasing torque.
4. Flare and Landing (Flight Segment 4): Includes the landing portion of flight beginning with a sharp increase in engine torque following descent prior to landing.
5. Hover (Flight Segment 5): Includes all portions of flight when the airspeed is below 40 knots."

The variation among the three groups of definitions appears to be significant. It is of course possible to compare data that have been gathered under one consistent set of definitions, and this has been done for the data of References 1, 2, and 3. This is shown in Figures 1 and 2, which provide a basis for evaluating the mission segment time distribution for three modern turbine-powered Army helicopters assigned to three different missions. To achieve a broader data base and to permit evaluation of all available data, it is necessary to convert all data to a common basis. The bulk of the data having common mission segment definitions is that which divides the total time into climb, enroute, and descent segments in accordance with the  $\pm 300$  feet per minute rate-of-climb criterion. The mission segment data from References 1, 2, 3, 4, 11, and 12 were adjusted to agree with this form of definition by considering that the time spent between the smallest negative rate of climb reported and the smallest positive rate of climb reported was proportional to enroute time. Time spent at larger positive rates of climb was considered to be proportional to climb or ascent time, and time spent at larger negative rates of climb was considered to be proportional to descent time. Table II presents the mission segment results based on this criterion. As noted in Table II, the data of References 3, 5, 6, 7, 8, and 10 are based on the  $\pm 300$  feet per minute rate of climb. Data from References 1 and 2 are based on a rate of climb of  $\pm 500$  feet per minute, and data from References 11 and 12 are based on a rate of climb of  $\pm 400$  feet per minute. A statistical analysis was made to determine the possible error that could exist if data based on these three rate-of-climb criteria were combined. Results showed average errors to be 0.75% for the enroute segment, 0.5% for the climb or ascent segment, and 1.4% for the descent segment. It was thus concluded that all of the data of Table II could be utilized to establish mission segment trends. Figure 1 presents these data in graphical form to assist in establishing comparisons and correlations. Data derived from CAM-6, Reference 13, are also included.

Figure 2 shows the comparison of Army flight load survey data based on mission segment definitions of References 1, 2, and 3 and the same data as modified to the three-segment mission definition. Mission segment breakdowns derived from the CAM-6 spectrum, Reference 13, and those obtained from fatigue substantiating data are also presented for comparison. The CAM-6 spectrum is segregated into mission segments corresponding to the four-segment and the three-segment mission definitions as shown in Table III. Although only flight time is being considered, 1% of the ground time

listed in the CAM-6 spectrum is considered to be either steady-state or enroute time. In a like manner, the load spectrums used in the calculation of component fatigue life for the three helicopters were converted to agree with these mission segment definitions. In some instances, the available fatigue life spectrum data were not in the form for easy comparison or were not complete enough to obtain the desired degree of correlation. For these reasons, the data presented in Figure 2 are intended to be used only as an approximate comparison of measured load spectrums and analytical spectrums.

As a further aid in establishing basic mission segment trends, the data shown in Table II were plotted in statistical form on log-probability paper, Figure 3. Data for each mission segment were ranked from the lowest to the highest value of percent time, and the respective plotting position on the probability scale was determined for each of the percentages of time by the method of median ranks, Reference 14. This method was derived principally for use in plotting fatigue test data in cases where small samples were available; however, it has been found generally useful for data of other types.

Using the principle of "least squares", the line that best fits the data was calculated and drawn through these points as shown in the figure. This plot is a statistical method for estimating the trend of the total population based on a relatively few data points. Thus, at the 50% probability value, there is a 50% probability that the percent time for a mission segment for any helicopter will not exceed the percent time associated with this probability. Similarly, at the 90% probability value, there is a 90% probability that the percent time for a mission segment for any helicopter will not exceed the percent time associated with this probability. It should be noted that the percents for each mission segment at a given probability cannot be added together, since this total would not necessarily be equal to 100%. The decision as to what mission segment is to be used in establishing the corresponding percentages of time for the other two segments is determined by the particular nature of the part or component being investigated. If, for example, the fatigue life of a component is to be calculated, and preliminary calculations have shown that the major portion of the fatigue damage occurs during the descent segment, then the descent curve would be selected as the base to which the other two segments, enroute and ascent, are adjusted, such that the total time for all three segments would equal 100%. The reliability of the prediction would vary with the probability selected. Thus,

if a high reliability of the predicted life is desired, the percent time for the descent segment would be selected at a correspondingly high probability of success, say, 99% or 99.9%.

The foregoing method of establishing mission segment trends is quite general and does not reflect the individual characteristics or capabilities of a given helicopter. In an effort to improve this situation, the percent time that each helicopter spent in each of the three segments was plotted as a function of the helicopter's design normal gross weight/maximum takeoff power ratio in Figure 4. As shown in this figure, as well as in Figure 1, the enroute data appear to band together in a fairly tight group with the exception of those for the CH-47A, Reference 1; the UH-34D, Reference 4; the H-13 military trainer, Reference 6; and the YH-40 experimental helicopter, Reference 8. Study of these references led to the conclusion that this variance existed because of the particular types of missions being flown at the time that the flight data were recorded. A study of the percent time that the CH-47A and UH-34D spent at various altitudes revealed that these two helicopters flew at altitudes of less than 1000 feet for a large percentage of the total time. This fact plus the general mission description reported, i.e., troop-supporting missions in simulated combat conditions, led to the conclusion that these missions could be considered to be nap-of-the-earth-type flying where many short-range, low-altitude shuttles were being flown in the time that was reported to be one flight. This type of mission would then account for a lower than average time being spent in the enroute segment. The low enroute time reported for the H-13 military trainer and the YH-40 experimental helicopter is considered to be a typical trend of helicopters being utilized as primary trainers, where the basic principles of helicopter operation and control are demonstrated or where the handling characteristics of a new helicopter are being investigated. This type of flying would be characterized by many landings, takeoffs, and maneuvers, resulting in a lower enroute time.

The nature of the data shown in Figure 4 suggested that a more precise definition of mission segment trends could be obtained if two groups of mission types were considered instead of just one. This was accomplished by establishing the standard mission and the nonstandard mission categories. The distinction between these two mission types is tentatively defined as follows:

Nonstandard Mission would have one or more of the following characteristics:

1. Flight training missions, where considerable time is spent in demonstrating and practicing takeoffs, landings, maneuvers, and autorotative flight.
2. Test flight of experimental or prototype helicopters, where considerable time is spent in determining the flying qualities and/or flight loads associated with given flight conditions. Test flying of production helicopters after overhaul would also be included here.
3. Cargo- or troop-carrying missions, where relatively many short-range, low-altitude shuttles are made during a flight.

Standard Mission would, in general, be devoid of the characteristics associated with the nonstandard mission, and a considerable percent of the total flight time would be spent at altitudes in excess of 1000 feet. Typical missions included in this category are:

1. Utility-type flights
2. Airmail flights
3. Civil transport flights
4. Relatively long-range cargo- and troop-carrying flights
5. Military navigational or cross-country-type flying such as experienced by the H-34 Instrument Flight Rules Trainer, Reference 8
6. General load-lifting flights

The general results of the study of these two mission types are shown in Figure 4. The scatter bands illustrated are derived from Figures 5 and 6, the probability plots of the data, which also show the relatively good fit of the data to the log-normal distribution. The width of the scatter bands in Figure 4 is  $\pm 1\sigma$ , and it is therefore not unusual that a few data points should fall outside of these limits.

## SUMMARY

Figure 1 presents a general pictorial review of the results of the prominent helicopter flight spectrum surveys conducted to date when each mission is viewed on the basis of the three segments, ascent, enroute, and descent. Review of this figure, which is presented in order of increasing weight, shows no general correlation between gross weight and mission segment. In this rather superficial view, a surprising degree of uniformity is apparent with only an occasional exception. The first column on the left in the figure is that derived from CAM-6, Reference 13, while the last column on the right is the average of the measured survey data. The general applicability and reasonableness of the CAM-6 spectrum are demonstrated by the fact that the CAM-6 spectrum blends quite well with the bulk of measured data. It is, of course, true that any specific mission or aircraft may vary significantly from the CAM-6 spectrum; however, as a general specification for helicopters of many varied missions, CAM-6's basic mission segment breakdown appears to be well chosen.

The data of References 1, 2, and 3 are studied in somewhat more detail in Figure 2. Here, the data recorded under simulated Army combat conditions for three modern turbine-powered helicopters are presented basically as recorded in the four-segment breakdowns (ascent, descent, maneuver, and steady state) and also as modified to the three-segment breakdown. For comparison, the CAM-6 spectrum and the originally assumed fatigue spectrum for each helicopter are shown for both the three- and four-segment mission.

The generally favorable correlation of the CAM-6 spectrum to the spectrum measured in service is seen to be slightly improved for the four-segment breakdown. The CH-47A flight-measured data appear to deviate from the CAM-6 spectrum by the largest amount. Further study of the mission data for this aircraft reveals that virtually all of the flight time was spent at low altitudes and that flight duration was typically very short. This is undoubtedly due to the nature of the particular mission that the aircraft was assigned and is therefore an example of the effect that specific missions can have on flight profile.

It can also be noted in Figure 2 that relatively poor correlation exists between the flight-measured spectrum and the fatigue spectrum that was originally assumed for the purpose of determining the fatigue life of components for each aircraft shown. For the UH-1B and CH-47A, the

enroute or steady-state time determined in the service load surveys is significantly less than that assumed, while the ascent, descent, or maneuver segments exceed that assumed by substantial margins. For the CH-54A, the enroute or steady-state time assumed in the fatigue spectrum is a reasonable approximation of the measured data; however, no ascent, descent, or maneuver schedule was available for comparison. This is due to the manner in which the fatigue spectrum is presented. Only the level-flight portion of the fatigue spectrum is presented in terms of percent time, while the remainder of the spectrum is in terms of maneuvers per 100 hours. Converting maneuvers per 100 hours into percent time cannot be accomplished without additional information defining the duration of each type of maneuver being considered.

The full meaning and importance of these deviations cannot be assessed without detailed knowledge and analysis of the accompanying loads and strength for a particular helicopter component. In this study we are concerned with the portions of the flight spectrum which contribute significantly to fatigue damage and therefore limit component fatigue life. There is no single flight condition that is critical from this point of view, for all helicopters or for all components of a given helicopter.

The flight conditions which contribute significant fatigue damage are those which produce high vibratory loads and which are sustained for a sufficient time to accumulate the damaging cycles. Severe maneuvers may produce loads or stresses which are far in excess of a component's endurance limit; however, the relatively few stress cycles per maneuver combined with the infrequency of such maneuvers result in these loads being generally noncritical in the fatigue damage assessment. Steady-state flight conditions which may produce loads only slightly in excess of the endurance limit but which may be sustained for long periods are generally more damaging. Components which accrue damage in straight and level flight will normally have a very low fatigue life. Other steady-state conditions such as high power climb, rapid descent, or banked turns may prove to be the life-limiting conditions for other components. Mild maneuvers which have a relatively long period, such as cyclic flare just before touchdown, are also of considerable interest here. Sizeable errors in assigning time to any of these critical flight conditions may lead to component lives which are either dangerously long or, conversely, unnecessarily short and thereby penalize the aircraft economically.

Review of Figure 2 leads to observations that the steady-state or enroute time assumed in the fatigue spectrums for the UH-1B and CH-47A far exceeds that which is experienced in service; while the ascent, descent, and maneuver segments assumed are far less than those measured. If level flight is the critical fatigue damage regime, then the fatigue spectrums may be quite conservative; however, this conclusion depends on the airspeed distribution, which is analyzed later in this report. If, however, one of the other flight regimes is the more critical, then it must be concluded that component lives based upon the fatigue spectrum are probably quite optimistic when considering the effects of mission segment alone. In the case of the CH-54A, the steady-state or enroute time assumed in the fatigue spectrum matches quite well that determined in the survey and, therefore, may be considered to be fairly accurate. The lack of available fatigue spectrum information for other flight regimes eliminates any further consideration for this aircraft.

Some additional study of the general mission segment breakdown is presented in Figures 3 through 6. Figure 3 is a plot of percent time in each of the three primary mission segments versus probability. The slope of the lines on the plot is a measure of the variability in the data. The enroute data line reveals that only 10% of all helicopters would be expected to spend less than 63% of total flight time in the enroute segment (i.e., 90% of all helicopters would spend more than 63% of time in the enroute segment). Toward the higher end of the scale, it is seen that only 10% of all helicopters would spend more than 79% of all time in the enroute segment (i.e., 90% of all helicopters would spend less than 79% of all time in the enroute segment). Similar observations may be made for the ascent and descent segments.

Figure 3 may be used as a guide in the selection of the basic mission segment breakdown for a new aircraft. To do this, it would be necessary to know from preliminary calculations which segment is critical for the component under consideration. Let us assume the hypothetical case of a tail rotor blade root section that is known to accumulate a considerable amount of fatigue damage during high-power ascents but, during descents or while enroute, accumulates only a moderate amount of fatigue damage. A reasonable choice of spectrum for this component could be derived from Figure 3 as follows. The percent time spent in the critical flight regimes should be chosen at a high probability level. If 99% is chosen as the probability level, then the aircraft would be considered to spend 23% of all flight time in ascent and 26% in descent. The

remaining time is then considered to be enroute time, 51%. For certain aircraft or certain missions, it may be quite unrealistic to use a very high ascent and descent time. In such a case, it would be proper to use some lower probability level; however, this decision should still be weighed in favor of the critical fatigue damaging conditions. In this example, only 1% of all helicopters would be expected to exceed the ascent and descent times chosen; however, the enroute time is only that required to account for the remaining flight time and may bear no specific relation to Figure 3. Other components on the same aircraft will probably be found to be critical for other flight regimes, and these may be handled in a similar fashion with the emphasis on the critical fatigue damage-producing segment for that component. While this may lead to an apparent inconsistency in the schedule of operation for a given aircraft, a more important result is that a better level of uniformity of conservatism in assigning fatigue lives can be achieved.

Further analysis of the mission segment structure for helicopters is shown in Figures 4, 5, and 6. Figure 4 shows a grouping of the data for the enroute, ascent, and descent segments vs gross weight/power ratio for the aircraft studied. A relatively narrow scatter band was found to exist for most of the data; however, certain aircraft consistently fell outside of this band. Review of the basic data sources for these aircraft revealed that there was some cause to expect that utilization of these aircraft was not representative of typical helicopters. The aircraft in question were not alike in any way, with the one exception that the mission or duty assignment at the time that they were surveyed was such that enroute time would be relatively short and that many takeoffs and landings would occur. These aircraft are the H-13 military trainer, the YH-40 experimental, the UH-34D, and the Army CH-47A. As discussed previously, the mission that these helicopters were assigned required low-altitude, nap-of-the-earth flying with many takeoffs and landings and has been designated a nonstandard mission, as opposed to a standard mission which would require flying to some remote point at a relatively constant altitude and airspeed. Since the nonstandard mission would include pilot training and familiarization, it is quite likely that every type helicopter will be subjected to this type of flying for some portion of its total useful lifetime. In evaluating a fatigue spectrum for a helicopter that is expected to be assigned a standard type of mission, Figures 4 and 5 may be used as a guide. The scatter band widths shown in Figure 4 are based on the average time plus

and minus one standard deviation and would, therefore, be expected to include 68% of all cases. Other probabilities may be used by working from Figure 5. The effects of operations in nonstandard missions should also be evaluated to assure that these operations do not drastically affect component lives. Figures 4 and 6 are useful in establishing the required mission times and probabilities for this purpose.

## AIRSPPEED

### DATA REDUCTION

The airspeed frequency distribution for a helicopter could be one of the most important factors influencing the fatigue life of its components. This is particularly true for rotor systems where, in many cases, vibratory loads acting on the system are fairly high at the lower transition from hover to forward flight, are lower at moderate airspeeds, and then steadily increase with increasing airspeed up to  $V_{NE}$ , where  $V_{NE}$  is the never-exceed airspeed usually redlined on the airspeed indicator or specified in the flight manual. If the load-strength relationship is such that fatigue damage is experienced at these higher level flight loads, then the percentage of time spent at the high load-producing airspeeds becomes increasingly significant. As a result of this, either the airspeeds that produce appreciable component fatigue damage may be avoided or, if this is impractical, the time spent at these airspeeds may be limited. Such a restriction could influence the characteristics and the types of missions that may be flown. The converse of this may also be true: the type of mission flown could influence the airspeed frequency distribution.

Other interrelated factors that may influence the airspeed frequency distribution of a helicopter are its airspeed capabilities, the type of power plant installed or its available power, and the design normal gross weight. The influences of these factors are the subject of this section.

In general, airspeed frequency data reported in References 1 through 12, for the helicopters listed in Table I, are presented in the form of univariate or bivariate tables and/or in the form of frequency histograms. These tables and histograms relate the percentage of total or steady-state time with corresponding airspeed intervals expressed in terms of knots or miles per hour or as nondimensional ratios such as  $V/V_{max}$  or  $V/V_{NE}$ . To standardize the presentation of these data for comparison purposes, the percentage of the attainable level-flight velocity,  $V_A$ , was selected as the airspeed parameter, where  $V$  is the airspeed being considered and  $V_A$  is the maximum attainable level-flight airspeed, considering design gross weight, usable power, blade stall, and structural limitations. Values of the attainable level-flight airspeed  $V_A$ , design gross weights, and usable power are presented in Table 1.

The helicopters listed in Table I were subdivided into four classes, dependent on helicopter design gross weight and the type of propulsion system installed. These classes are defined as follows:

1. Reciprocating engine-powered helicopters having a design normal gross weight of less than 10,000 pounds.
2. Turbine-powered helicopters having a design normal gross weight of less than 10,000 pounds.
3. Reciprocating engine-powered helicopters having a design normal gross weight of 10,000 to 15,000 pounds.
4. Turbine-powered helicopters having a design normal gross weight of greater than 15,000 pounds.

Percentages of time for each helicopter were converted to cumulative percentages of time to form cumulative airspeed frequency distributions in the manner shown in the example presented in Figure 7. The transformation of percent time frequency distributions presented in tabular or histogram form, Figure 7a, to cumulative frequency distribution curves, Figure 7b, is accomplished by cumulatively summing the percentages of time corresponding to given airspeed intervals, starting with the lowest airspeed. The cumulative sum of percent time at an airspeed interval is plotted at the upper class boundary for that interval. This procedure is repeated for each interval, and a smooth curve is faired through the resulting points. This graph then permits the determination of the cumulative frequency for airspeeds equal to or less than the desired airspeed. To facilitate comparisons with helicopters of different airspeed capabilities, the airspeed is expressed as a percent of the attainable level flight airspeed,  $V_A$ , as shown in Figure 7b. The interpretation of this curve can be illustrated by an example. At 60%  $V_A$  (see Figure 7b), it can be stated that 70% of the time will be spent at an airspeed of 60%  $V_A$  or less; at 80%  $V_A$ , it can be stated that 95% of the time will be spent at an airspeed of 80%  $V_A$  or less; and at 100%  $V_A$ , it can be stated that 100% of the time will be spent at an airspeed of 100%  $V_A$  or less.

Another feature of the cumulative frequency distribution curve is that the relative frequencies at airspeeds either higher or lower than a given airspeed can be estimated by noting the characteristics of the curve slope in the desired area. In general, steeper slopes are associated with higher percentages of time being spent at a given

airspeed interval, and lower slopes are associated with lower percentages of time being spent at a given airspeed interval.

Cumulative airspeed frequency distribution curves similar to that of Figure 7b were developed for each helicopter. After these curves were grouped according to helicopter class, a statistical analysis was made to determine the scatter bands corresponding to a variation of plus and minus one standard deviation from the mean ( $\pm 1\sigma$ ). The results of these calculations are shown in Figure 8 for the four classes of helicopters being considered. Composite scatter band curves for these classes are presented in Figure 9 to facilitate the determination of airspeed frequency distribution trends with power plant type and design gross weight.

The airspeed frequency distribution portion of the flight-measured spectrums for the CH-47A, UH-1B, and CH-54A helicopters, References 1, 2, and 3, respectively, is compared in Figure 10. These same curves are also compared to the airspeed portions of the fatigue spectrums used to establish component lives and to the airspeed portion of CAM-6, Reference 13, in Figure 11. The airspeed portion of CAM-6 used for this comparison is shown in the last column of Table III. Time listed in CAM-6 for the forward flight-power on, right and left turns, at 30, 60, and 90%  $V_{NE}$  conditions and for the autorotation-power off, steady forward flight, right and left turns, at 30, 60, and 90%  $V_{NE}$  conditions was reapportioned to match the 20, 40, 60, 80, and 100%  $V_{NE}$  increments. The values were then normalized so that total time equaled 100%. These percentages of total time were then cumulatively summed and plotted in Figure 11 as a function of the attainable level-flight airspeed. For the purposes of this comparison,  $V_A$  and  $V_{NE}$  are considered to be interchangeable.

A comparison of the variations of the cumulative airspeed frequency distribution with altitude is presented in Figure 12 for the CH-47A, UH-1B, and CH-54A helicopters. Individual cumulative airspeed frequency distribution curves were developed for several altitude ranges, the summation of which equals the total airspeed frequency experience.

#### SUMMARY

Airspeed data for the helicopters listed in Table I and reported in References 1 through 12 were analyzed for the purpose of establishing basic airspeed frequency distribution trends and characteristics for these helicopters, so

that the distributions for future helicopters may be anticipated. The importance of this information in the determination of component fatigue lives has been demonstrated in the past by the difficulties experienced in predicting fatigue lives prior to the availability of a considerable amount of in-flight frequency data.

The effect that mission assignment has on the airspeed frequency distribution is first investigated in Figure 8. Figure 8a presents the cumulative airspeed frequency distribution curves (scatter band) based on a variation of  $\pm 1\sigma$  for seven reciprocating engine-powered helicopters having a design normal gross weight of less than 10,000 pounds. Also shown are the helicopter designations and the types of missions flown at the time that the frequency data were recorded. It is evident from the width of the scatter band that there is a fairly high variability in the data. This is principally due to the inclusion of data for the H-13 high-altitude helicopter and the H-13 military trainer. If a statistical analysis were performed on the remaining five airmail-utility-type helicopters, a much narrower scatter band would result. This grouping of the data suggests that the distribution of airspeed frequency data is very much dependent on the type of mission flown. This conclusion is further supported by considering the four different missions of the four H-13 helicopters. One is used for high-altitude missions, one is used as a military trainer, one is used to deliver airmail, and the remaining one is used for utility-type missions. The airspeed capabilities, gross weight, and usable power are essentially the same, but the cumulative airspeed distributions shown in Figure 8a for the military trainer and for the high-altitude helicopters differ considerably from those for the airmail and for the utility helicopters. In general, it can be concluded that special-purpose helicopters of this class, such as the trainer and the high-altitude ships, spend less time at the higher airspeeds than do helicopters performing basic utility missions.

Airspeed frequency data for five turbine-powered helicopters having a design normal gross weight of less than 10,000 pounds, shown in Figure 8b, exhibit a relatively narrow scatter band. With the exception of the UH-1B, the curve shapes or relative airspeed distributions are quite similar, varying only in their placement along the airspeed axis. The curve for the UH-1B is much steeper than the others, signifying that it spends a larger percentage of its forward flight time within a fairly narrow airspeed range (60% to 75%  $V_A$ , or a spread of only 15%  $V_A$  compared to an average spread of approximately 30%  $V_A$  for the other four ships).

It should be noted that the UH-1B is the heaviest helicopter included in this group.

Although the correlation of airspeed frequency distribution with mission type is not as evident for this class as it was for that shown in Figure 8a, Figure 8b indicates that the UH-1B utility and the YH-40 experimental helicopters spend less time at the higher airspeeds than do the three observation helicopters. It is not possible to determine whether this trend can be attributed to mission assignment, gross weight as with the UH-1B, or other aircraft characteristics such as power required, pilot comfort, etc.

Figure 8c presents cumulative airspeed frequency distributions for four reciprocating-engine helicopters having a gross weight of 10,000 to 15,000 pounds. At the lower airspeeds up to approximately 40%  $V_A$ , the  $\pm 1\sigma$  scatter band is relatively narrow but becomes increasingly wider for the remainder of the airspeed range. Since these four helicopters have approximately the same gross weight and usable power, it is considered that this divergence is caused by differences in the missions flown. It is noted that if only the UH-34D, H-21C, and H-34A were considered, the uniformity of the low-speed scatter band would be continued for the full airspeed range. This suggests that the characteristics of the mission flown by the H-34 IFR (Instrument Flight Rules) trainer are significantly different from those of the mission flown by the other three utility ships. This seems to be a reasonable assumption when it is considered that the H-34 IFR trainer would be spending a large percentage of its total forward flight time at moderate airspeeds, practicing instrument or blind flying procedures; whereas the utility helicopters, usually flying in favorable weather conditions, would be more intent on reaching their destination quickly.

Cumulative airspeed frequency distribution data for five turbine-powered helicopters having a design normal gross weight greater than 15,000 pounds are presented in Figure 8d. The  $\pm 1\sigma$  scatter band width is relatively large at the lower- and middle-range airspeeds but decreases slightly at the higher airspeeds. There appears to be a close correlation between the two studies of CH-54A load lifters and a close correlation between the S61N and the V-107-II civil transports. The heavier load lifters spend a considerable amount of time at the lower airspeeds. For the two CH-54A helicopters shown, this amounts to 25% to 30% at airspeeds of 35%  $V_A$  or less. The two civil transports, on the other hand, spend only 8% to 9% of the total time at an airspeed of 35%  $V_A$  or less. This difference can be attributed to the mission each is expected to perform. The

CH-54A helicopters are primarily designed to transport heavy loads either suspended below the helicopter by cables or carried internally in detachable compartments. In cases where the cargo is suspended below the ship, the airspeeds flown are limited by aerodynamic effects created by the cargo, thus limiting the amount of time that could be spent at higher airspeeds. The mission performed by the civil transport is one that is primarily dictated by schedules and economics (i.e., the more passenger miles per hour, the greater the financial return). Thus, a large percentage of the total time would be spent at the higher airspeeds, 90% to 100%  $V_A$ , as shown in Figure 8d.

The airspeed frequency distribution curve for the CH-47A cargo helicopter is similar to that of the civil transports at the low-speed range but diverges rapidly beyond 45%  $V_A$ . Thus, small percentages of time are spent at the lower and higher airspeeds, with the majority of the time being spent between airspeeds of 60% to 90%  $V_A$ .

Figure 8d may also be interpreted as showing a trend of airspeed frequency distribution with gross weight. In general, it can be stated that as the gross weight increases, the time spent at the higher airspeed decreases.

Airspeed frequency distribution scatter bands obtained from Figure 8 for the four classes of helicopters are compared in Figure 9. Figure 9a compares the scatter bands from Figures 8a and b for reciprocating engine- and turbine-powered helicopters having a design normal gross weight of less than 10,000 pounds. The similarity of these two classes is readily noted, particularly at the higher airspeeds. Differences in the lower airspeed boundaries appear to be the result of the type of missions flown. It is interesting to note that if the data for the H-13 high-altitude helicopter and for the H-13 military trainer had been omitted from the data shown in Figure 8a, the resulting scatter band would be almost identical to that of Figure 8b. The conclusion that can be drawn from the comparison made in Figure 9a is that the lighter reciprocating engine-powered and turbine-powered helicopters spend approximately the same percentages of time at the same proportion of their airspeed capability. Exceptions to this trend are usually the result of the differences in the mission assignment, with special-purpose helicopters such as the high-altitude and military trainers spending more time at lower airspeeds.

Figure 9b compares the airspeed frequency distributions for the heavy reciprocating engine- and turbine-powered helicopters. Although the ranges of gross weight are different for each class, 10,000 to 15,000 pounds for the reciprocating

engine-powered helicopter and greater than 15,000 pounds for the turbine-powered helicopter, several general trends can be noted. At the lower airspeeds, up to 40%  $V_A$ , the scatter bands have considerable overlap, with the turbines actually spending more time at low speeds. This is largely attributable to the data obtained for two CH-54A load lifters, which show 35% to 30% of the total time being spent up to an airspeed of 35%  $V_A$ . It is considered that this trend is more associated with the type of mission flown than with any effects due to gross weight. The heavier turbine-powered helicopters spend a much greater percentage of the total time near the high end of their airspeed capability than do the reciprocating engine-powered helicopters. Although the type of mission flown probably plays the most important role in producing this trend, it is felt that the lower weight/power ratios associated with the turbine-powered helicopters are also a factor.

Figure 9c compares the two classes of reciprocating engine-powered helicopters having design normal gross weights of less than 10,000 pounds, Figure 8a, and 10,000 to 15,000 pounds, Figure 8c. At the lower airspeeds, the trends for both classes are approximately the same; but as the airspeed increases, the lighter class spends slightly more time at the higher airspeeds than does the heavier class, indicating a modest trend of airspeed frequency distribution with gross weight. The wider scatter band for the heavier class at approximately 80% cumulative time is due to the mission flown by the H-34 IFR trainer, as previously discussed. This again emphasizes the fact that the type of mission flown by a helicopter has an important effect on the resulting airspeed frequency distribution.

Figure 9d compares two classes of turbine-powered helicopters, one class having design normal gross weights of less than 10,000 pounds and the other class having design normal gross weights of greater than 15,000 pounds. The heavier ships spend a larger cumulative percentage of the total time at the lower airspeeds than do the lighter ships. This is principally due to the type of mission flown by the CH-54A helicopter, as previously discussed. It is also noted that because of the data from the two civil transports, the heavier class spends a substantial percentage of time near the higher airspeed limit. In general, it is concluded that light turbine-powered helicopters tend to concentrate the majority of forward flight time in a fairly narrow airspeed range (60% to 70%  $V_A$ ), whereas the heavier turbine-powered helicopter spreads its total forward flight time more uniformly over the full airspeed range but is strongly influenced by mission assignment.

Airspeed frequency data for the CH-47A cargo helicopter,

UH-1B utility helicopter, and CH-54A load-lifting helicopter (References 1, 2, and 3) are shown in Figure 10. The airspeed range where the majority of forward flight time is spent is 60% to 90%  $V_A$  for the CH-47A, 60% to 75%  $V_A$  for the UH-1B, and 65% to 95%  $V_A$  for the CH-54A. It is seen that the lighter utility helicopter, the UH-1B, spends the majority of its flight in a relatively narrow airspeed range. Although these data are quite limited, they do suggest that at airspeeds up to 30%  $V_A$ , the cumulative percent of the total time varies directly with gross weight; at the higher airspeeds, 80%  $V_A$ , the opposite trend appears.

No one factor is considered adequate to explain the variations shown in Figure 10. As mentioned previously, the assigned mission of the aircraft is an important factor affecting airspeed distribution. However, it is recognized that design parameters and aircraft characteristics may be equally important. In the case of the UH-1B doing general utility flying in support of field units, it would be anticipated that periodic high-priority missions would require a significant portion of time to be spent near the maximum airspeed capability and that other utility missions would tend to spread the time over the airspeed range. The fact that an extremely small amount of time is spent in the higher speed range indicates that some other factor or factors inhibit such operation and actually tend to group the majority of time in the narrow band between 60 and 75%  $V_A$ . The reason that relatively little use is made of the available higher speed range is not apparent from these data. It is probable that the distribution is influenced by pilot preference due to flying or handling qualities considerations, such as an increase of vibration level with higher airspeed.

The airspeed distribution for the CH-47A shown in Figure 10 exhibits a relatively smooth and normal trend, while that for the CH-54 illustrates the tendency to spend substantial amounts of time in the low-speed range. This latter observation is considered to be normal for the CH-54A operations, that is, transporting heavy external loads.

Figure 11 presents a comparison of flight-measured airspeed spectrums with the airspeed portion of the fatigue spectrums for the CH-47A, UH-1B, and the CH-54A helicopters. The CAM-6 airspeed spectrum is also shown on these plots. In Figure 11a, the flight spectrum for the CH-47A and the CAM-6 spectrum are seen to be in fairly close agreement. If the CAM-6 spectrum allowed for approximately 12% of the total time spent at airspeeds of 30%  $V_A$  or less, the two spectrums would match extremely well. The airspeed portion

of the fatigue spectrum does not compare as favorably with the flight-measured spectrum. The effects of this deviation on component fatigue lives cannot be estimated without further knowledge of the corresponding flight loads and the fatigue strength. If fatigue damage occurs only at airspeeds greater than 90%  $V_A$ , then the fatigue spectrum, which predicts a higher percent time spent at these airspeeds than does the flight-measured spectrum, would be conservative.

A comparison of the flight-measured airspeed spectrum for the UH-1B with the fatigue spectrum and CAM-6 spectrum, Figure 11b, shows a fairly close correlation at the low-speed range. Above approximately 60% to 70%  $V_A$ , the fatigue spectrum and the CAM-6 spectrum predict a larger percentage of time than was obtained from the flight-measured spectrum. Of the two, CAM-6 is in closer agreement with the flight-measured spectrum. The fatigue spectrum is undoubtedly conservative with regard to damage accrued in high-speed flight.

Figure 11c presents the comparison of the flight-measured, CAM-6, and fatigue spectrums for the CH-54A helicopter. Generally good agreement is seen at the higher airspeeds. However, CAM-6 deviates significantly at airspeeds below 60%  $V_A$ . The fatigue spectrum is a close approximation of the flight-measured data at 40%  $V_A$  but predicts more utilization than was recorded for airspeeds between 40% and 75%  $V_A$ . Since the slope of the line is a measure of time spent at that velocity, the fatigue spectrum is seen to predict somewhat less time in the interval from 75% to 100%  $V_A$  and, therefore, may underestimate fatigue damage accrued if loads in this range exceed the endurance limit for any component.

The manner in which the cumulative airspeed frequency distribution varies with altitude is shown in Figure 12 for the CH-47A, UH-1B, and CH-54A helicopters. Airspeed-altitude data for the CH-47A, Figure 12a, are divided into three altitude ranges: less than 1000 feet, 1000 to 2000 feet, and 2000 to 3000 feet. The summation of the time for these three altitude ranges equals the total airspeed experience. Figure 12a signifies that the time spent at altitude becomes smaller with increasing altitude and that the majority of the forward flight time is spent between approximately 60% and 90%  $V_A$ , regardless of the altitude.

The airspeed-altitude data for the UH-1B, Figure 12b, are divided into four altitude ranges: less than 1000 feet, 1000 to 2000 feet, 2000 to 5000 feet, and above 5000 feet. The curve shapes for each altitude range are very similar with the exception of the curve obtained for the above-5000-foot

range. The majority of the forward flight time for the lower three altitude ranges is spent at airspeeds of approximately 60% to 75%  $V_A$ , whereas the maximum percentage of time at the above-5000-foot range is spent at airspeeds of 65% to 75%  $V_A$ . This is probably due to the fact that  $V_A$  is considered to be a constant which is independent of altitude for the purposes of this study, whereas in reality some reduction in attainable airspeed probably occurs for altitude changes of this magnitude. Also the size of the data sample in the range above 5000 feet is quite small, and this result could therefore be influenced by additional data. The time spent at altitude increases with altitude up to approximately 5000 feet. However, the amount of time spent above 5000 feet accounts for only a small percentage of the total time.

Figure 12c presents the airspeed-altitude data for the CH-54A. Like the UH-1B, the time spent at altitude increases with altitude up to 5000 feet, with the CH-54A spending a slightly higher percentage of time at the higher altitudes, though no time was recorded above 5000 feet. Curve shapes for altitude ranges of less than 1000 feet, 1000 to 2000 feet, and 2000 to 5000 feet are fairly similar, with the majority of forward flight time being spent at airspeeds of approximately 65% to 95%  $V_A$ .

The possibility that differences in the recorded density altitude data for these three helicopters, particularly those for the CH-47A, resulted from differences in outside air temperature was also explored. Data presented in References 1, 2, and 3 showed that the percentages of steady-state time spent between 50 and 80 degrees were approximately 70% for the CH-47A, 64% for the UH-1B, and 73% for the CH-54A. Below 50 degrees, the percentages of steady-state time were approximately 22% for the CH-47A, 22% for the UH-1B, and 9% for the CH-54A. Above 80 degrees, the percentages of time were approximately 8% for the CH-47A, 14% for the UH-1B, and 18% for the CH-54A. It would be expected that if the three helicopters spent all of their time flying at the same absolute altitude, differences in the density altitude would be reported due to differences in outside air temperatures. The ship that spends a large percentage of time at the colder outside air temperatures would report a larger percentage of time at lower altitudes. Thus, if outside air temperature was the only variable, it would be expected that the CH-45A would spend the same amount of time at the lower density altitudes as does the UH-1B (22%).

Actually, the CH-47A spends approximately 44% of the steady-state time at density altitudes lower than 1000 feet, compared to only 25% for the UH-1B. Comparing outside air

temperature with the altitude data for the CH-54A, relatively low percentages of time are spent at lower outside air temperatures, whereas density altitude data show a fairly high percentage of time being spent at the lower altitudes. It would appear from these contradictory trends that outside air temperature does not significantly affect the reported density altitude frequency distributions and that these distributions therefore do reflect a true difference in the mode of operation for the various helicopters.

## GROSS WEIGHT

### DATA REDUCTION

The available gross weight frequency data found in References 1, 2, 3, 11, and 12 for the CH-47A, UH-1B, CH-54A, S61N, and V-107-II helicopters are presented as bivariate tables and frequency histograms. Four of these helicopters, the CH-47A, CH-54A, S61N, and V-107-II, fall into the class of turbine-powered helicopters having a design normal gross weight of greater than 15,000 pounds, whereas the UH-1B falls into the class of turbine-powered helicopters having a design normal gross weight of less than 10,000 pounds. Frequency data for these five helicopters are shown in Figure 13 as cumulative percent time versus the ratio of operating gross weight/design normal gross weight to facilitate comparison. The frequency data for the four heavier ships are analyzed statistically to determine the width of the scatter band corresponding to a variation of plus and minus one standard deviation from the mean ( $\pm 1\sigma$ ). Data for the UH-1B are also shown.

Figure 14 shows the breakdown of total gross weight frequency experience into the four mission segments defined in References 1, 2, and 3 for the CH-47A, UH-1B, and CH-54A helicopters. These segments are: ascent, maneuver, descent, and steady state.

### SUMMARY

The cumulative gross weight frequency distributions for the CH-47A, UH-1B, CH-54A, S61N, and V-107-II helicopters, References 1, 2, 3, 11, and 12, are compared in Figure 13. Since the CH-47A, CH-54A, S61N, and V-107-II are in the class of turbine-powered helicopters having a design normal gross weight greater than 15,000 pounds, previously established in the airspeed portion of this report, the data for these four helicopters are statistically analyzed to obtain the  $\pm 1\sigma$  scatter band for this class. The cumulative frequency curve for the UH-1B is included for comparison purposes and was not included in the scatter band determination.

Cumulative gross weight frequency curves for the four heavier helicopters do not appear to have much similarity if considered singularly. If, however, the data for these four helicopters are statistically analyzed, the width of the  $\pm 1\sigma$  scatter band is fairly uniform throughout. Up to approximately 60% cumulative time, which corresponds to operating gross weight/design normal gross weight ratios

of roughly 0.77 to 0.85, the scatter bands are nearly straight. This implies that, as a class, the percentages of time spent at these lower gross weight ratios are approximately uniform. As the operating gross weight/design normal gross weight ratio increases, the percentages of time spent at each ratio decrease; so that at ratios between .95 and 1.23, only small percentages of time are experienced.

If curves are drawn through the data points plotted in Figure 13 for each of the four heavier helicopters, the individuality of each can be seen. When the curve shapes of the two civil transports are considered, it is noted that the time spent by the V-107-II is uniformly distributed across the gross weight range, as the straight line up to a ratio of approximately 0.96 signifies. Above the gross weight ratio of 0.96, the percentages of time decrease with increasing weight, until at a ratio of 1.05 the percentage of time becomes negligible. The percentage of time distribution experienced by the S61N, on the other hand, falls primarily in a narrow range and shows little evidence of a uniform distribution. The differences are probably due to differences in route schedule and passenger loadings for these two civil operations. However, such information is not available in the referenced reports.

Of the four heavier helicopters considered in Figure 13, the data obtained for the CH-47A and the CH-54A helicopters appear to be spread over a larger gross weight range than those obtained for the two civil transports. Up to a gross weight ratio of about .84, corresponding to 85% cumulative time, data for the CH-47A reveal little change in the steep slope of the curve, indicating a high, and roughly uniform, utilization of this range. Above this ratio, the remaining 15% of the total time is evenly distributed up to an operating gross weight/design normal gross weight ratio equal to approximately 1.19. Data for the CH-54A show three distinctive gross weight experience ranges: 55% of the total time was spent at gross weight ratios up to 0.79, 35% of the total time was spent at gross weight ratios of 0.79 to 1.0, and the remaining 10% of the total time was spent at gross weight ratios of 1.0 to 1.21. As each of these portions of the cumulative gross weight frequency curve is fairly straight, the percentages of time spent within a portion are uniformly distributed throughout each range.

The cumulative gross weight frequency curve for the UH-1B utility helicopter shown in Figure 13 is similar in shape to the scatter band curves obtained for the four heavier helicopters, with the exception that it is displaced along

the gross weight axis. This displacement implies that the utility helicopter generally flies at higher percentages of design gross weight than do the heavier ships. The straight portion of the curve shows that the 80% of the total time spent at gross weight ratios of 1.10 or less is uniformly distributed over this range, whereas the upper curved portion signifies that the percentage-of-time increments for the remaining 20% of the total time decrease with increasing gross weight ratios. It should also be noted that the maximum gross weight ratio encountered was 1.36 for the UH-1B versus 1.19 for the CH-47A, 1.21 for the CH-54A, and 1.00 to 1.05 for the V-107-II and the S61N helicopters.

The nonuniformity of the cumulative gross weight frequency distribution curves is considered to be principally due to the different types of missions flown by these helicopters. It would be expected that gross weight limitations would be more restrictive and more rigidly adhered to for civil transports than for military helicopters. This is borne out by the data, in that the civil transports rarely fly at operating gross weight/design normal gross weight ratios greater than 1.0, whereas the military cargo and load lifter spend approximately 7% to 10% time in excess of 1.0 and the utility helicopter spends up to 60% time in excess of 1.0. If the gross weight frequency data obtained for the CH-47A, UH-1B, and CH-54A helicopters were compared to the maximum allowable gross weight instead of to the design normal gross weight, further trends could be developed. The maximum allowable gross weights obtained from pilots' handbooks or operators' manuals for the CH-47A, UH-1B, and CH-54A are 33,000, 8500, and 42,000 pounds, respectively, which result in maximum allowable gross weight/design normal gross weight ratios of 1.16, 1.29, and 1.10, respectively. When these ratios are plotted on Figures 13 and 14, it can be seen that the time spent at gross weights in excess of the maximum allowable gross weight is approximately 0.5% for the CH-47A, 0.1% for the UH-1B, and 4.7% for the CH-54A. The relatively large percentage of time spent above the maximum allowable gross weight experienced by the CH-54A is, as explained in Reference 3, due to flights flown to demonstrate the load-lifting capabilities of this helicopter and therefore may not be representative of operational-type mission assignments.

Figure 14 presents the cumulative gross weight frequency distribution by mission segment for the CH-47A, UH-1B, and CH-54A helicopters. The upper curves labeled "Total" are based on the same data that are presented in Figure 13 for these three helicopters and are also equal to the summation of the ascent, maneuver, descent, and steady-state mission

segment curves shown in Figures 14a, 14b, and 14c. In general, trends in one mission segment result in similar trends in the other three segments which are also reflected in the totals. Slight variations from this general rule are noted in the data obtained for these three helicopters, but the significance of these variations cannot be ascertained without supplementary information. It does appear, however, that the steady-state mission segment experiences proportionately more time at the higher gross weight levels than the ascent, maneuver, or descent segments.

## RATE OF CLIMB

### DATA REDUCTION

Available rate-of-climb data presented as frequency tables and/or histograms for the helicopters listed in References 1 through 12 were converted to cumulative rate-of-climb frequency distributions in a manner somewhat similar to that shown in Figure 7. By starting at the fastest rates of climb, the percentages of time for each rate-of-climb increment were cumulatively summed and plotted at the proper rate-of-climb value. This procedure was repeated for the rate-of-descent data, starting with the fastest rate of descent (highest negative rate of climb). It should be noted that cumulative distribution curves such as those that start cumulatively summing at the high values are called "or more" curves compared to the "or less" type defined in Figure 7. Thus, when the rates of climb or descent corresponding to a given cumulative percent time are read, it is stated, for example, that 70% of the total time is spent at a rate of climb of 1000 feet per minute or more. As shown previously in this report, the total percentage of time spent in the positive rate-of-climb category is equal to the time spent in the climb portion of the mission segment breakdown, and the total percentage of time spent in the rate-of-descent (or negative rate of climb) category is equal to the descent portion of the mission segment breakdown. The summation of the time spent in the rate-of-climb and rate-of-descent categories plus the percentage of time spent in the enroute segment accounts for 100% of the total time. Percentage of time values for the climb, enroute, and descent mission segments of each helicopter considered may be found in Table II.

The cumulative rate-of-climb frequency distributions obtained for each helicopter were segregated into the following three helicopter classes, which are dependent on the design normal gross weight and the type of power plant installed:

1. Reciprocating engine-powered helicopters having a design normal gross weight of less than 12,000 pounds.
2. Turbine-powered helicopters having a design normal gross weight of less than 10,000 pounds.
3. Turbine-powered helicopters having a design normal gross weight of greater than 15,000 pounds.

After the  $\pm 1\sigma$  scatter band limits for the rate-of-climb and rate-of-descent data of each class were established by statistical analysis, the resulting scatter band curves and data points were plotted in Figure 15.

To be of further aid in establishing basic trends and relative rate-of-climb characteristics, the  $\pm 1\sigma$  scatter band curves presented in Figure 15 are repeated in Figure 16 as a composite for the three classes of helicopters being considered.

A comparison of the cumulative rate-of-climb and rate-of-descent frequency distribution curves for the CH-47A, UH-1B, and CH-54A helicopters, References 1, 2, and 3, is also shown in Figure 17.

#### SUMMARY

Figure 15a presents the cumulative rate-of-climb and-descent frequency distribution  $\pm 1\sigma$  scatter band curves and data points for reciprocating engine-powered helicopters having a design normal gross weight of less than 12,000 pounds. The portions of the rate-of-climb and-descent curves above 2% cumulative time are fairly similar, with possibly slightly higher rates of descent being experienced. Below the 2% cumulative time, there is a general trend of rates of descent being higher than rates of climb for equal cumulative percentage of time values.

The increased scatter of data points at the lower values of cumulative percentage of time could possibly be associated with the types of mission flown, the weight/power ratios, or the limited data available in this range. Noting that the rate-of-climb and-descent data obtained for the H-13 high-altitude helicopter are concentrated over a relatively narrow band varying between a rate of descent of -1000 feet per minute to a rate of climb of +1000 feet per minute, it is conjectured that this may be the result of power limitations during climbs and blade stall or power recovery considerations during descent at the higher altitudes. Data for the H-25 utility helicopter, on the other hand, are spread over a wide band varying between a rate of descent of -3000 feet per minute to a rate of climb of +1000 feet per minute. As this ship has the highest weight/power ratio of the four helicopters considered, its ability to climb at the higher rates should be more limited than that of the other three ships. This is not the case, however, as the data show that the H-25 spends as much time at the higher rate of climb as does the H-34 IFR trainer, which has the lowest weight/power ratio of the four. It is thus considered that the type of mission flown is the controlling factor that

accounts for the apparent scatter. As also noted in the data for the H-25, the maximum rate of descent experienced is almost twice the maximum rate of climb experienced. This trend is thought to be associated with rates of climb being limited by the available power, whereas factors such as rotor blade stall, controllability, or structural considerations limit the rate of descent. This trend is also noted for the H-13 high-altitude helicopter and the S-55 airmail helicopter. The reverse is true, however, for the H-34 IFR trainer. At cumulative time values in excess of 1% where there are comparable data for both rates of climb and descent, higher rates of climb are experienced than are rates of descent. This may be explained by considering the nature of an IFR training flight. If it is assumed that, with the exception of takeoffs and landings, all flight time is spent flying blind, then higher rates of climb would be expected due to the lack of obstructions overhead during climbs. Descents, on the other hand, would be performed more cautiously, particularly at lower altitudes or over varying terrain.

Figure 15b presents the cumulative rate-of-climb and-descent frequency data for five turbine-powered helicopters having a design normal gross weight of less than 10,000 pounds. When the  $\pm 1\sigma$  scatter band curves for climb and descent are compared, it is noted that both sets of curves are quite uniform and that, in general, slightly higher rates are experienced during descent than are experienced during climb. The uniformity of the data obtained for the three observation helicopters is to be expected, as they are fairly similar in design and in the type of missions flown at the time that the data were recorded. Data for the UH-1B utility helicopter agree quite well with those for the three observation helicopters, although there is a trend for the UH-1B to experience slightly higher rates of climb and descent above 10% cumulative time. The YH-40 experimental helicopter experiences higher rates of climb and descent than do the other four ships throughout the full range. This tendency is considered to be associated with the nature of experimental-type flights, where the capabilities and handling characteristics of a helicopter are being evaluated in relation to the assigned mission. It would be expected that a considerable amount of time would be spent at or possibly beyond the extremities of the flight envelope to assess these qualities.

Figure 15c presents the cumulative rate-of-climb and frequency distribution curves for five turbine-powered helicopters having a design normal gross weight greater than 15,000 pounds. A comparison of the  $\pm 1\sigma$  scatter band

curves shows that there is more variability in the climb data than there is in the descent data, with slightly higher rates of climb being experienced. Higher rates of climb are encountered by the tandem-rotor V-107-II civil transport than are experienced by the other four helicopters, with slightly lower rates of climb being experienced by the single-rotor S61N civil transport. The data for the CH-54A load lifter obtained from Reference 10 are in the middle of the scatter band, and the data for the CH-47A obtained from Reference 3 are at the inner scatter band limits. The trend for rate-of-descent data is similar to that for the rate-of-climb data, with the exception that the CH-54A data obtained from Reference 10 are at the outer scatter band limits at cumulative times lower than 0.5%. It is of interest to note that the data for the tandem-rotor H-25 utility helicopter presented in Figure 15a and the data for the tandem-rotor V-107-II civil transport presented in Figure 15c exhibit the same characteristic of being at the outer limits for both the rate-of-climb and the rate-of-descent scatter bands, though it is conjectured that this is due to the characteristics of the basic missions flown and the operational procedures, rather than any differences between single-rotor and tandem-rotor helicopters.

Data for the CH-47A appear to be modified somewhat from the general trends established by the scatter band curves. The CH-47A curves for both rate of climb and descent have steeper slopes, signifying that the ranges of values experienced are narrower than those for the other ships.

A composite for the three classes of helicopters considered in Figure 15 is shown in Figure 16. Rate-of-climb data for the two classes of turbine-powered helicopters are in close agreement throughout the full rate-of-climb range, showing no appreciable trends with gross weight or power available. Rate-of-climb data for the reciprocating engine-powered helicopter show a great deal of variability at cumulative times less than 1%. At cumulative times in excess of 2%, the scatter bands for the three classes are approximately the same.

Rate-of-descent data show that, in general, the lighter turbine-powered helicopters experience slightly higher rates of descent than do the heavier turbine-powered helicopters. Data for the light reciprocating engine-powered helicopters above 1% cumulative time are quite similar to those for lighter turbine-powered helicopters. Below 1% cumulative time, the scatter band increases in a manner somewhat similar to that experienced for rate-of-climb data.

Cumulative rate-of-climb and-descent frequency distribution curves for the CH-47A, UH-1B, and CH-54A helicopters (References 1, 2, and 3) are presented in Figure 17. Rate-of-climb data for these three helicopters are surprisingly similar, considering the differences in gross weight and types of missions each performs.

Data for the CH-47A and UH-1B reflect similar rate-of-descent trends. Rate-of-descent data for the CH-54A load lifter, while quite similar to those for the CH-47A and UH-1B, signify that this maneuver is performed with more caution than is used for the other two, perhaps due to the fact that external sling loads are frequently present.

## NORMAL LOAD FACTORS

### DATA REDUCTION

The frequency of occurrence of normal acceleration or load factor peaks for the helicopters reported in References 1 through 12 is, in general, presented in the form of single-variable or bivariate frequency tables or may be plotted in the form of cumulative frequency distribution curves called exceedance curves. The abscissa of these exceedance curves is expressed either as the normal load factor  $n_z$  or as the incremental load factor  $\Delta n_z$  defined as:

$$\Delta n_z = n_z - 1$$

Ordinates of the exceedance curves are defined in several ways:

1. Hours to reach or to exceed  $n_z$  or  $\Delta n_z$ .
2. Frequency of load factor peaks per 100 hours.
3. Frequency of load factor peaks per 1000 hours.
4. Average number of flights to reach or exceed  $n_z$  or  $\Delta n_z$ .

Comparison of these data could not be accomplished without first establishing a common base. To this end, the incremental load factor  $\Delta n_z$  was selected as the abscissa, and the frequency of cumulative load factor peaks per 1000 hours was selected as the ordinate. Cumulative load factor peaks per 1000 hours were obtained by cumulatively summing the occurrences of load factor peaks starting with the largest positive and the largest negative load factor peaks reported, and then converting these cumulative occurrence values to cumulative peaks per 1000 hours by the use of the appropriate increment of time during which these occurrences were noted. The applicable data obtained from the tables of References 1 through 12 were converted to this standardized form and were used consistently in Figures 18 through 27.

The dispersion of data points about the mean of the data was analyzed statistically to determine the width of the scatter band corresponding to a variation of plus and minus one standard deviation. This was accomplished by obtaining

values of  $\Delta n_z$  at a common frequency level for each applicable helicopter, plotting these data on log-probability paper using median ranks to obtain the abscissa, establishing the best-fit line passing through the data points by the method of least squares, and calculating the values of  $\Delta n_z$  corresponding to 84.13% probability (plus one standard deviation) and 15.87% probability (minus one standard deviation). This process was repeated at a sufficient number of frequency levels to insure that a representative scatter band curve could be presented.

The total normal load factor experience is presented in Figures 18a, b, and c. Three general helicopter classifications that are dependent upon the design normal gross weight of the helicopter and upon the type of propulsion system installed are:

1. Reciprocating engine-powered helicopters having a design normal gross weight of less than 12,000 pounds (Figure 18a).
2. Turbine-powered helicopters having a design normal gross weight of less than 10,000 pounds (Figure 18b).
3. Turbine-powered helicopters having a design normal gross weight of greater than 15,000 pounds (Figure 18c).

Statistical methods, previously described, were used to establish the width of the scatter band corresponding to a variation of plus and minus one standard deviation from the mean. The resulting scatter band curves for the three groups of helicopters are presented as a composite in Figure 19 to aid in establishing total load factor experience trends.

Comparing the variation of load factor experience with mission segments is complicated by the differences in mission segment definitions used in References 1 through 12, as previously discussed in the mission segment portion of this report. Although it was feasible to reduce all mission segment data to a common base by using the three-segment-mission criterion, the load-factor/mission-segment data could not be reduced in a similar manner due to the absence of data relating load factor to rate of climb. Because of this, the load-factor/mission-segment data were divided into two groups:

1. Load-factor/mission-segment data based on the three-segment criterion, where the total data are divided

into climb, enroute, and descent mission segments.

2. Load-factor/mission-segment data based on the four-mission-segment criterion, References 1, 2, and 3, where the total data are divided into ascent, maneuver, descent, and steady-state segments.

The combined load-factor/mission-segment experienced, based on the three-segment mission definitions for reciprocating engine-powered helicopters having a design normal gross weight of less than 12,000 pounds, is shown in Figures 20a, b, and c for the climb, enroute, and descent segments, respectively. Scatter bands corresponding to a variation of plus and minus one standard deviation from the mean, shown in these figures, are also shown in Figure 21, which is presented as a composite summary of this mission segment category. Similarly, the combined load-factor/mission-segment experience based on the three-mission-segment criterion for turbine-powered helicopters having a design normal gross weight of less than 10,000 pounds is shown in Figures 22a, b, and c for the climb, enroute, and descent segments, respectively. Scatter band curves shown in the figures are also presented in Figure 23 as the composite summary for this category. Data for the large turbine-powered helicopters were generally in the four-segment-mission format and could be compared only to data of that type.

Load-factor/mission-segment data based on the four-segment-mission criterion, References 1, 2, and 3, are presented in Figures 24, 25a, b, c, and d for the total, ascent, maneuver, descent, and steady-state segments, respectively. Since these data are limited to three helicopters of different weight categories (CH-47A, UH-1B, and CH-54A), statistical analysis was not attempted. However, comparisons for these three helicopters as they are used in the Army environment are presented.

References 1, 2, 3, and 11 distinguish between maneuver- and gust-induced normal load factors. These data for the CH-47A, UH-1B, CH-54A, and S61N helicopters are presented in Figures 26a, 26b, and 27. Figure 26a shows the experience for maneuver-induced normal load factors, and Figure 26b shows the experience for gust-induced normal load factors. Curves showing variation of the data from the mean for plus and minus one standard deviation are also presented. Figure 27 shows these scatter band curves for both maneuver- and gust-induced normal load factors for comparison purposes.

## SUMMARY

Various maneuvers and gusts which produce normal accelerations or load factors can play an important role in setting the static strength requirements and in evaluating the fatigue life of helicopter components. Loads corresponding to the design limit maneuvers will rarely, if ever, be encountered in the service life of a helicopter model; however, these loads will generally form the basis for the design static strength, the stress analysis, and the static test substantiation. Loads produced in maneuvers of less severity will be encountered more frequently and, though they may not pose a threat to the static strength of the aircraft, they may well be very important in establishing the fatigue life of critical rotor components. In a well-designed helicopter, little if any fatigue damage will be accrued in level flight or in any steady-state flight regime. The mild maneuvers which produce vibratory loads that exceed component endurance limits even by a small amount are of primary importance in the determination of component fatigue lives. To establish the frequency of occurrence of these loads, surveys have been conducted for many different helicopters with varying results.

As might be expected, the occurrence of load factors for a particular helicopter model is related to the ability of that model to achieve increased load factors. This, in turn, is related to design parameters, such as the capacity of the rotor to produce excess thrust, the control responsiveness, and the fuselage inertia. Study of the data from References 1 through 12 has revealed that plotting of all data on a single exceedance curve produces extremely wide scatter in results; however, certain logical groupings can be made which narrow the scatter significantly.

### Maneuver History by Helicopter Size Category

Figures 18a through 18c present all of the basic data divided into the three major groupings as previously described. From Figure 18a, which presents the data for reciprocating engine-powered helicopters having a design normal gross weight of less than 12,000 pounds, several basic observations can be made. The abscissa for all of these graphs is in terms of load factor increment as measured for 1.0 "g" level flight. It is, therefore, reasonable to expect that small increments, representing modest deviations from 1.0 g, will occur most frequently. As seen in Figure 18a, this is the case; in fact, the frequency of occurrence of modest increments is many times that for larger increments. The vertical scale of the graph is logarithmic for convenience in plotting and reading; however, this scale tends to disguise

the drastic variation that occurs with all such load factor data. Statistical analysis of the scatter has been carried out, and the solid lines on the plot represent  $\pm 1\sigma$  (one standard deviation from the mean) scatter bands. These bands should include 68% of all data, and it is therefore not surprising that some data points should fall outside of these limits.

Some interesting observations can be made in regard to the relative position of particular aircraft within the scatter bands. For instance, the H-13 military trainer generally falls on or near the upper bound of scatter, while the data for the Los Angeles airmail operation generally approximate the lower bound. This difference could be entirely due to the vast difference in types of flying that these two operations embrace. In the case of the military trainer, a majority of time is spent with a novice pilot at the controls while he is practicing the more intricate maneuver and control operations. Excessive control displacements and flight path corrections are expected. The airmail operation provides a decided contrast, since it involves routine flying over well-known routes by highly experienced pilots.

When the  $\pm 1\sigma$  bounds are used to approximate the maneuver experience for these two operations, it is seen from Figure 18a that a positive load factor increment of 0.6 g or greater will be experienced 1800 times in 1000 flight hours of military training, while the airmail operation will encounter this "g" level only 100 times in 1000 flight hours - a ratio of 18 to 1. Similarly, for a negative load factor increment of 0.6 g or greater (+ 0.4 g absolute load factor or less), Figure 18a shows that the military trainer will encounter increments of this magnitude 850 times in 1000 hours, while the airmail operation will encounter it only 70 times - a ratio of 12 to 1. Differences of this magnitude will have a pronounced effect on fatigue life of the helicopter components. In the case of a component which accrues fatigue damage only in maneuvers, component life will vary directly as the occurrence of maneuvers and is, therefore, seen to be highly sensitive. If the variation in occurrence shown in this example is due to mission assignment alone, then a component whose fatigue life is determined by maneuver loadings will accrue fatigue damage approximately 12 to 18 times faster in a military training assignment than it would in airmail usage. If a single retirement life is assigned, regardless of mission, then the airmail operation must suffer a substantial penalty in usable component life. The fact that the data for the airmail and military training operations were gathered on two different helicopters in different locales means that other factors, such as design parameters and local atmospheric conditions, may have contributed to the apparently vast difference.

Additional information of this general type could be gathered by surveying two different helicopters employed in identical missions and flight conditions, and by surveying a particular helicopter model as it is used in two significantly different missions. Numerical results from such studies could be viewed with more confidence regarding the source of any resulting difference. Some data of this type are included in Figure 18a, as there are three surveys on the H-13 and two on the H-34 aircraft included here; however, detailed variations of the helicopter models did occur between these surveys. It is still interesting to note that the H-13 data generally fall in the upper half of the scatter band, while the H-34 data tend toward the lower bound. It would seem justified to conclude that basic design parameters for these two aircraft have played a role in the relative position of their load factor spectrum.

In Figures 18b and 18c, which present load factor data for turbine-powered helicopters with a design normal gross weight of less than 10,000 pounds and turbine-powered helicopters with a design normal gross weight of greater than 15,000 pounds, respectively, it is noted that a clear trend appears. For each succeeding category, the boundaries of the load factor spectrum are generally lower; that is, turbine-powered helicopters appear to encounter fewer load factor peaks than do reciprocating-engine helicopters of similar weight. Also, the high gross weight turbine machines encounter significantly fewer load factor peaks than do the smaller helicopters with similar power plants. A composite plot showing the relative position of the scatter bands for all three categories is presented in Figure 19. Here it is seen that although there is considerable overlap, substantial trends are established. Proper design consideration should recognize these differences, allow for them in the fatigue criteria, and take advantage of them where it is possible to do so.

A more detailed study of Figure 18b shows that all of the data are for Army helicopters: three light observation machines and two versions of the basic utility helicopter. An outstanding feature of this plot is the very narrow scatter bands that result. It is probable that this is largely attributable to the fact that these aircraft were designed and flown under very similar requirements and conditions. This fact makes it very difficult to identify trends in the data. It is undoubtedly true that certain specific missions for these same aircraft could produce load factor experience which would fall entirely outside of these narrow scatter bands. It is also possible that a new helicopter, in this basic category but designed to different requirements, would have a load factor spectrum which differed significantly from that shown. Such

new bounds could be approximated from the present data by using a bandwidth of  $\pm 2\sigma$  or  $\pm 3\sigma$ , depending upon the degree of deviation anticipated.

Figure 18c presents the load factor experience for large turbine-powered helicopters covering a fairly broad range of gross weights and mission assignments. In this plot the  $\pm 1\sigma$  scatter bands are quite broad, as would be expected for the variety of aircraft and missions that are included. As mentioned previously, this category produces the lowest occurrence of load factor peaks of those categories studied. It is interesting to note that the upper and lower bounds are very nearly defined by the two civil transports, with the military utility and load-lifting missions generally filling in the center of the bands.

While the two civil transports provide basically the same type of service, their operations are conducted in different locales and under somewhat different conditions. However, a more significant difference probably lies in the basic aircraft configuration, since one is a tandem-rotor configuration while the other is a single main and tail rotor configuration. Other factors would tend toward similarity, and so it must be concluded that the vast difference in load factor experience for the two civil transports is due to geographic location and to design parameters, with the proportion that each contributes undetermined.

The CH-47A and CH-54A military helicopters provide primarily a cargo and load-lifting function. On occasion, they perform other utility missions. These aircraft often fly at very heavy weights and, as a result, do very little maneuvering that would produce significant load factors. In the case of the CH-54A, the heavy load is usually represented as an external sling load, which creates substantial aerodynamic drag and which has a pendular degree of freedom, thereby further inhibiting maneuvers. Two separate studies of the CH-54A load factor experience are included in Figure 18c. Although the results of these studies are in reasonably good agreement, the earlier, less extensive data did produce two positive load factor points which are well above the  $\pm 1\sigma$  boundary. While these points appear to be unrelated to the bulk of the basic data, it is quite probable that in early fleet introduction, during the course of development of piloting techniques with external load, the vertical load factors will reach unexpectedly high values. It is therefore considered that the later survey, reported in Reference 3, will much more accurately represent the total fleet experience for this aircraft. It will be noted in Figure 18c that the CH-47A and the CH-54A have nearly identical load factor experience.

Since these two aircraft again present the configuration difference of tandem rotors versus single main rotor, it would appear that this fact alone is not enough to cause differences in load factor spectrum.

#### Maneuver History by Mission Segment

Figures 20a, b, and c and 22a, b, and c present the vertical load factor experience for the lightweight reciprocating and turbine-powered helicopters, respectively. These plots are divided according to the three-segment-mission definitions, climb, enroute, and descent. The solid lines drawn on the plots represent the scatter band width of plus and minus one standard deviation, so that approximately 68% of all data points should fall within these bounds. A review of these figures and of the summary plots, Figures 21 and 23, reveals that no substantial difference in load factor experience is encountered during the climb and enroute segments, but that significantly more load factor peaks, both positive and negative, are encountered during the descent mission segment. It is seen that the H-13 military trainer has experienced an outstanding number of load factor peaks. The fact that the most severe experience occurs in the descent segment is undoubtedly due to the fact that the pilot has a close visual reference to the ground and is approaching other potential obstacles. In the case of pilot training, one can readily recognize the probability of excessive control inputs and corrections which would result in frequent and severe load factor peaks.

Much of the most recent and voluminous data on helicopter load factor spectrums has been recorded using the four-segment mission definitions, ascent, steady-state, descent, and maneuver. The addition of a specific maneuver segment, wherein the control stick displacements are used to differentiate from other mission segments, permits a finer and more useful breakdown of data. References 1, 2, and 3 are the primary sources of these data which cover the UH-1B, CH-47A, and CH-54A. The total load factor experience for these three aircraft is presented in Figure 24. It is seen that the two large cargo machines experience nearly identical load factor spectrums and that the smaller, more maneuverable UH-1B encounters all levels of load factor increment more frequently. Figures 25a, b, c, and d present the load factor experience for these helicopters according to the mission segment in which it is encountered. Review of these figures shows that the UH-1B load factor spectrum is the most severe in all four mission segments and that the CH-54A spectrum is slightly greater than that of the CH-47A in all but the steady-state segment. Since the data were limited to three aircraft, a statistical reduction of data was not attempted.

The descent segment of flight is seen to contribute a substantial number of load factor peaks; in fact, it competes with the specific maneuver segment for the highest levels and frequencies. The UH-1B, for instance, experiences the higher negative load factor increments more frequently in the descent segment than in the maneuver segment, although positive load factors are encountered more frequently in the maneuver segment. For the cargo aircraft, the differences are less clear but favor higher occurrences in the maneuver segment.

Due to their great depth and additional detail, the data of References 1, 2, and 3 are considered to provide a substantial demonstration of the basic trend of helicopter load factor experience with aircraft size and maneuverability. These same references contain a further analysis of the source of the load factors. Study of the traces prior to and during load factor variations permits a judgment to be made as to whether the load factor increment was pilot induced or due to an external source, considered to be atmospheric turbulence. Those instances which are accompanied by control stick displacement are considered to be intentional pilot-induced maneuvers, while load factor increments in the presence of relatively constant stick position are considered to be the result of gusts. Figures 26a and 26b present the exceedance curves for maneuvers and gusts, respectively. Comparison of these two figures reveals that the maneuver-induced load factors are considerably more significant in terms of magnitude and occurrence than those due to gusts. Solid lines drawn on the figures represent a bandwidth of plus and minus one standard deviation, and it is seen that the scatter due to maneuvers is much broader than that attributable to gusts. The differences in size and maneuverability appear to be an important factor in the maneuver-induced load factors; however, no clear trend occurs for those induced by gusts. The gust response of helicopters is a function of basic design parameters, and it would appear that no substantial difference in this characteristic was present for the four aircraft surveyed. In general, these data would lead to the conclusion that gust-induced load factors are of far less significance in helicopters than are those induced by maneuvers. The relative frequencies are shown on Figure 27, where the scatter bands of the two prior figures are reproduced.

## ESTABLISHING A FLIGHT SPECTRUM

In the design and fatigue substantiation of a new helicopter model, one of the steps that must be accomplished is the establishment of a representative schedule of flight operation. More than one such schedule may be required to evaluate various parts of the helicopter conservatively. The best schedule to use for a given area or component will usually be derived only after preliminary calculations have indicated the critical portions of the flight envelope from the point of view of fatigue damage. Typically, it will be operation at high gross weight, high airspeeds, and maneuvering flight that will be most influential in producing fatigue damage, though some components will also be critical in rapid climb, descent, hover turns, and other specific flight regimes.

By starting with a knowledge of the general size, maneuverability, and mission for a new helicopter, a projected flight spectrum is usually established using either contractor experience with the helicopter type or some published schedule. Data presented in this report may also be used as will be described. During the early phases on a new model, an arbitrarily chosen schedule will be used with available loads and strength data to estimate component fatigue life and to ascertain any need for changes or redesign. In this early stage, the strength and load data will be largely analytical but will be replaced by experimental data as rapidly as they become available. The final and most accurate component fatigue lives will be based on in-flight-measured loads obtained for the entire flight regime, on fatigue test results establishing the fatigue strength of the components, and on a flight spectrum obtained from in-flight data after the utilization of the helicopter has been well defined. The fact that substantial scatter in fatigue strength will be present is widely recognized and almost universally accounted for; however, a similar scatter that occurs in loads and in flight spectrum is often ignored. The scatter that occurs in vibratory flight loads for a specific flight condition can and should be handled statistically, as is the scatter in strength. Plots presented in this report can be used to establish a flight spectrum for helicopters of various types with some statistical background for the choice.

The parameters that are usually of significance in the flight time distribution for a helicopter are the various mission segments, gross weights, airspeeds, rates of climb or descent, and load factors. To illustrate the use of these plots, let us assume the case of a main rotor blade that has been shown by preliminary fatigue life calculations to be critical in

the production of fatigue damage during operation at high gross weight, at high airspeed, and in maneuvers. The mission assignment for the helicopter will be considered to be a standard military utility mission, with no known heavy utilization in any specific flight regime. When the mission segments enroute, ascent, and descent are considered, it would appear that the critical segment would be enroute, since fatigue damage occurs in high-speed level flight with no substantial contribution from the other segments. If the example helicopter has a design gross weight/usable power ratio of 7.0, an enroute time, read from the upper scatter band of Figure 4, would be 76%, leaving 24% to be divided about equally between the less critical ascent and descent segments, with perhaps slightly more time allotted for descent than for ascent. Since all of the scatter bands presented in this report represent  $\pm 1\sigma$  from the mean, it may be interpreted that approximately 84% of all similar helicopters will spend less than 76% of total flight time in the enroute segment. Further allowance could of course be made by choosing enroute time in excess of the upper scatter band with a corresponding improvement in probability, and in that case less time would remain for the other two mission segments. Operation at high gross weight is also critical, and Figure 13 can be used as a guide to the choice of a gross weight schedule. Data of this nature were not available for all classes of machines. However, Figure 13 presents scatter bands for the large turbine-powered helicopter. The discrepancy that appears in that figure between the UH-1B and the other helicopter is considered to be due to the large difference between the design normal gross weight and the maximum allowable gross weight of the UH-1B, thus permitting a substantial amount of operation above the design normal gross weight. When it is assumed that our example helicopter will have only modest overload allowance, the scatter band for the majority of helicopters in Figure 13 is considered to apply. When the boundary on the right is used, it is seen that approximately 10% of the time may be spent above the design gross weight and that 27% of all flight time may be spent at weights above 90% of the design gross and 60% of the time at weights above 80% of design gross. The schedule of gross weights could then be constructed by allowing 10% of all time at weights between design normal gross weight and maximum allowable gross weight, 17% of the time at weight between 90 and 100% of design gross weight, 33% of the time between 80 and 90% of design normal gross weight, and the remaining time at low gross weights. In establishing such a schedule, the minimum flight weight and the maximum allowable gross weight should, of course, be taken into account. Some allowance should be made for flight at weights higher than those officially permitted,

as evidenced by some of the data in this report.

For illustration purposes in the practical use of some curves developed in this report, assume the imaginary helicopter to be turbine-powered and to have a design normal gross weight of less than 10,000 pounds. The airspeed spectrum for this class vehicle can be gleaned from Figure 9a. The right-hand boundary of the cross-hatched area represents the  $+1\sigma$  cumulative airspeed line for this aircraft category. It is seen that approximately 3% of the flight time can be expected at airspeeds above  $V_A$ . Such an allowance is not at all unrealistic, particularly if the helicopter has the capability to reach level flight airspeeds beyond the selected limit. Approximately 17% of the time will occur between 90 and 100%  $V_A$ , and 63% of all flight time could be expected to be spent at airspeeds between 60 and 90%  $V_A$ . For the example utility helicopter, such an airspeed distribution may be modestly conservative. However, for some mission assignments it could be unnecessarily severe. If, for instance, the same basic type helicopter were being designed for Navy plane guard duty, it could be expected that the vast majority of flight time would be spent at airspeeds in the neighborhood of 50%  $V_A$  and that there would be much less utilization of the range between 75 and 100%  $V_A$ . However, even in that case, it would be proper to make an allowance for time above  $V_A$  for the occasional high-priority mission. When the boundary of Figure 9a or a similarly constructed line is used, it is possible to establish an airspeed spectrum with any desired number and width of increments by simply subtracting successive curve ordinates to obtain the percentage of time within a particular interval. The resulting airspeed spectrum will then account for 100% of the flight time.

In the example problem under consideration, rate of climb was shown by preliminary calculations to be noncritical and, therefore, is not specifically included in the spectrum for the main rotor blade.

However, vertical load factor is significant since it is associated with increased vibratory blade loads. Figure 19 includes the scatter band for this helicopter category and may be used in establishing a load factor spectrum. This could be accomplished by using the upper bound of the scatter band for turbine-powered machines with a design normal gross weight of less than 10,000 pounds, reading the ordinates at desired load factor increments and subtracting successive values to obtain the frequency within the interval. The number and size of intervals should be based upon the importance of this parameter in the production of

fatigue damage. If the new aircraft is designed to have maneuverability that is superior to that of the aircraft on which these past studies are based, it would then be proper to make upward adjustments of the load factor exceedance curve from that shown in Figure 19. In addition, since it is desirable that the flight spectrum recognize the complete permissible flight envelope, it would be prudent to select load factors up to the maximum allowed by the pilots' handbook. Figure 19 is based on the results of a number of surveys, most of which covered substantially less than 1000 hours. Had their duration been longer and the data reading covered all flight time, it seems apparent that load factor increments of higher magnitudes would have been recorded. The frequency of these higher values would decrease with magnitude and could probably be approximated by extrapolation of the Figure 19 curves to include the complete load factor range. The very low frequency of the extreme load factors may make them negligible in the final fatigue damage assessment. However, this is not always the case and should be investigated. If for a particular component the critical flight loadings occur during a specific mission segment, Figure 23 could be used to determine the load factor frequency. It should be recalled that this plot is based on 100% of flight time spent in each segment; therefore, actual time and frequency must be adjusted according to the mission segment breakdown for the aircraft under consideration.

The foregoing describes a means for establishing the flight spectrum for a selected component, the main rotor blade. This spectrum will not be the proper choice for all components of the aircraft. If, for example, the machine under consideration has a tail rotor, it is quite probable that the tail rotor blade will be critical in flight regimes that are not critical for the main rotor blade, such as high-power climb. In order that all important components be treated with a uniform level of conservatism, it is desirable that the tail rotor spectrum emphasize climb rather than enroute segments and that rate of climb be included as a parameter. Other components will be critical for other combinations of conditions and may require variations in the aircraft flight spectrum. The fact that a variety of schedules are considered to apply for one helicopter model is not unrealistic when one considers the variations in conditions, assignments, and techniques that will be encountered by a large fleet dispersed throughout the world. The fact that the people operating the aircraft are continually meeting and solving local problems by new applications of the aircraft makes it imperative that the most severe duty for each critical component be anticipated and fully accounted for in the fatigue substantiation.

## CONCLUSIONS

Based upon the analysis of data contained herein, it may be concluded that:

1. Helicopter flight spectrum is largely influenced by the assigned mission of the helicopter.
2. Certain logical groupings by weight and power permit the establishment of relatively narrow scatter bands for the occurrence of significant flight parameters.
3. The flight schedule of CAM-6, Appendix A, provides a reasonable flight spectrum for general utility helicopters, but it may be relatively inaccurate for special-purpose machines or unusual missions.
4. The reduced flight spectrum data provided in this report may be used as a guide in the establishment of a flight spectrum for the helicopter categories that are included herein.
5. Additional flight survey data of the type evaluated herein, particularly for different mission assignments, would increase the reliability of the conclusions reached in this report by broadening the statistical base.
6. Extrapolation of these data to predict the flight load spectrums for new mission assignments or for new aircraft types should be approached cautiously until a more thorough understanding of the problem is developed.

## RECOMMENDATIONS

The following recommendations are based upon a study of the data presented herein and the references noted:

1. All future flight spectrum studies should contain a concise listing of the aircraft characteristics and limitations which were applicable at the time of the survey. Items such as maximum gross weight, maximum airspeed (as affected by other parameters), installed power, usable power, structural or aerodynamic limitations, and any other factors having a possible bearing on the resulting flight loads spectrum should be included.
2. A consistent set of criteria and definitions should be adopted for all future surveys. That used in Reference 3 is recommended.
3. Surveys involving more than one aircraft of a particular type should present data for each individual aircraft, and careful definition of mission and assignment for each should be included.
4. Aircraft having more than one basic mission should be surveyed for each mission.

TABLE I. HELICOPTER CHARACTERISTICS

SYMBOL	HELICOPTER	ROTOR SYSTEM	POWER PLANT	TYPE OF OPERATION	DESIGN NORMAL GROSS WEIGHT (LB) (A)	VA (KT) (B)	USABLE POWER (HP) (C)	ROTOR DIA (FT)	ROTOR RPM (MAX)	REF (D)
□	CH-47A	Tandem	Twin Turbine	Cargo	28,500	130	4940	59	230	1
◇	UH-1B	Single	Turbine	Utility	6,600	120	1000	44	324	2
◇	CH-54A	Single	Twin Turbine	Load Lifting	38,000	115	6600	72	204	3
◇	UH-34D	Single	Reciprocating Eng	Utility	11,400	135	1400	56	248	4
◇	S-51	Single	Reciprocating Eng	L.A. Airmail	5,000	90	450	48	-	5
◇	H-13	Single	Reciprocating Eng	Chicago Airmail	2,350	77	200	35.2	345	6
◇	H-13	Single	Reciprocating Eng	Mil. Trainer	2,350	77	200	35.2	345	6
◇	H-25	Tandem	Reciprocating Eng	Utility	5,500	91	450	35	273	7
◇	S-55	Single	Reciprocating Eng	L.A. Airmail	6,700	104	600	53	200	7
◇	YH-40	Single	Turbine	Experimental	5,500	105	770	44	314	8
◇	H-34	Single	Reciprocating Eng	IFR Trainer	12,000	135	1400	56	248	8
◇	H-37	Single	Reciprocating Twin Engine	Load Lifting	30,000	120	3450	72	193	8
◇	H-13	Single	Reciprocating Eng	High Altitude	2,350	88	222	38.2	345	8
◇	H-13H	Single	Reciprocating Eng	Utility	2,350	88	222	35.2	345	9
◇	H-21C	Single	Reciprocating Eng	Utility	13,238	110	1425	44	278	9
◇	H-34A	Tandem	Reciprocating Eng	Utility	11,867	135	1400	56	248	9
◇	OH-4A	Single	Reciprocating Eng	Utility	2,570	115	250	35	314	10
◇	OH-5A	Single	Turbine	Observation	2,500	110	250	33.3	368	10
◇	OH-6A	Single	Turbine	Observation	2,100	128	250	26.3	469	10
◇	CH-54A	Twin Turbine	Twin Turbine	Load Lifting	38,000	115	6600	72	204	10
◇	S61N	Single	Twin Turbine	Civil Transport	19,000	131	2100	62	225	11
◇	V-107-II	Tandem	Twin Turbine	Civil Transport	19,000	130	2100	50	264	12

- (A) If gross weight spectrum data were not available for a helicopter, the gross weight at which other spectrum parameters were obtained was used.
- (B) Airspeeds listed are the attainable level flight velocities considering maximum available power, blade stall, and structural limitations, but they do not necessarily represent the speed potential of the aircraft.
- (C) Power values listed are either military power (30 minutes), transmission limited power, or normal rated power in the absence of other data.
- (D) Supplementary data not presented in these reference reports are obtained from other sources such as pilots' handbooks and flight manuals.

TABLE II. COMPARISON OF FLIGHT TIME AND MISSION SEGMENTS FOR SEVERAL HELICOPTERS

SYMBOL	HELICOPTER	ROTOR SYSTEM	POWER PLANT	TYPE OF OPERATION	TOTAL FLIGHT HOURS	NUMBER OF FLIGHTS	HOURS PER FLIGHT	ASCENT % TIME	ENROUTE* % TIME	DESCENT % TIME	REF
□	CH-47A	Tandem	Twin Turbine	Cargo	165	769	.21	16.0	63.5(c)	20.5	1
◇	UH-1B	Single	Turbine	Utility	219	758	.29	13.7	70.5(c)	15.9	2
△	CH-54A	Single	Twin Turbine	Load Lifting	110	409	.27	12.6	71.2(a)	16.2	3
□	UH-34D	Single	Recip Eng	Utility	37	20	1.90	18.0	62.0	20.0	4
□	S-51	Single	Recip Eng	L.A. Airmail	253	1691	.15	14.5	73.8(a)	11.7	5
□	H-13	Single	Recip Eng	Chicago Airmail	140	963	.15	14.0	77.0(a)	9.0	6
□	H-13	Single	Recip Eng	Mil. Trainer	162	1385	.12	17.9	62.6(a)	19.5	6
□	H-25	Tandem	Recip Eng	Utility	90	486	.18	13.5	75.7(a)	10.8	7
□	S-55	Single	Recip Eng	L.A. Airmail	320	1880	.17	17.0	71.0(a)	12.0	7
□	YH-40	Single	Turbine	Experimental	205	480	.43	18.8	59.4(a)	21.8	8
□	H-34	Single	Recip Eng	IFR Trainer	69	110	.63	12.5	75.9(a)	11.6	8
□	H-37	Single	Recip Eng	Load Lifting	35	58	.60	16.0	66.6(a)	17.4	8
□	H-13	Single	Recip Eng	High Altitude	50	165	.30	12.2	75.9(a)	11.9	8
□	H-21C	Single	Recip Eng	Utility	78						9
□	H-34A	Tandem	Recip Eng	Utility	117						9
□	OH-4A	Single	Recip Eng	Utility	180						9
□	OH-5A	Single	Turbine	Observation	982			10.0	78.0(a)	12.0	10
□	OH-6A	Single	Turbine	Observation	907	3064	.94	10.0	77.0(a)	13.0	10
□	CH-54A	Single	Turbine	Observation	981			9.0	78.0(a)	13.0	10
□	S61N	Single	Twin Turbine	Load Lifting	125	149	.84	11.0	74.0(a)	15.0	10
□	V-107-11	Single	Twin Turbine	Civil Transp	372	2782	.13	16.4	67.6(b)	16.0	11
□		Tandem	Twin Turbine	Civil Transp	316	2344	.14	14.4	71.0(b)	14.6	12

\* Enroute time is defined as the percent time spent between the following rates of climb:

- (a) ± 300 feet per minute
- (b) ± 400 feet per minute
- (c) ± 500 feet per minute



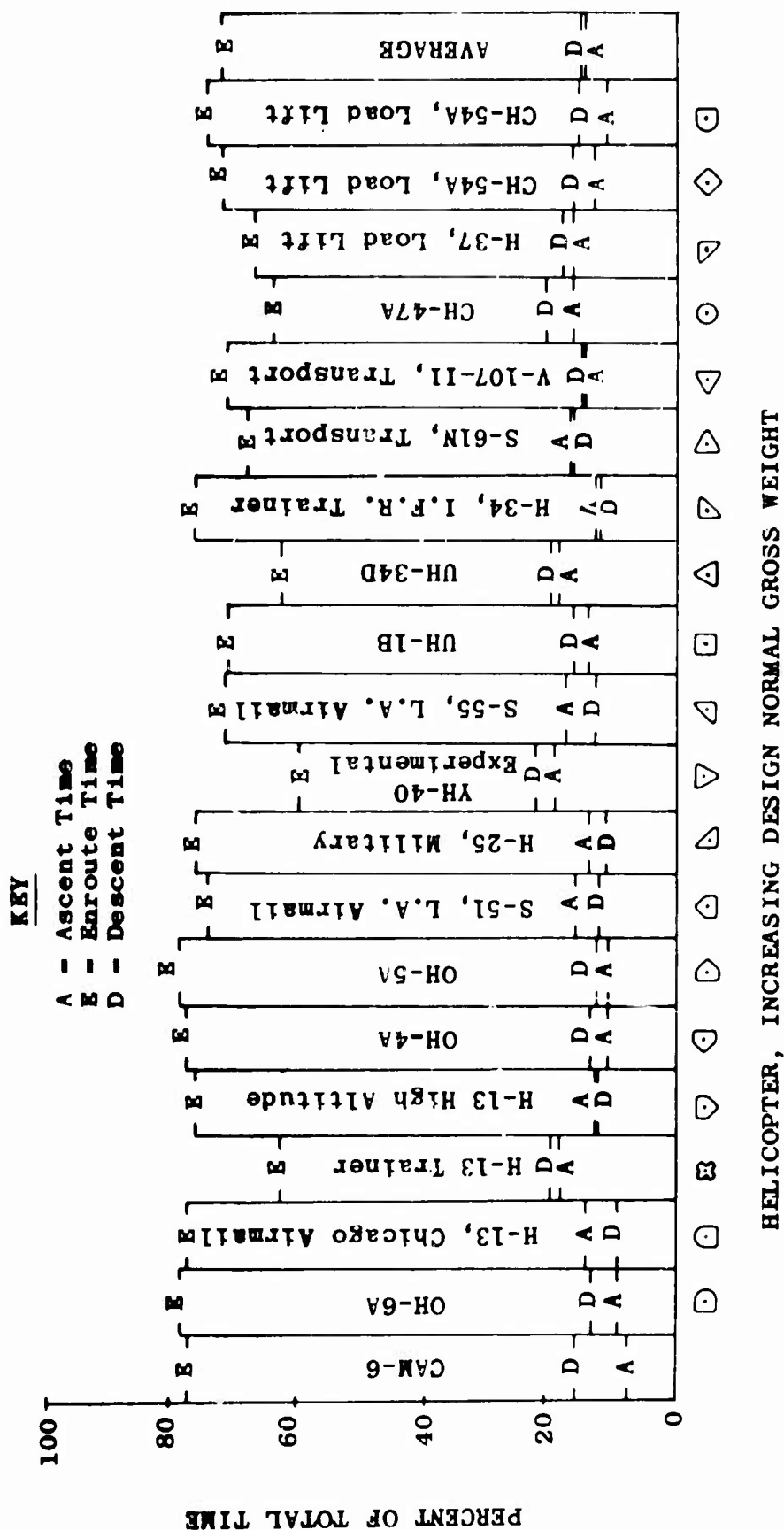


Figure 1. Percent of Total Time Spent in the Ascent, Enroute, and Descent Mission Segments for Several Helicopters.

KEY

S - Steady State  
M - Maneuver

A - Ascent  
E - Enroute  
D - Descent

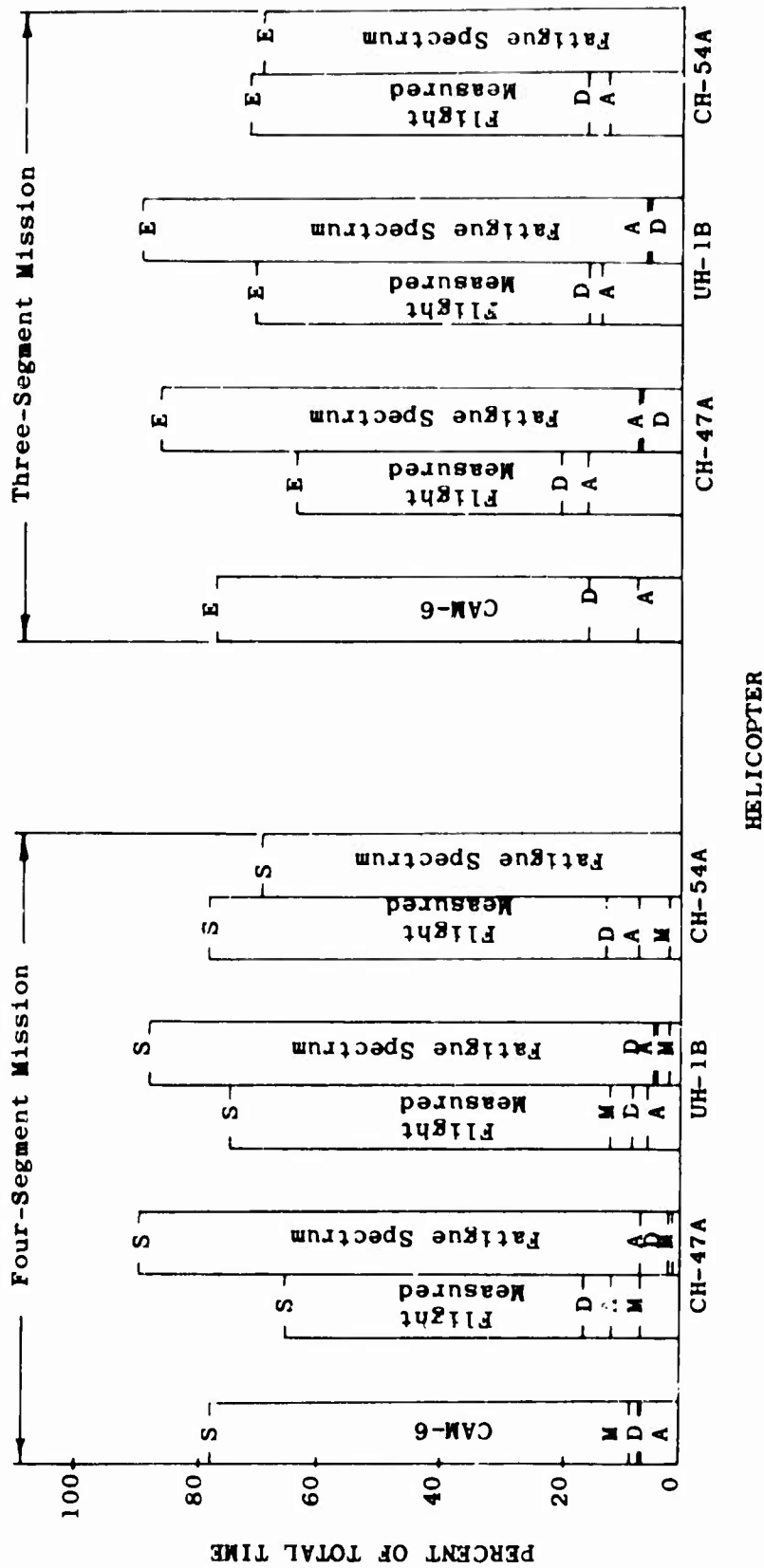


Figure 2. Percent of Total Time for the CH-47A, UH-1B, and CH-54A Helicopters Based on Two Different Mission Segment Breakdowns Including a Comparison of Flight-Measured Data with Fatigue and CAM-6 Spectrums.

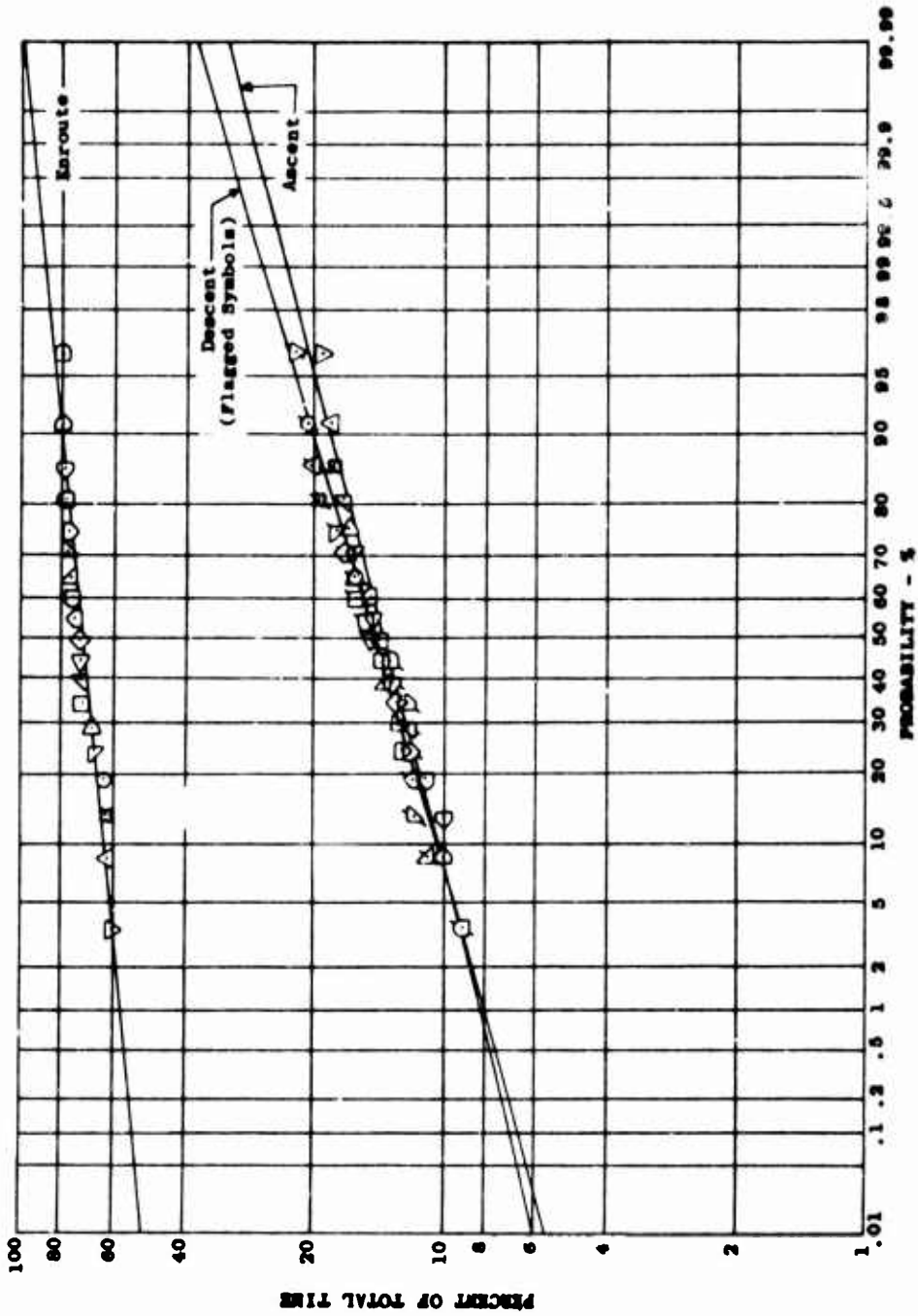


Figure 3. Mission Segment Probability Curves Based on Median Ranks - Three-Segment Breakdown. (See Table I for Symbol Definition).

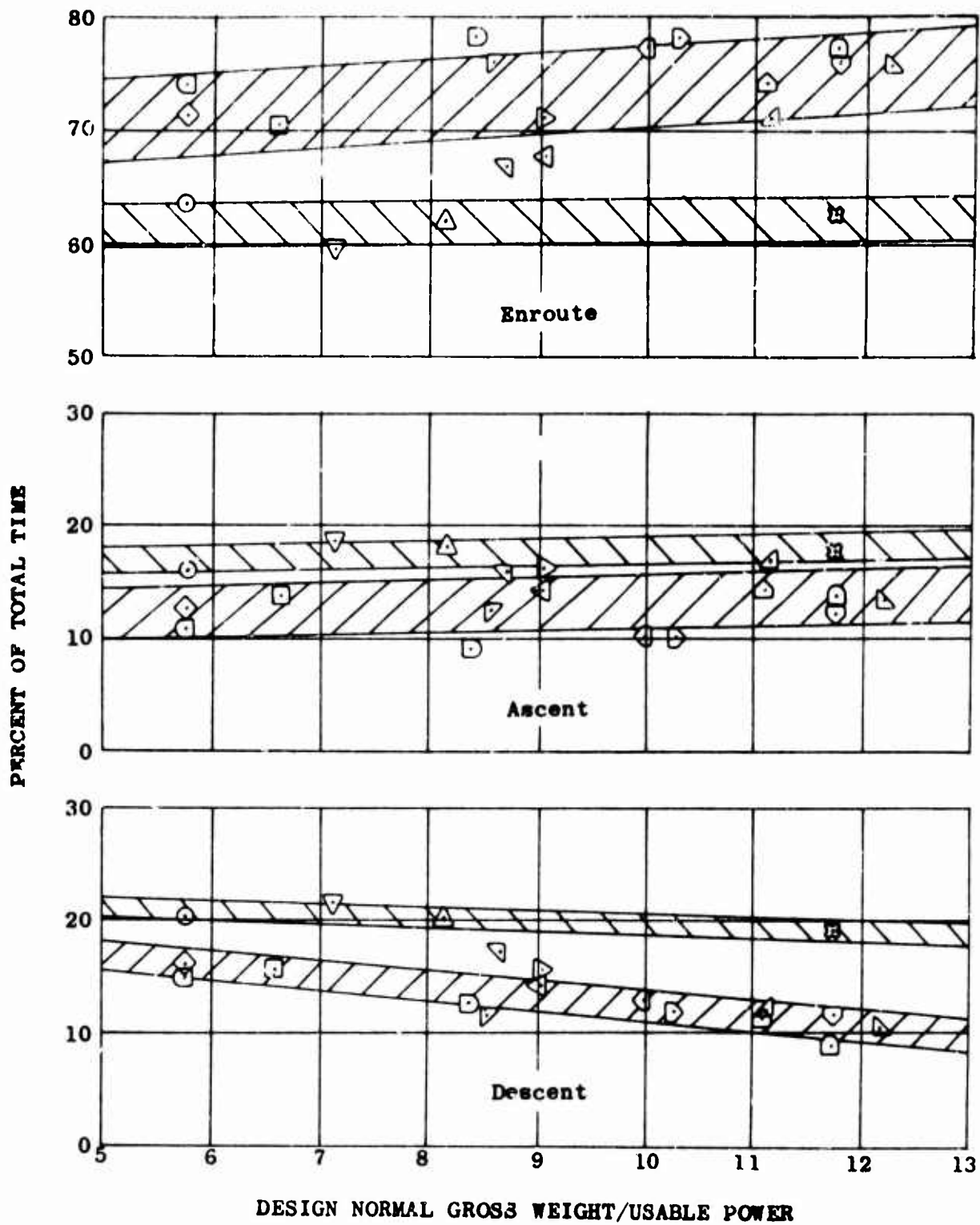


Figure 4. Percent Time Spent in Each Mission Segment for the Standard Mission  and for the Non-standard Mission . (See Table I for Symbol Definition). Scatter band width =  $\pm 1\sigma$ .

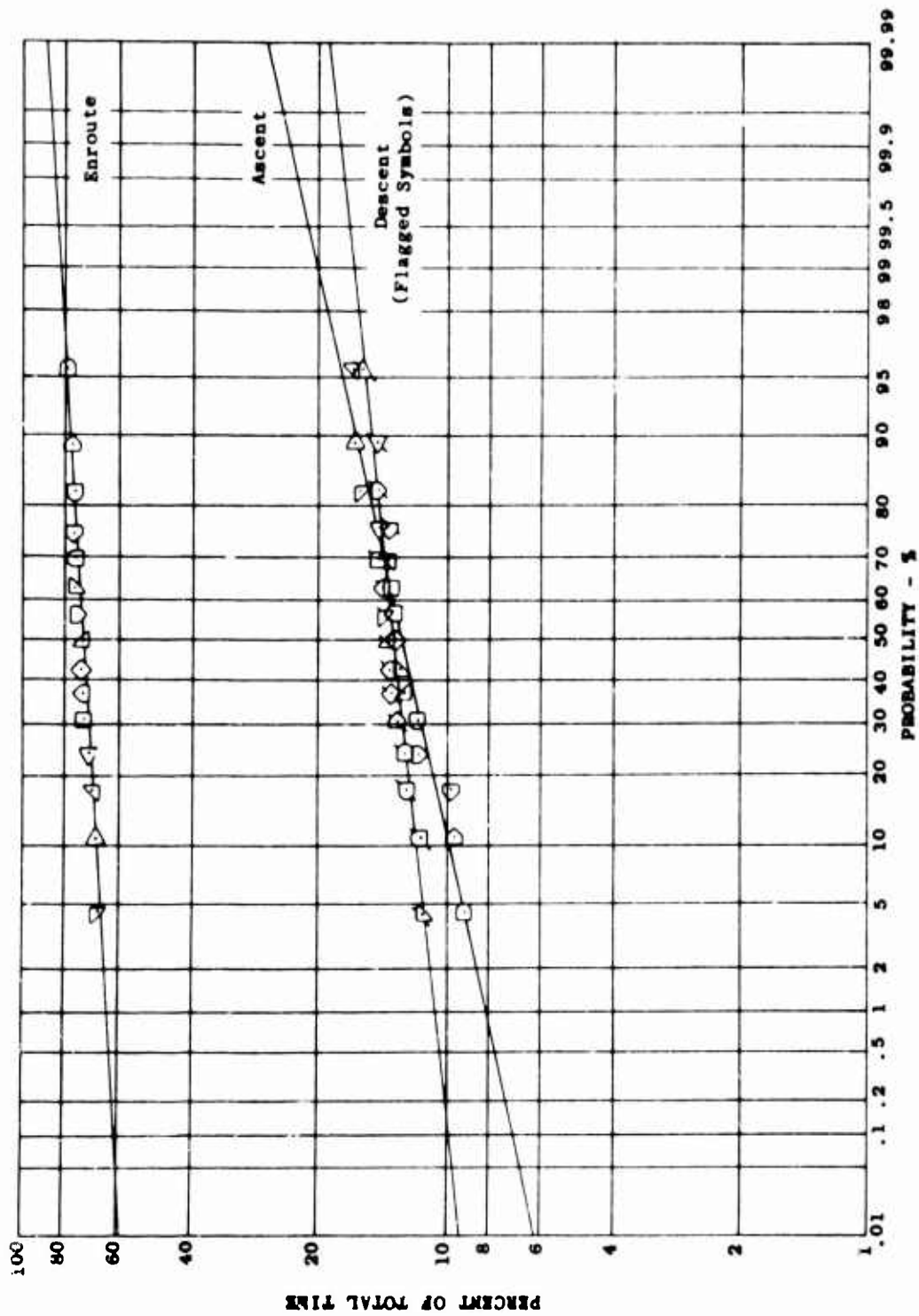


Figure 5. Standard Mission Scatter Band Determination for Plus and Minus One Standard Deviation Based on Median Rank. (See Table I for Symbol Definition).

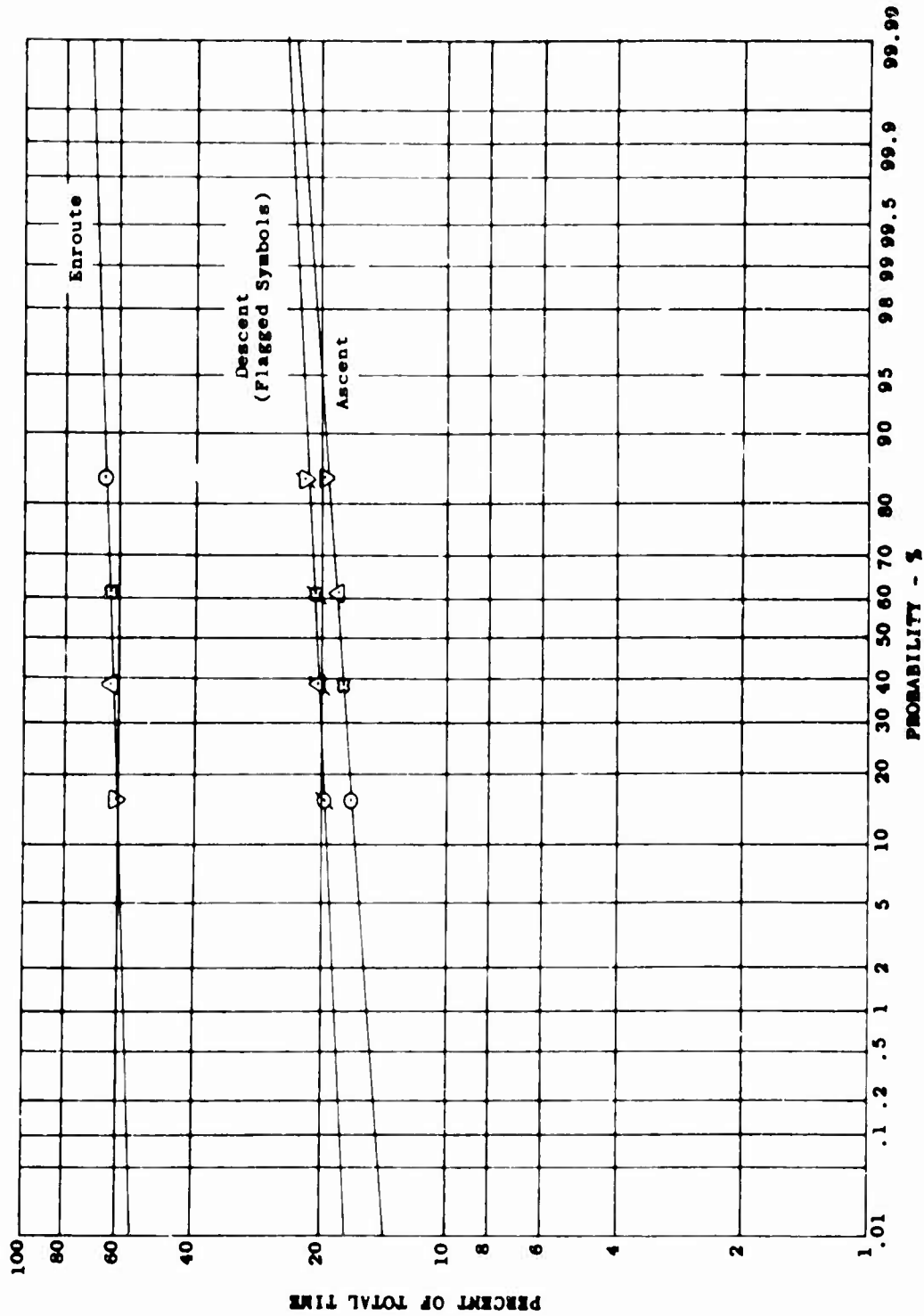
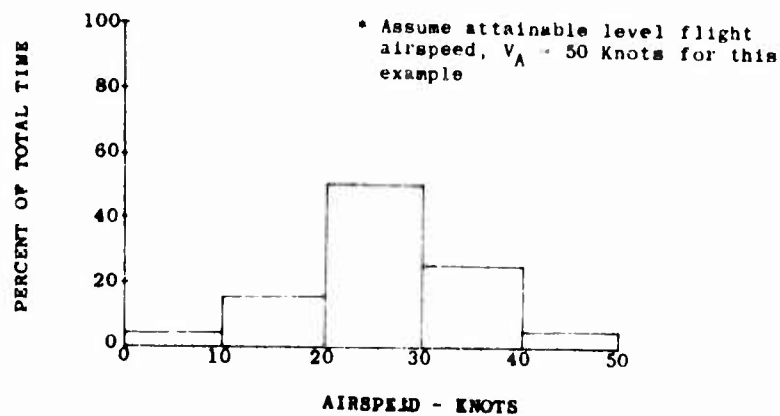


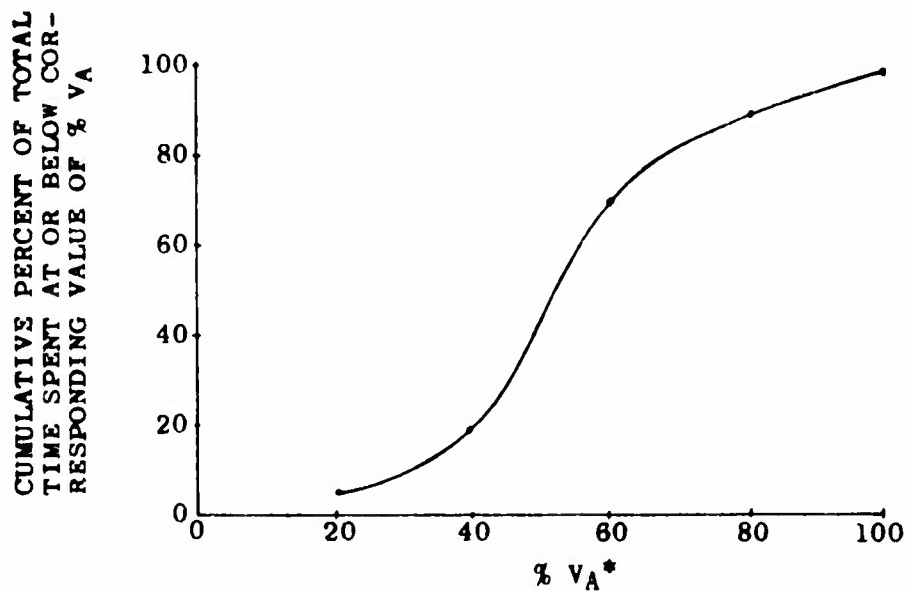
Figure 6. Nonstandard Mission Scatter Band Determination for Plus and Minus One Standard Deviation Based on Median Rank. (See Table I for Symbol Definition).

Airspeed (Knots)	% $V_A^*$	% Time	Cumulative % Time
0-10	0-20	5	5
10-20	20-40	15	20
20-30	40-60	50	70
30-40	60-80	25	95
40-50	80-100	5	100

Total - 100%



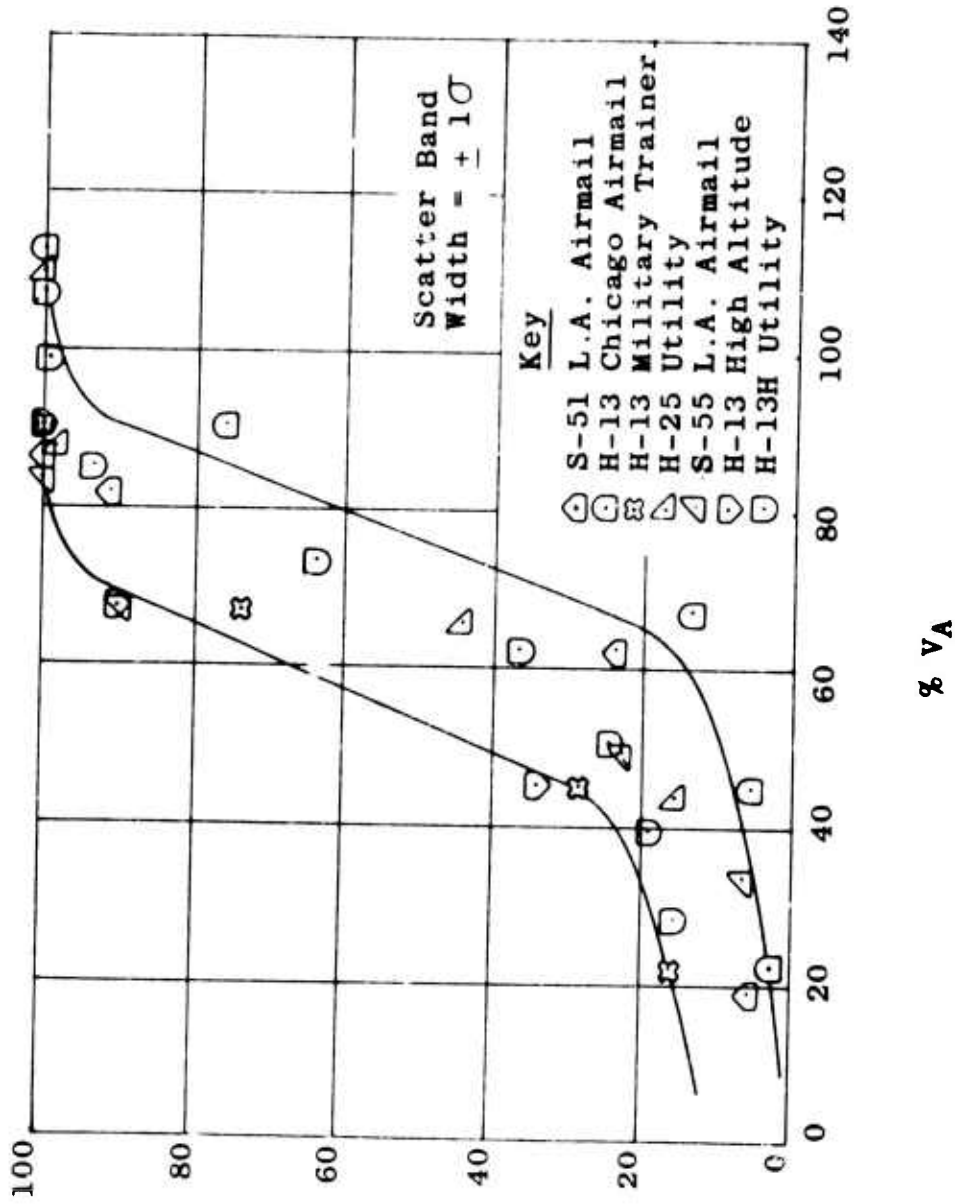
(a) Tabular Airspeed Frequency Data and Frequency Histogram.



(b) Cumulative Airspeed Frequency Distribution in Terms of %  $V_A$ .

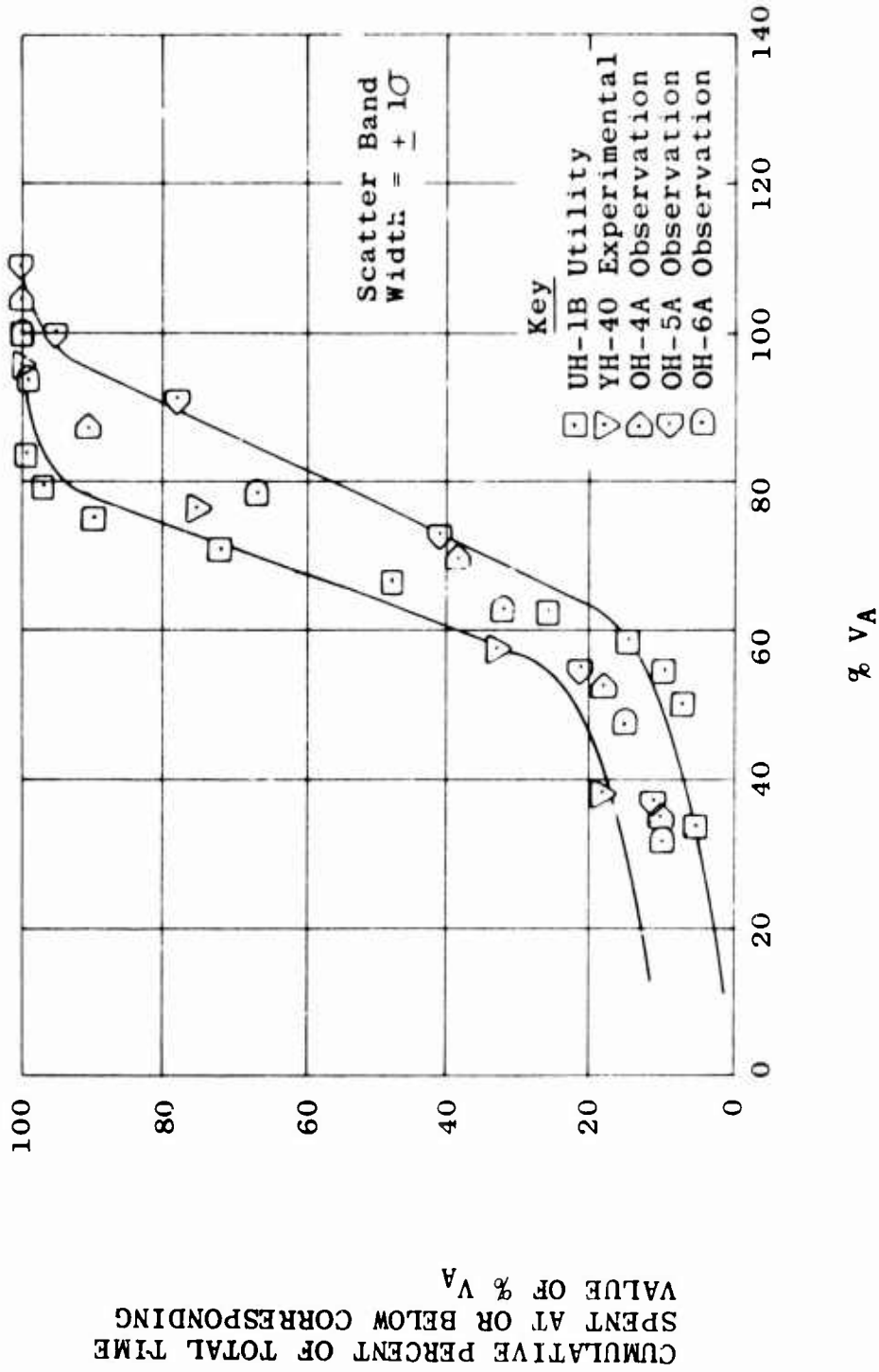
Figure 7. Example Showing the Conversion of Tabular Airspeed Frequency Data and a Frequency Histogram into a Cumulative Airspeed Frequency Distribution.

CUMULATIVE PERCENT OF TOTAL TIME  
 SPENT AT OR BELOW CORRESPONDING  
 VALUE OF % VA



(a) Reciprocating Engine-Powered Helicopters Having a Design Normal Gross Weight of Less Than 10,000 Pounds.

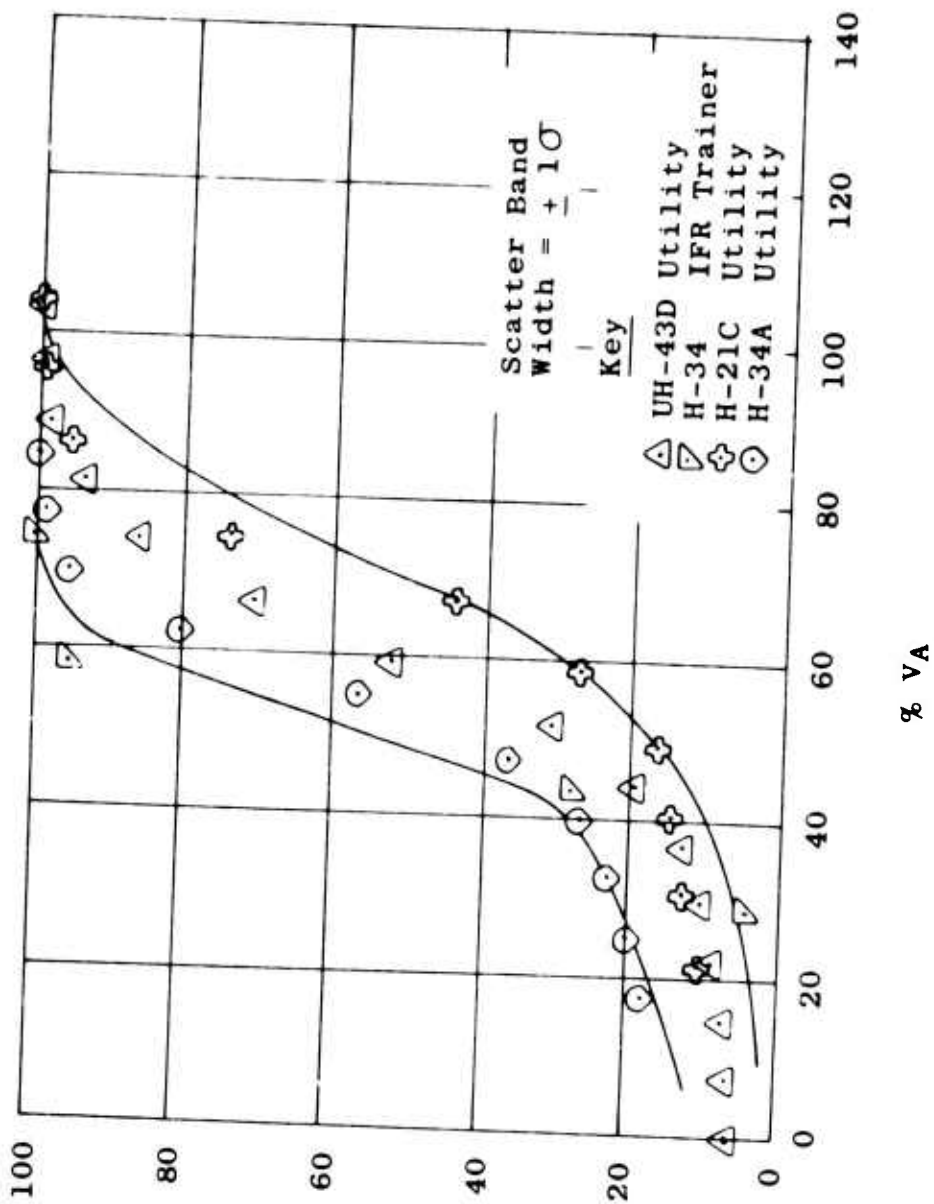
Figure 8. Cumulative Airspeed Frequency Distributions.



(b) Turbine-Powered Helicopters Having a Design Normal Gross Weight of Less Than 10,000 Pounds.

Figure 8. Continued.

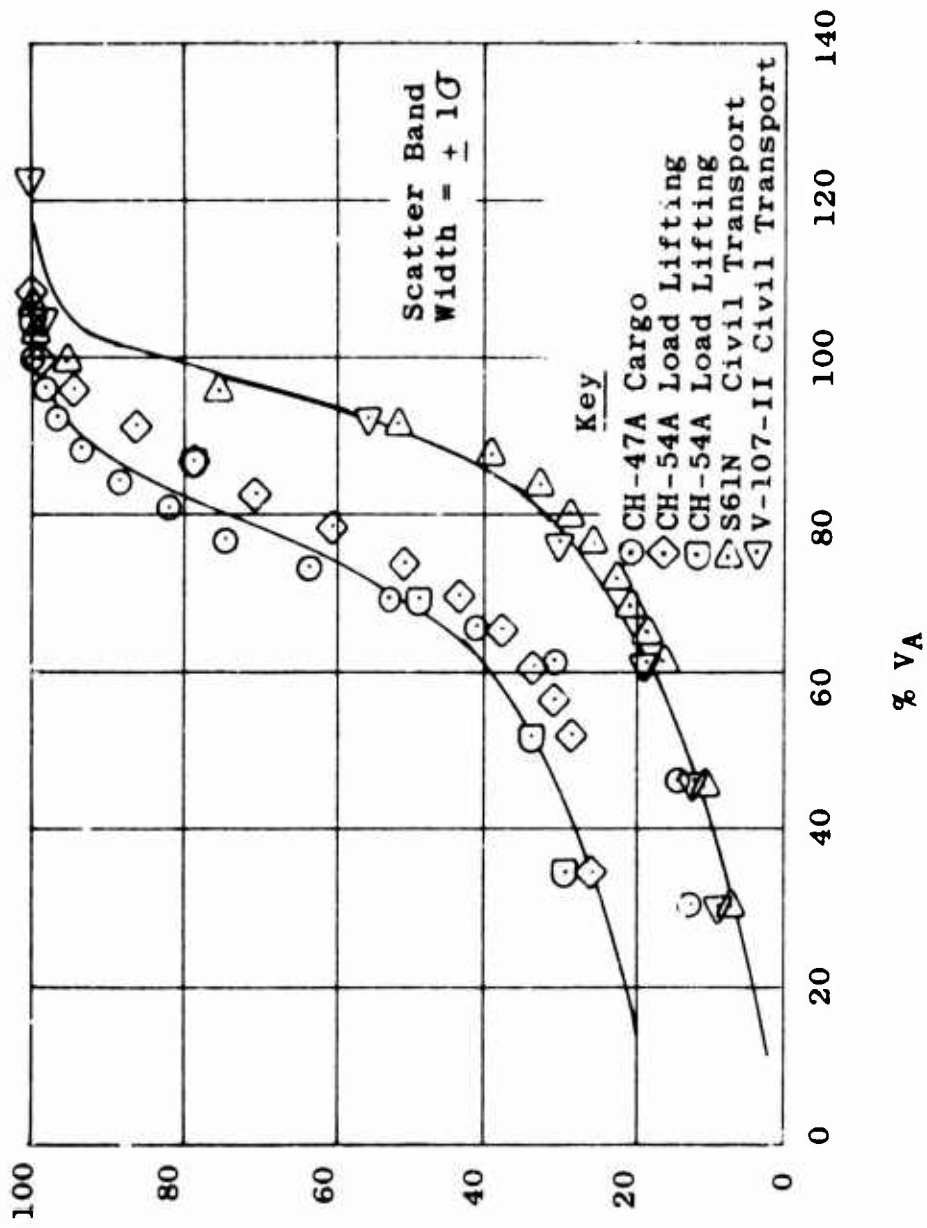
CUMULATIVE PERCENT OF TOTAL TIME  
 SPENT AT OR BELOW CORRESPONDING  
 VALUE OF % VA



(c) Reciprocating Engine-Powered Helicopters Having  
 a Design Normal Gross Weight of 10,000 to 15,000  
 Pounds.

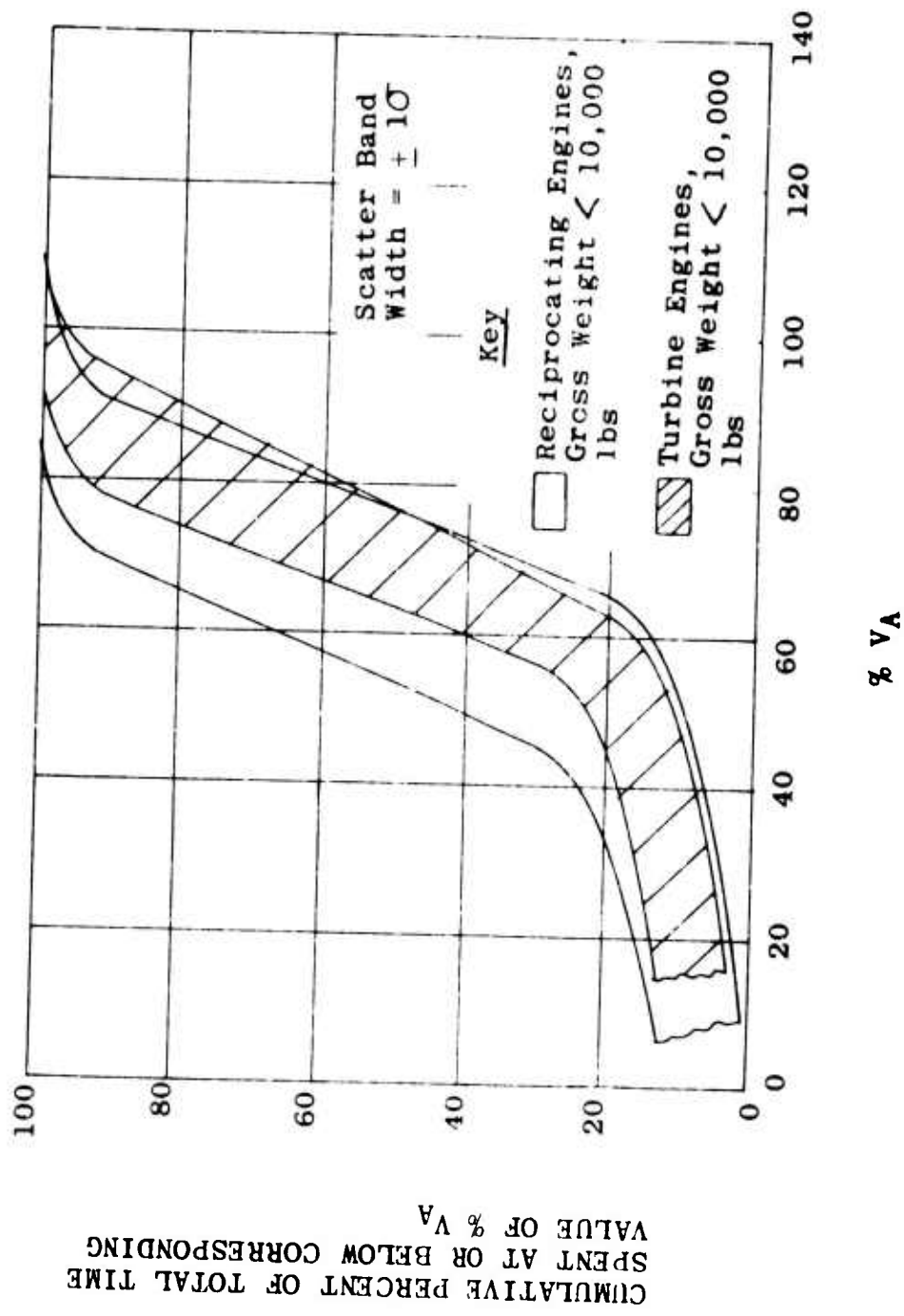
Figure 8. Continued.

CUMULATIVE PERCENT OF TOTAL TIME  
 SPENT AT OR BELOW CORRESPONDING  
 VALUE OF % VA



(d) Turbine-Powered Helicopters Having a Design Normal  
 Gross Weight of Greater Than 15,000 Pounds.

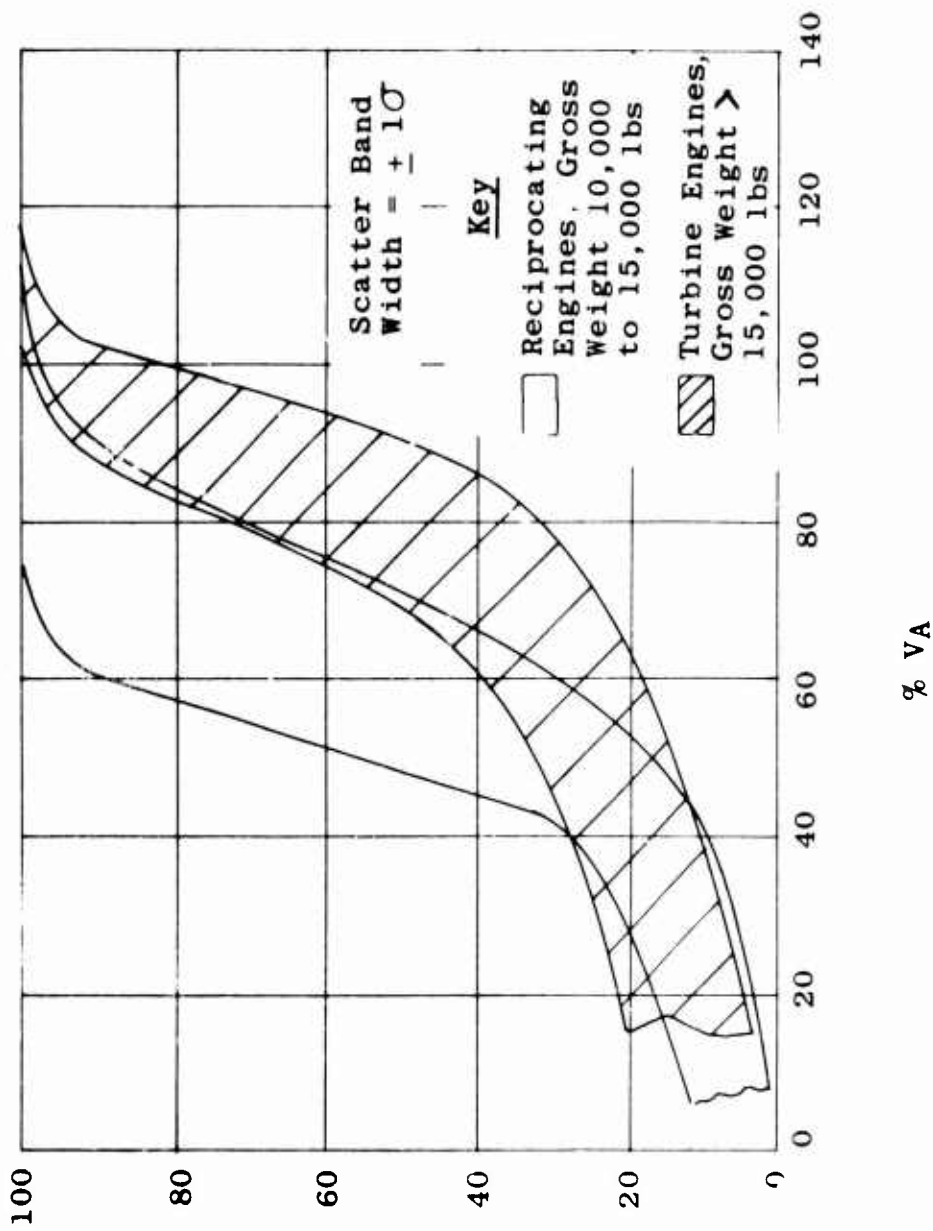
Figure 8. Continued.



(a) Reciprocating and Turbine Engine-Powered Helicopters Having a Design Normal Gross Weight of Less Than 10,000 Pounds.

Figure 9. Comparison of Cumulative Airspeed Frequency Distributions.

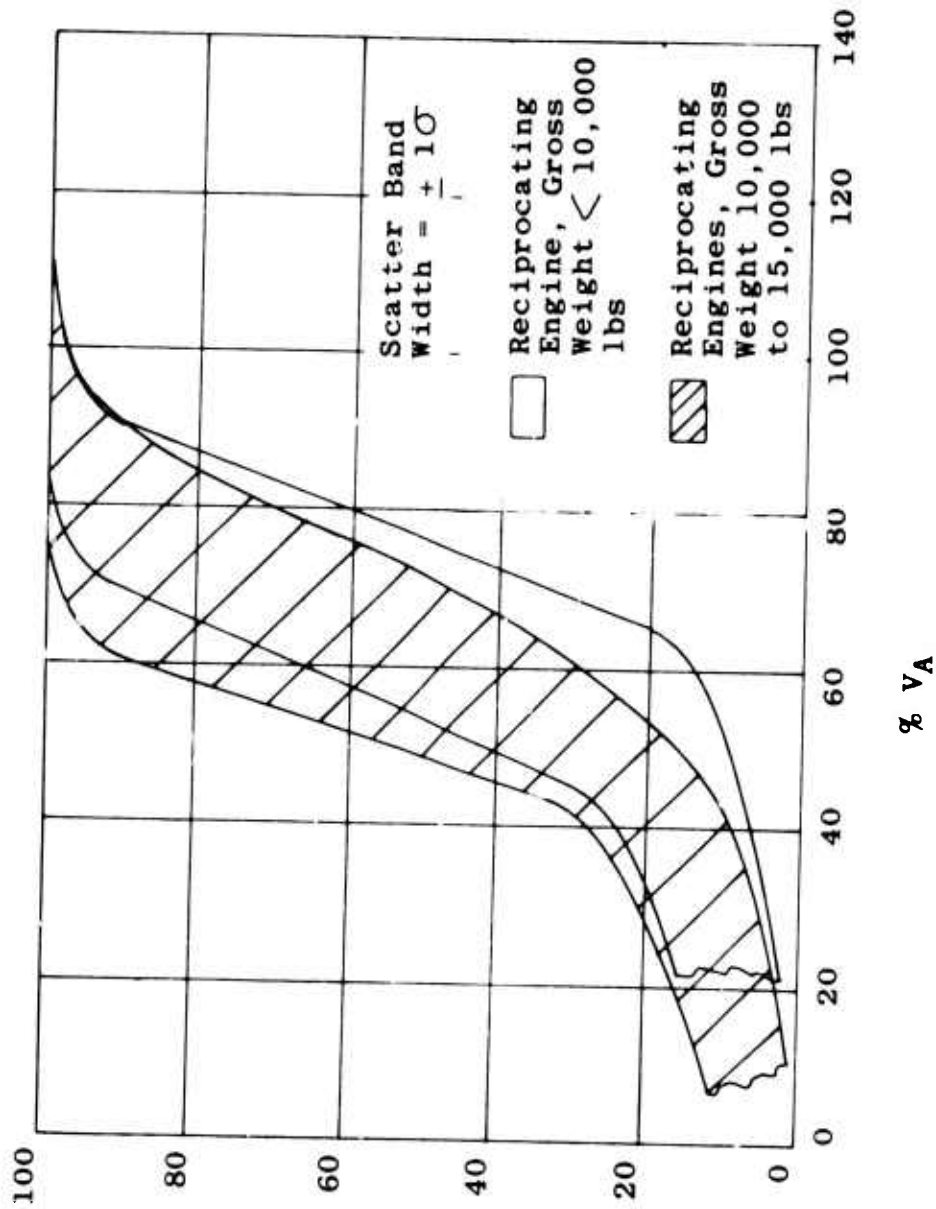
CUMULATIVE PERCENT OF TOTAL TIME  
 SPENT AT OR BELOW CORRESPONDING  
 VALUE OF % VA



(b) Reciprocating Engine-Powered Helicopters Having a Design Normal Gross Weight of 10,000 to 15,000 Pounds and Turbine Engine-Powered Helicopters Having a Design Normal Gross Weight of Greater Than 15,000 Pounds.

Figure 9. Continued.

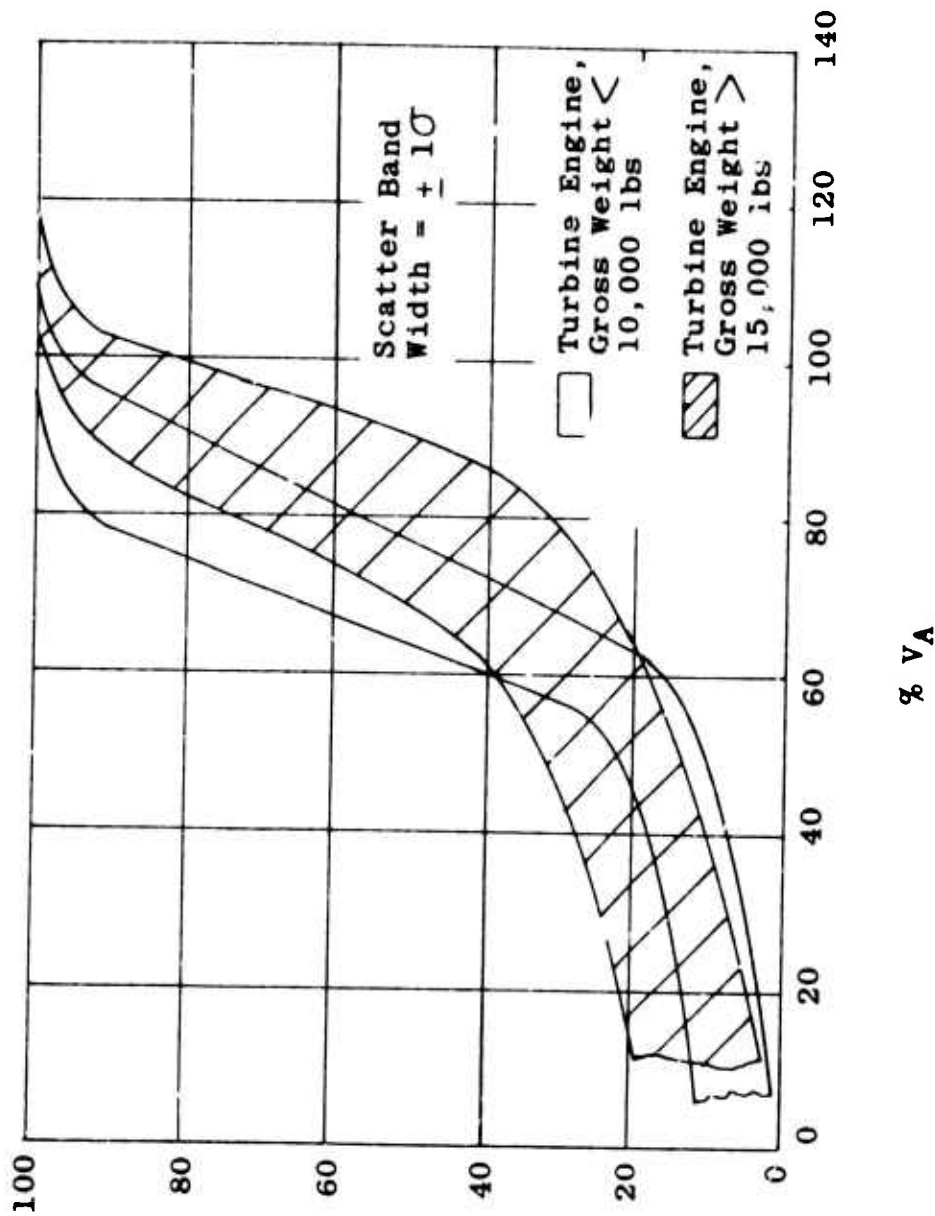
CUMULATIVE PERCENT OF TOTAL TIME  
 SPENT AT OR BELOW CORRESPONDING  
 VALUE OF % VA



(c) Reciprocating Engine-Powered Helicopters Having a Design Normal Gross Weight of Less Than 10,000 Pounds and Those Having a Design Normal Gross Weight of 10,000 to 15,000 Pounds.

Figure 9. Continued.

CUMULATIVE PERCENT OF TOTAL TIME  
 SPENT AT OR BELOW CORRESPONDING  
 VALUE OF % V<sub>A</sub>



(d) Turbine Engine-Powered Helicopters Having a Design Normal Gross Weight of Less Than 10,000 pounds and Those Having a Design Normal Gross Weight of Greater Than 15,000 Pounds.

Figure 9. Continued.

CUMULATIVE PERCENT OF STEADY-  
STATE TIME SPENT AT OR BELOW  
CORRESPONDING VALUE OF % VA

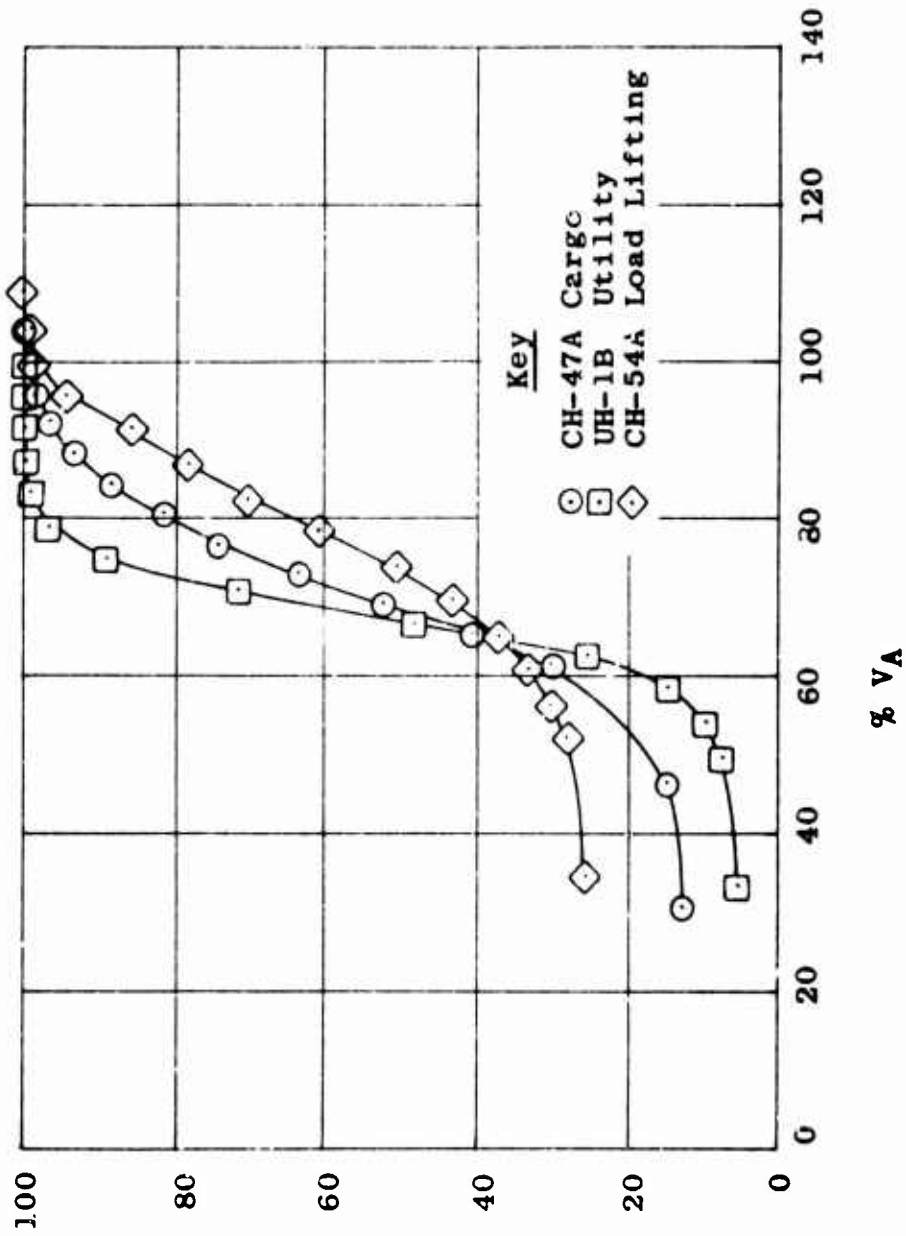
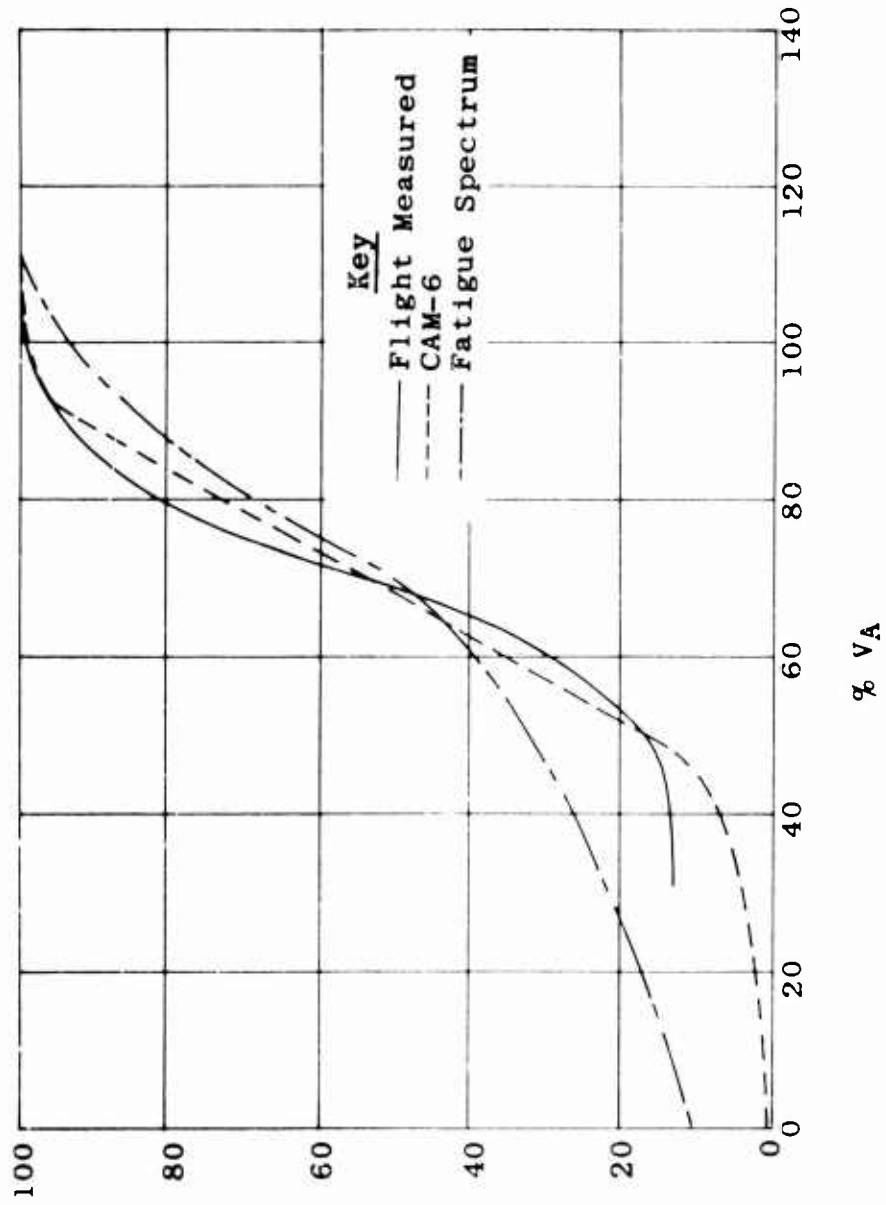


Figure 10. Cumulative Airspeed Frequency Distributions for the CH-47A, UH-1B, and CH-54A Helicopters.

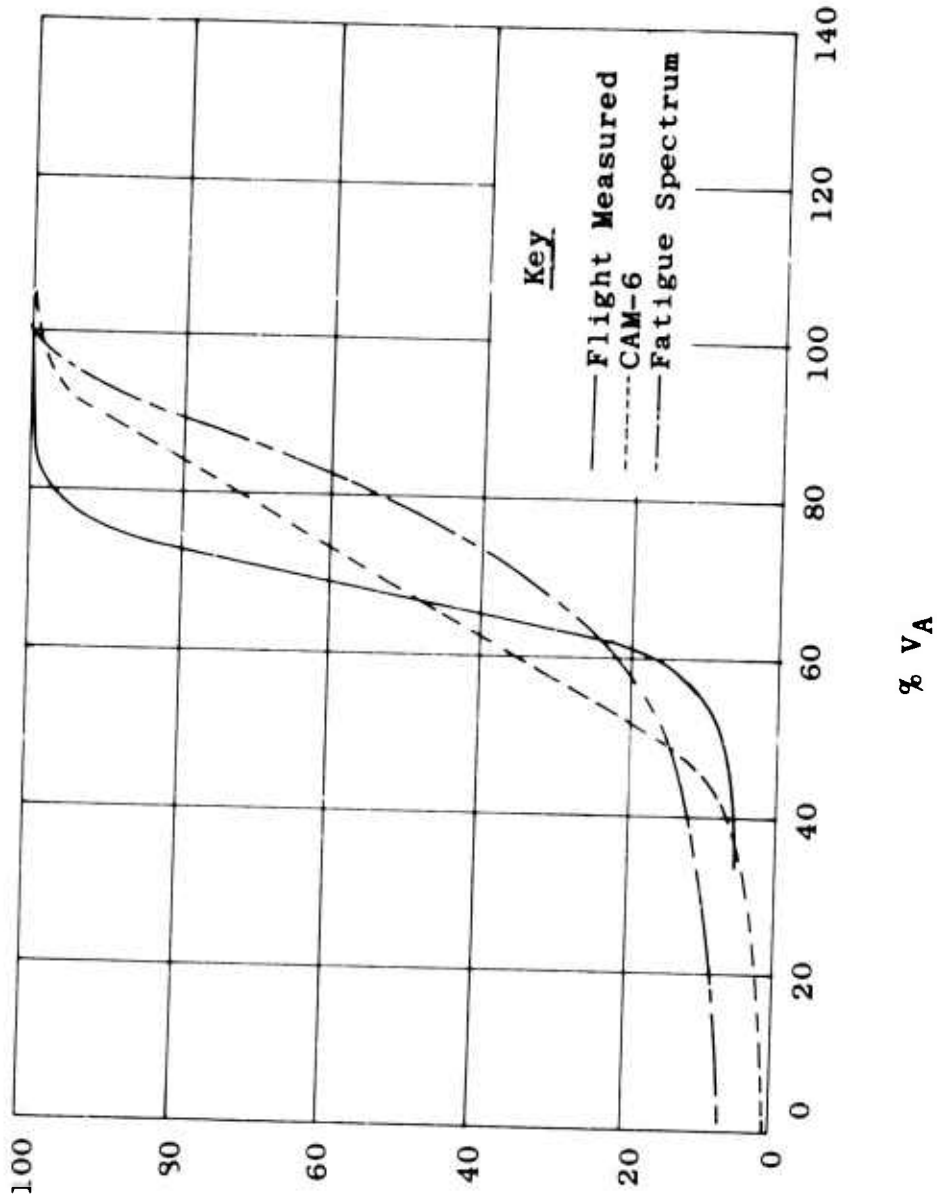
CUMULATIVE PERCENT OF STEADY-  
STATE TIME SPENT AT OR BELOW  
CORRESPONDING VALUE OF % V<sub>A</sub>



(a) CH-47A.

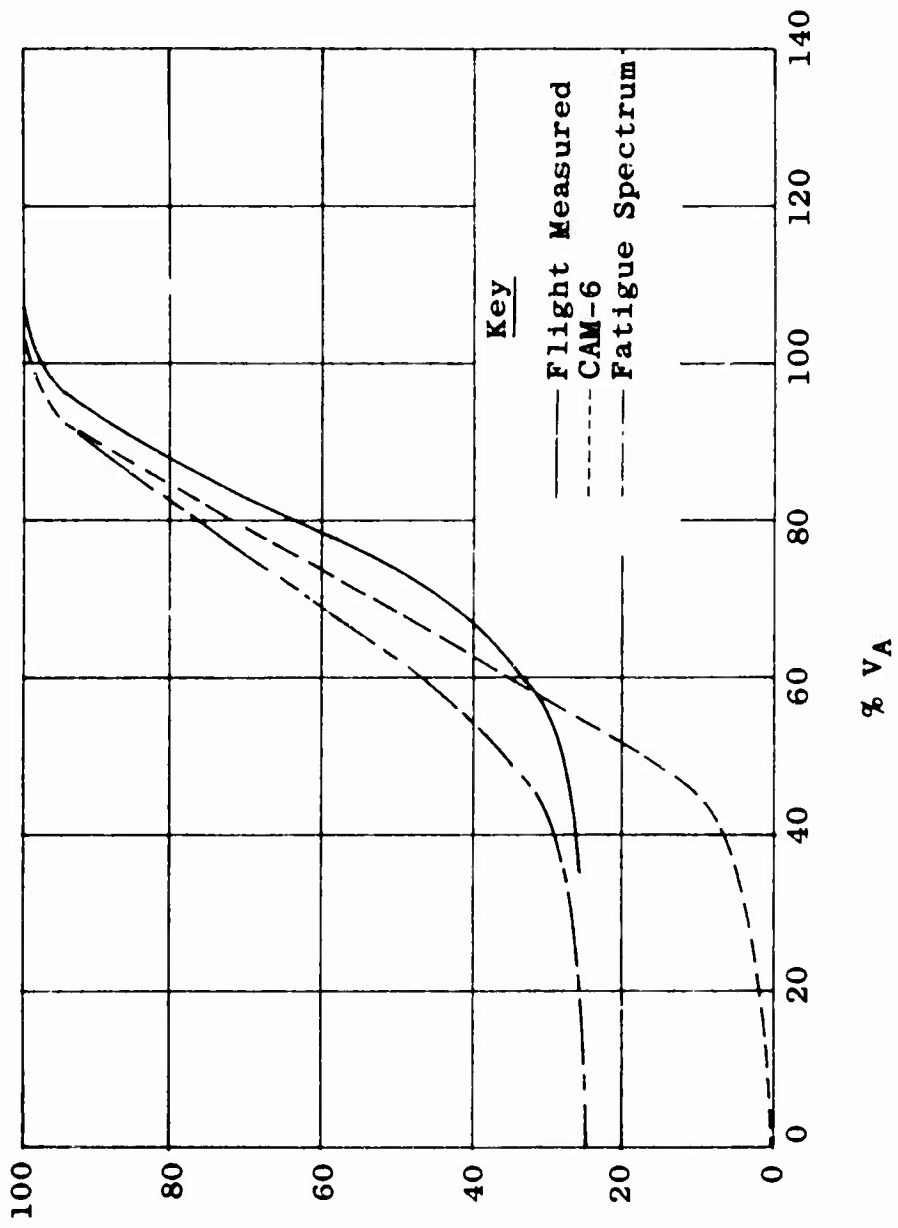
Figure 11. Comparison of Flight-Measured Cumulative Airspeed Frequency Distributions With Fatigue and CAM-6 Spectrums.

CUMULATIVE PERCENT OF STEADY-  
STATE TIME SPENT AT OR BELOW  
CORRESPONDING VALUE OF % VA



(b) UH-1B.

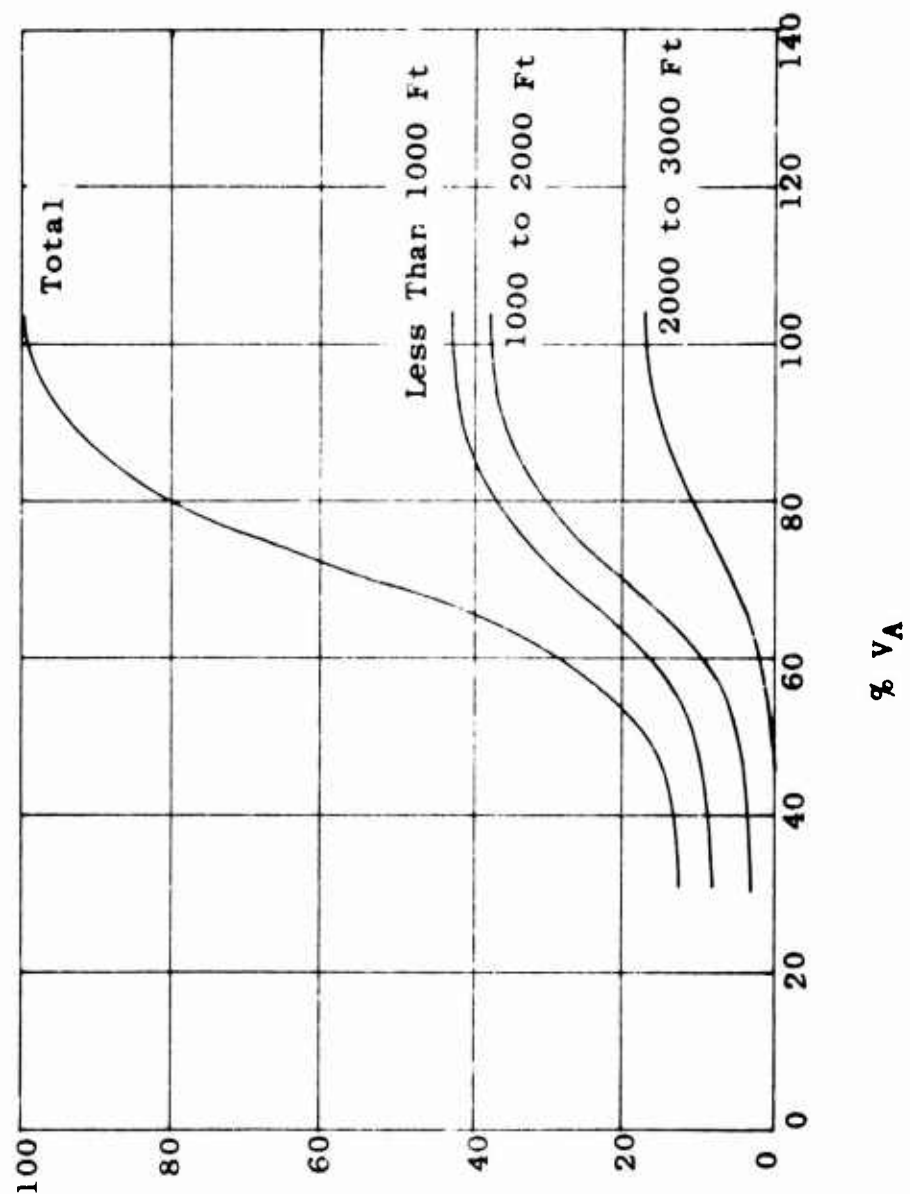
Figure 11. Continued.



CUMULATIVE PERCENT OF STEADY-STATE TIME SPENT AT OR BELOW CORRESPONDING VALUE OF % VA

(c) CH-54A.

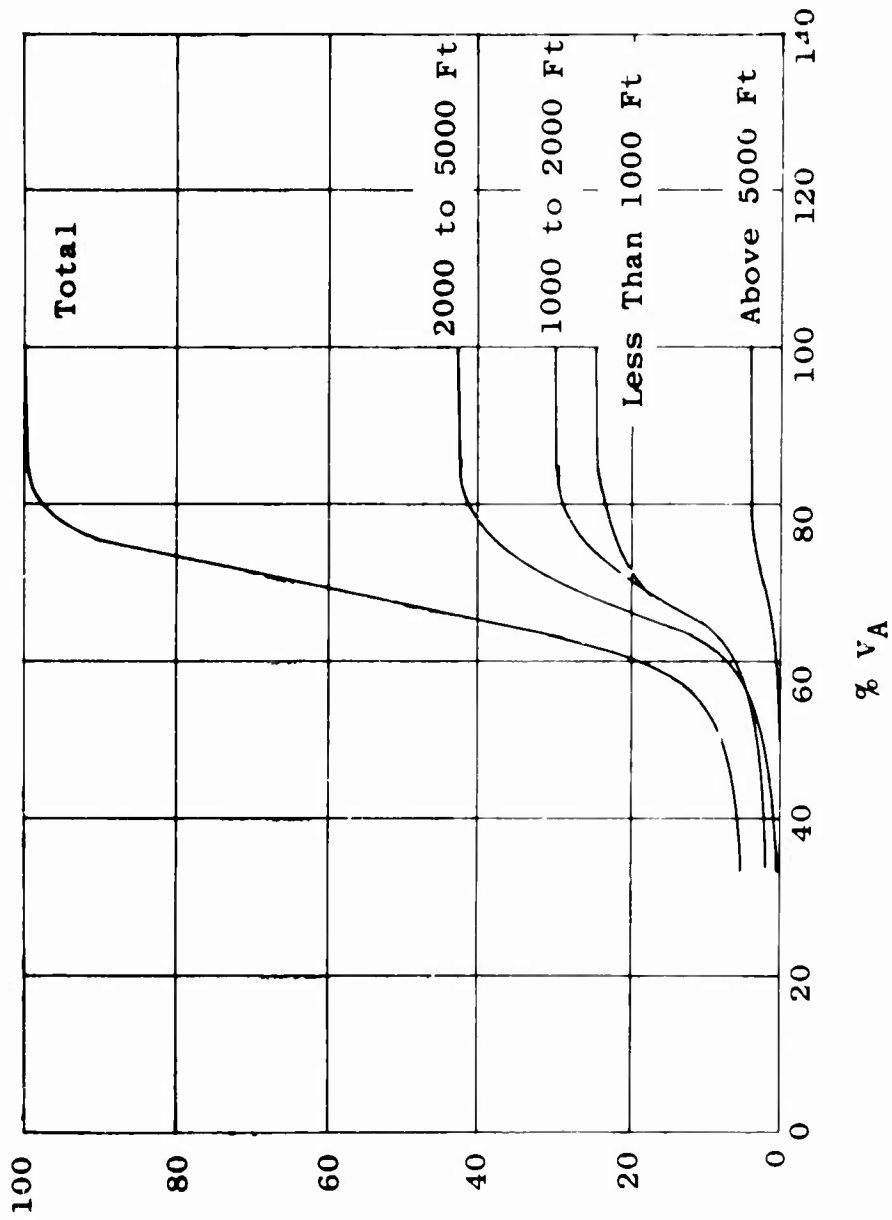
Figure 11. Continued.



(a) CH-47A.

Figure 12. Cumulative Airspeed Frequency Distribution by Altitude.

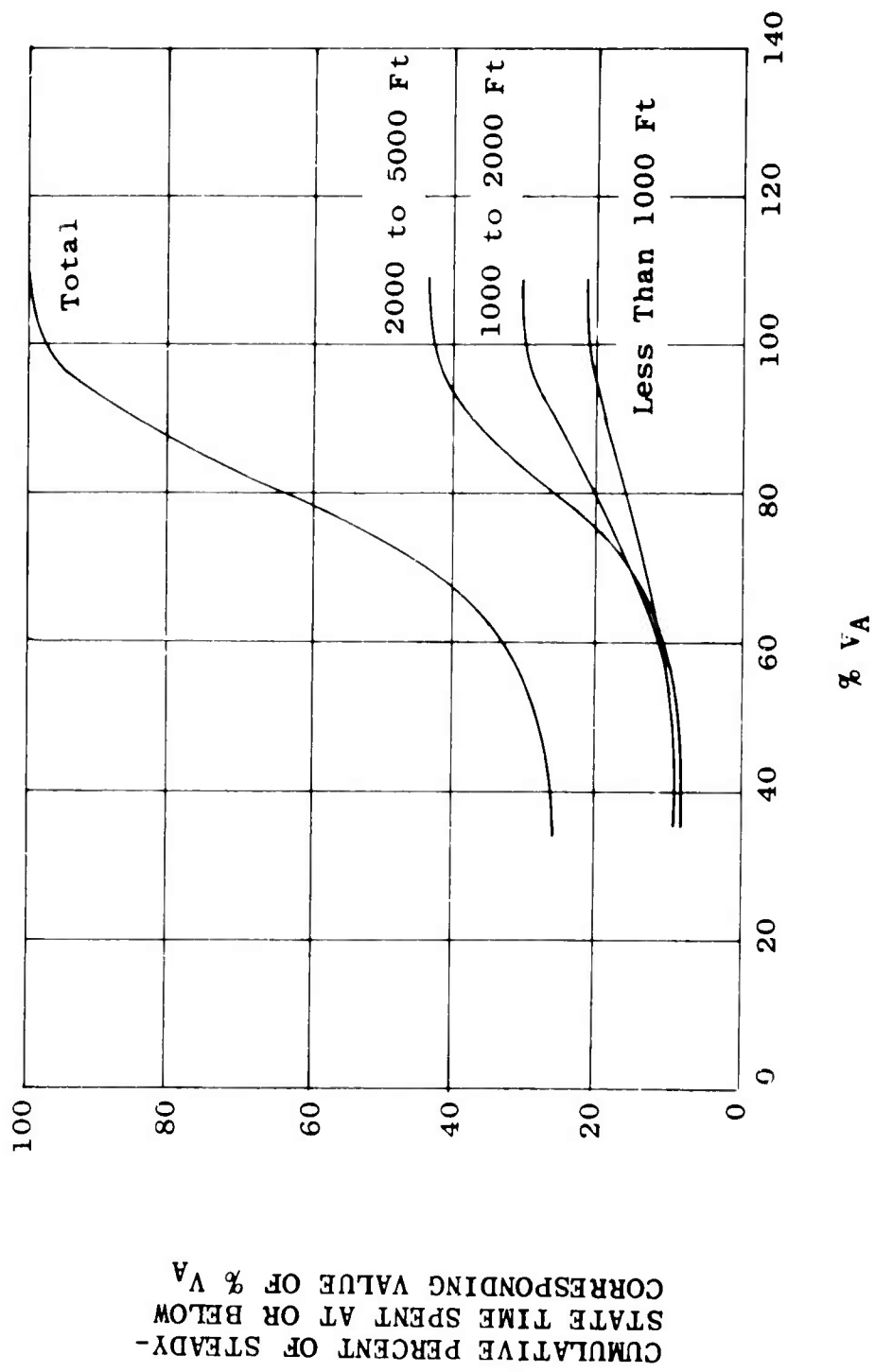
CUMULATIVE PERCENT OF STEADY-STATE TIME SPENT AT OR BELOW CORRESPONDING VALUE OF % VA



CUMULATIVE PERCENT OF STEADY-  
STATE TIME SPENT AT OR BELOW  
CORRESPONDING VALUE OF % VA

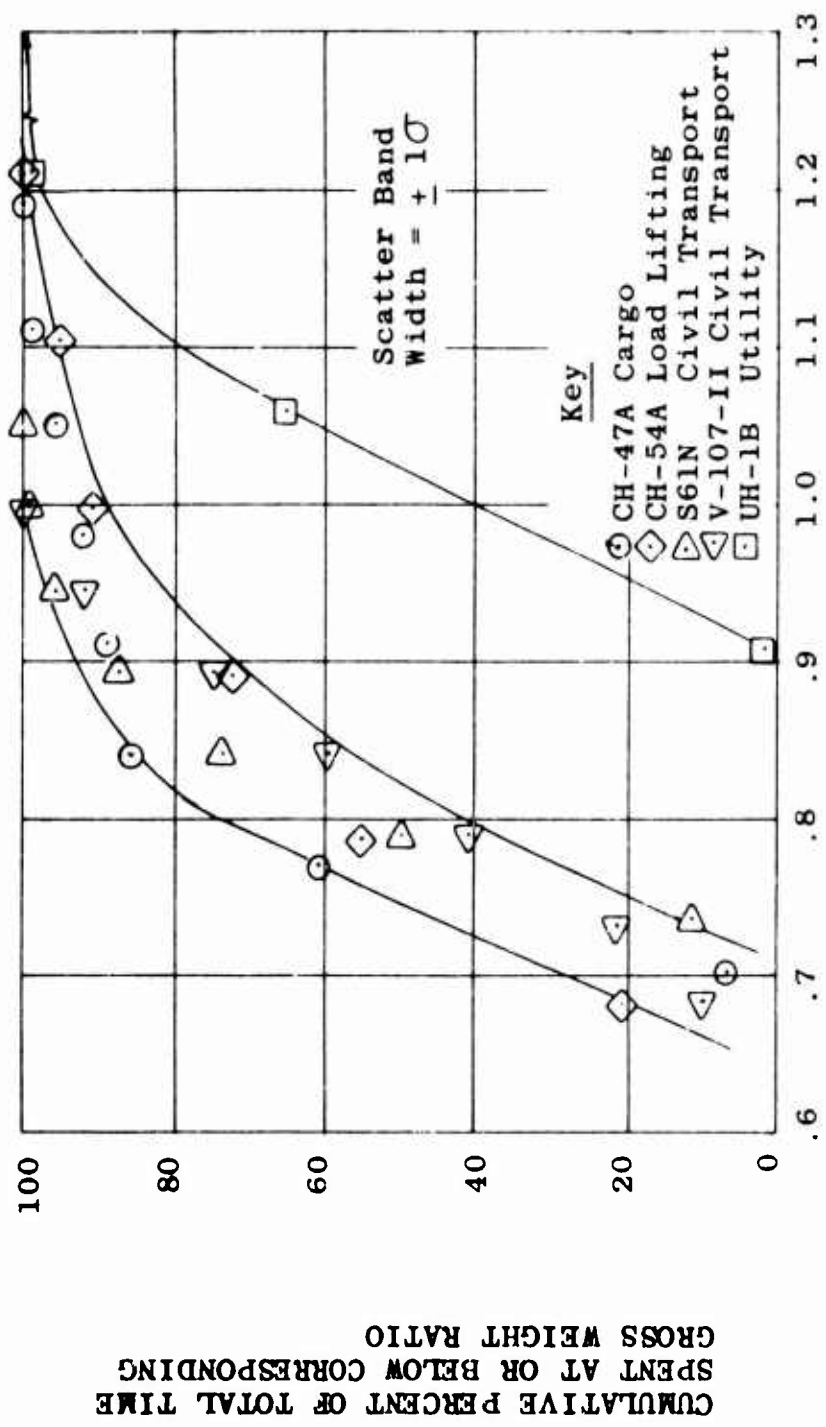
(b) UH-1B.

Figure 12. Continued.



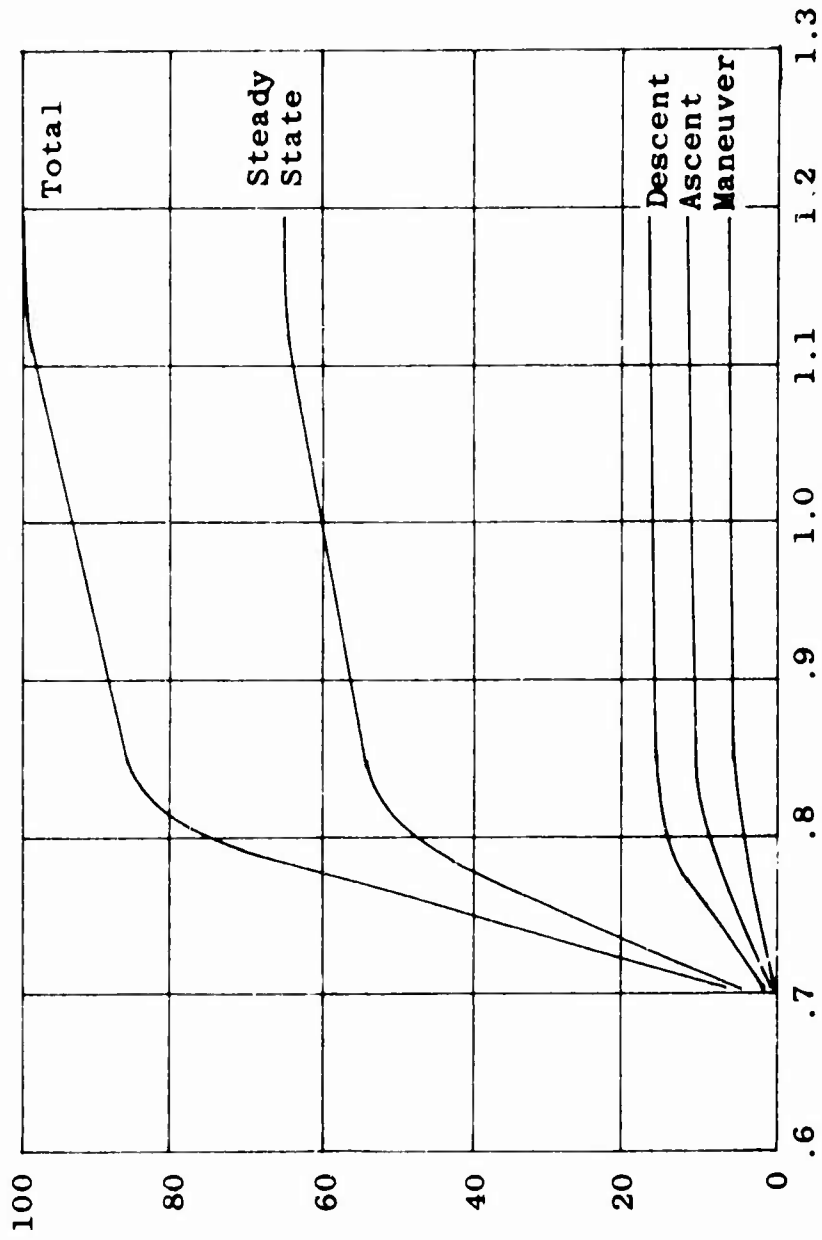
(c) CH-54A.

Figure 12. Continued.



OPERATING GROSS WEIGHT/DESIGN NORMAL GROSS WEIGHT

Figure 13. Cumulative Gross Weight Frequency Distribution for Turbine-Powered Helicopters Having a Design Normal Gross Weight of Greater Than 15,000 Pounds.

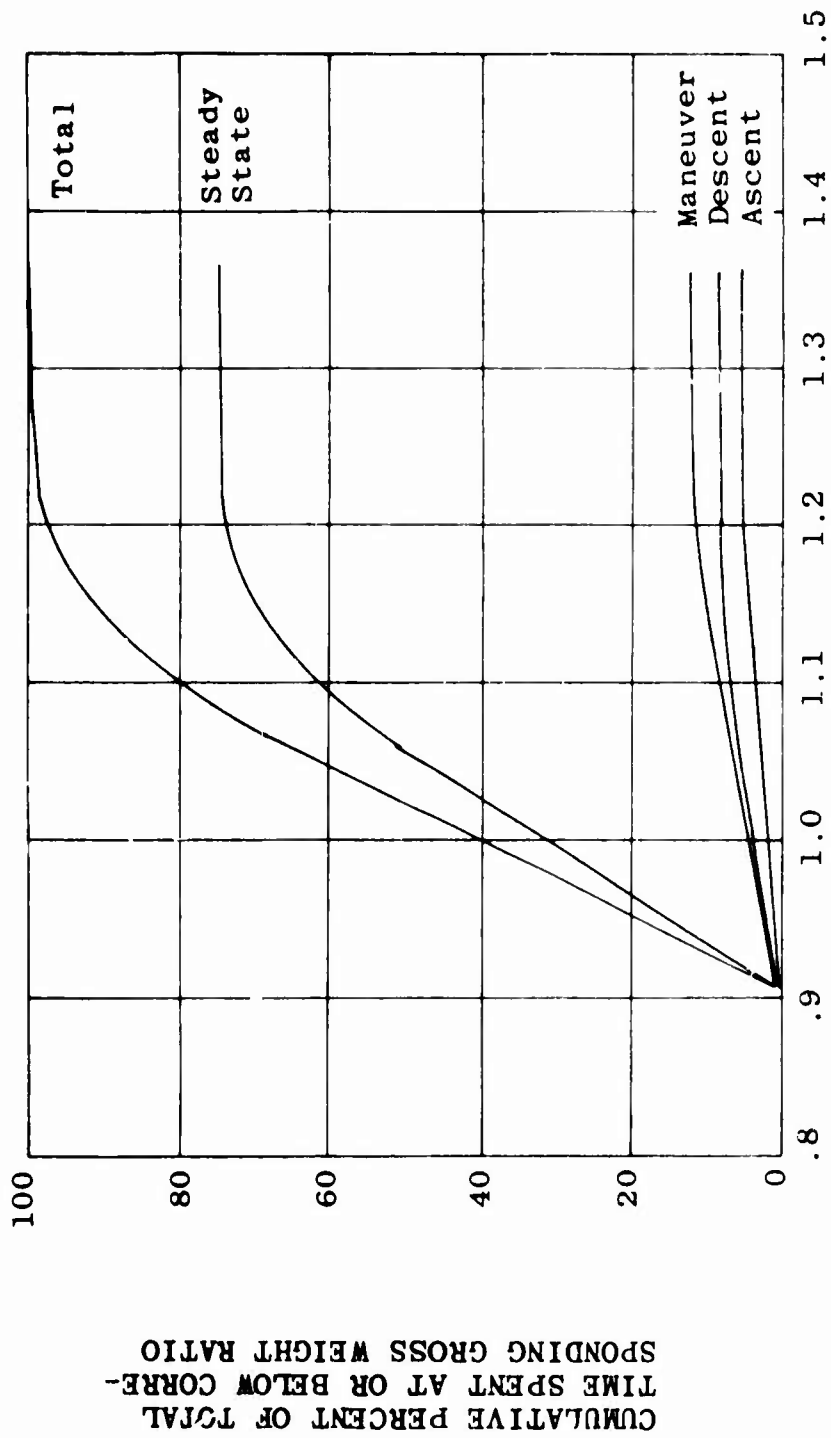


OPERATING GROSS WEIGHT/DESIGN NORMAL GROSS WEIGHT

(a) CH-47A.

Figure 14. Cumulative Gross Weight Frequency Distribution by Mission Segment.

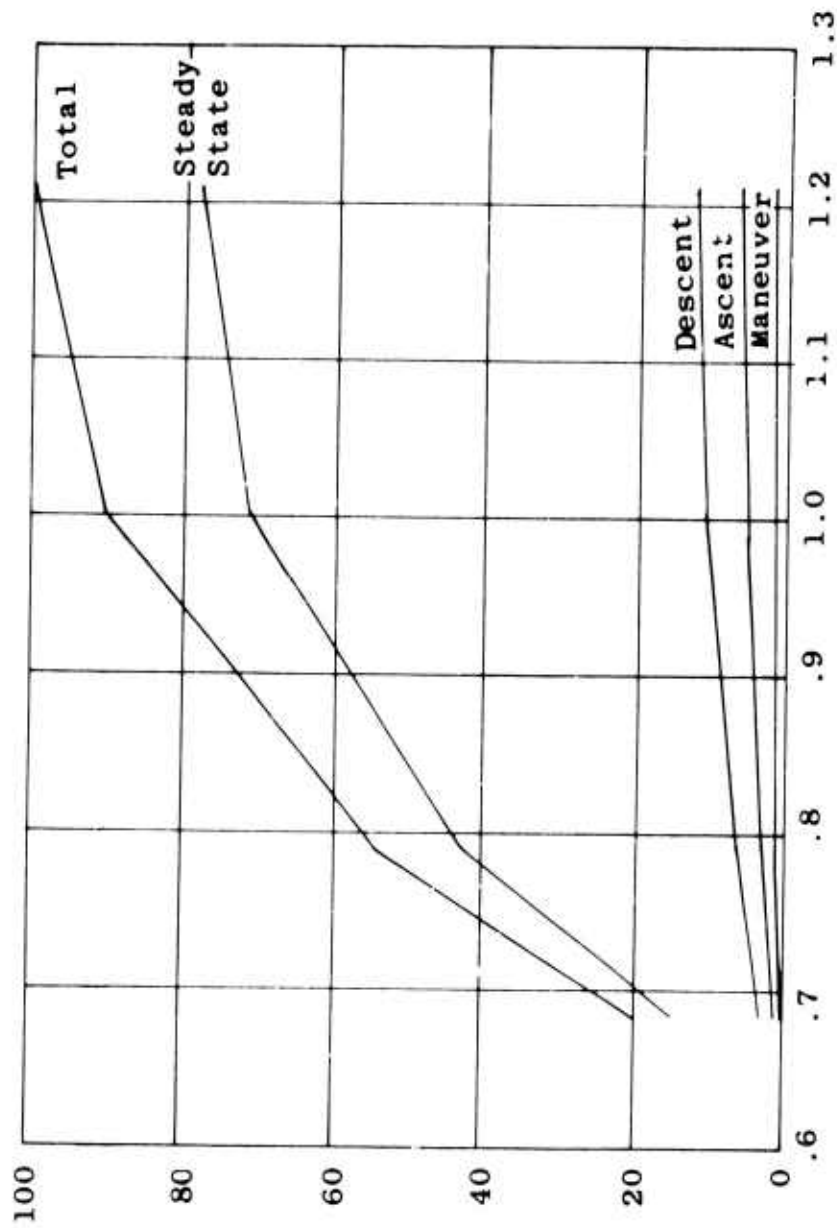
CUMULATIVE PERCENT OF TOTAL TIME  
SPENT AT OR BELOW CORRESPONDING  
GROSS WEIGHT RATIO



OPERATING GROSS WEIGHT/DESIGN NORMAL GROSS WEIGHT

(b) UH-1B.

Figure 14. Continued.

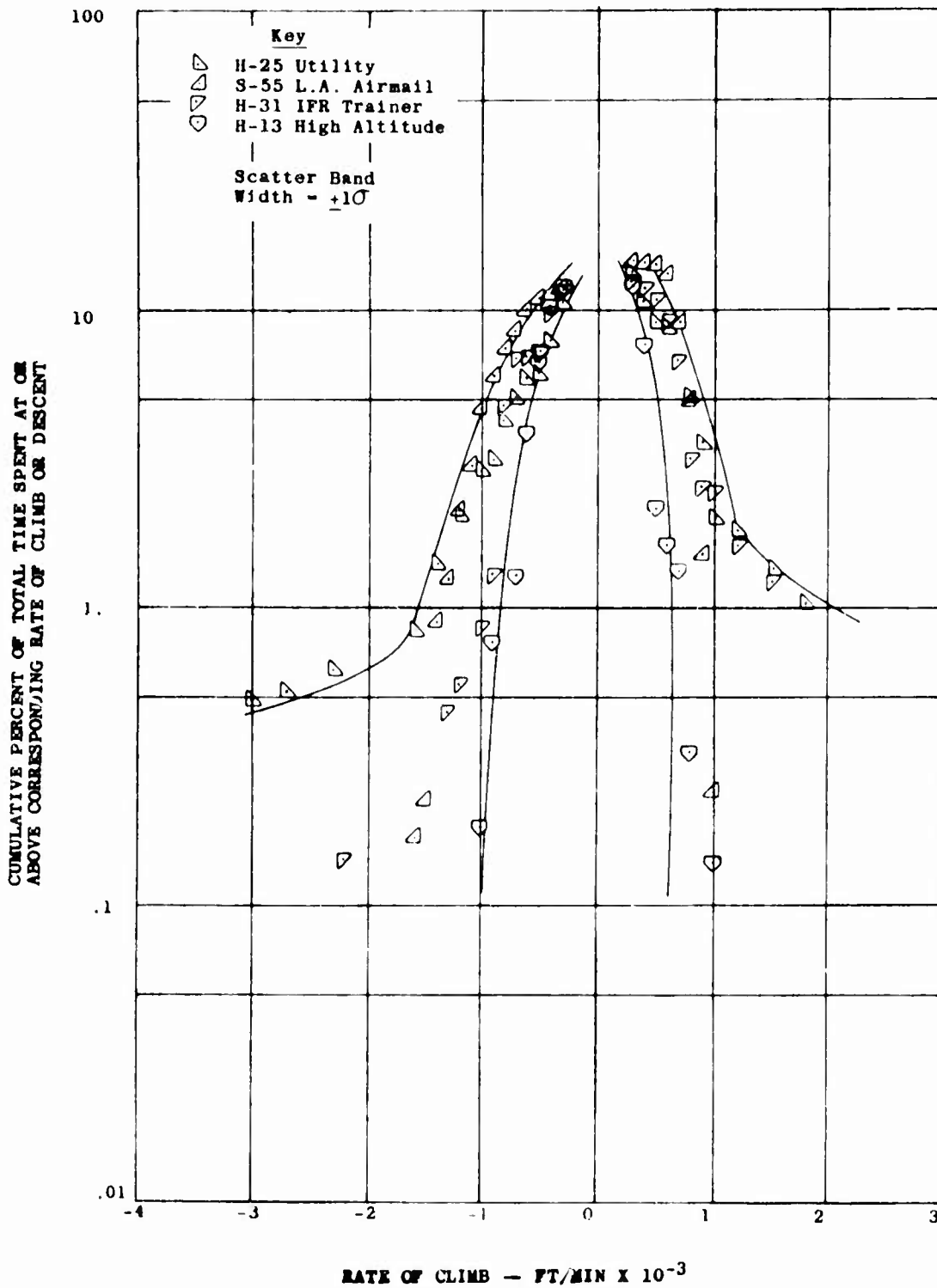


CUMULATIVE PERCENT OF TOTAL TIME SPENT AT OR BELOW CORRESPONDING GROSS WEIGHT RATIO

OPERATING GROSS WEIGHT/DESIGN NORMAL GROSS WEIGHT

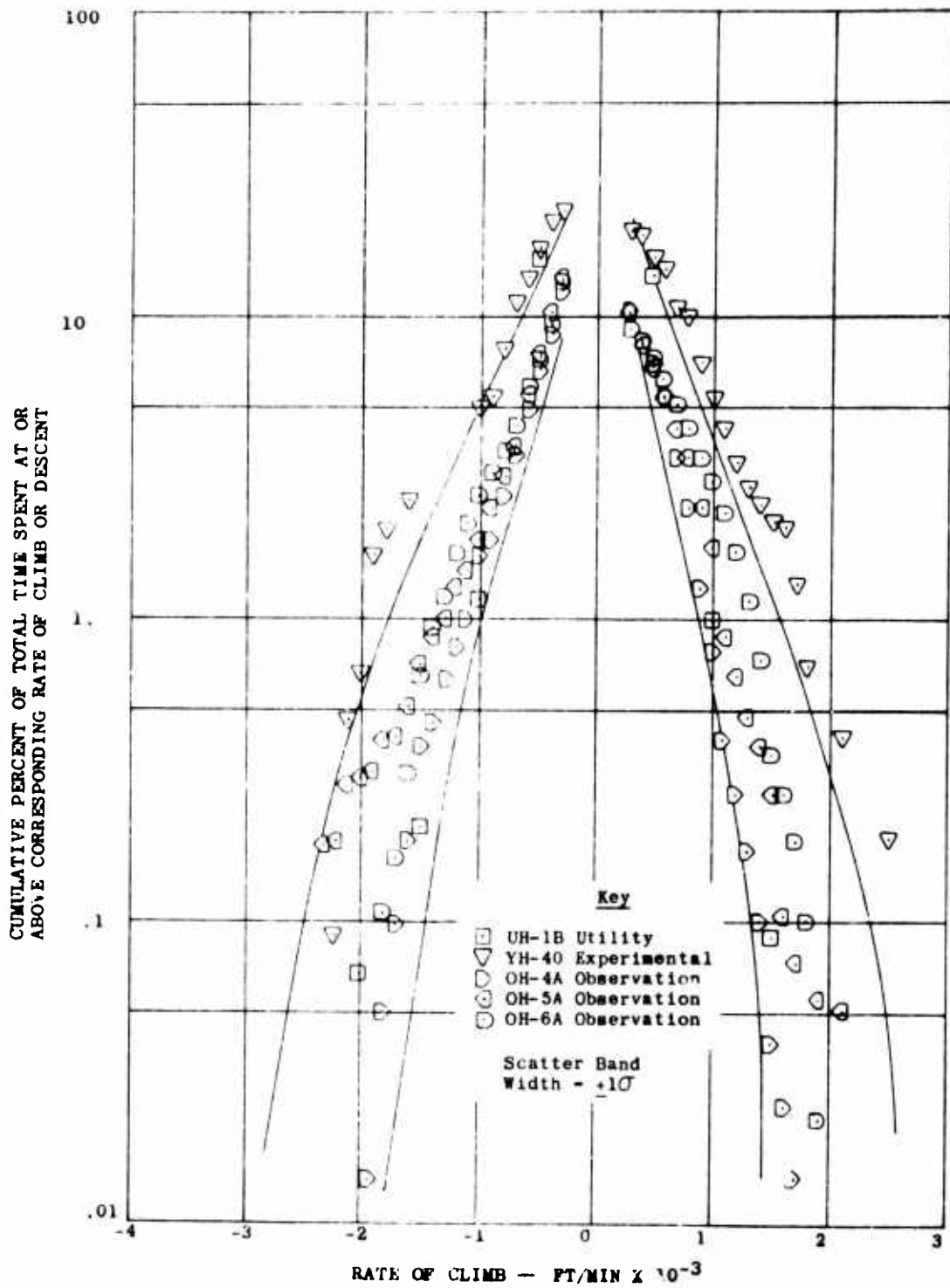
(c) CH-54A.

Figure 14. Continued.



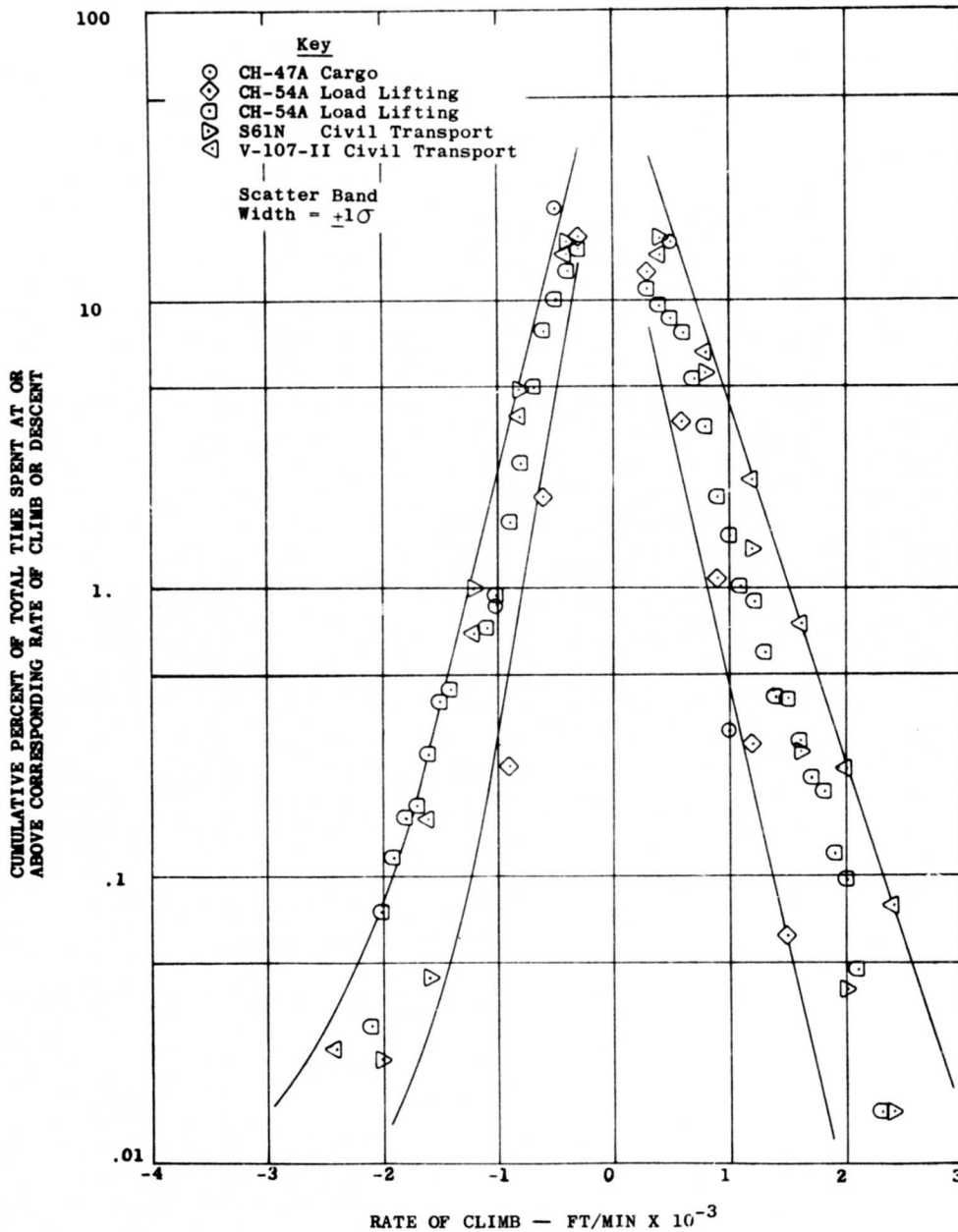
(a) Reciprocating Engine-Powered Helicopters Having a Design Normal Gross Weight of Less Than 12,000 Pounds.

Figure 15. Cumulative Rate-of-Climb Frequency Distribution.



(b) Turbine Engine-Powered Helicopters Having a Design Normal Gross Weight of Less Than 10,000 Pounds.

Figure 15. Continued.



(c) Turbine Engine-Powered Helicopters Having a Design Normal Gross Weight of Greater Than 15,000 Pounds.

Figure 15. Continued.

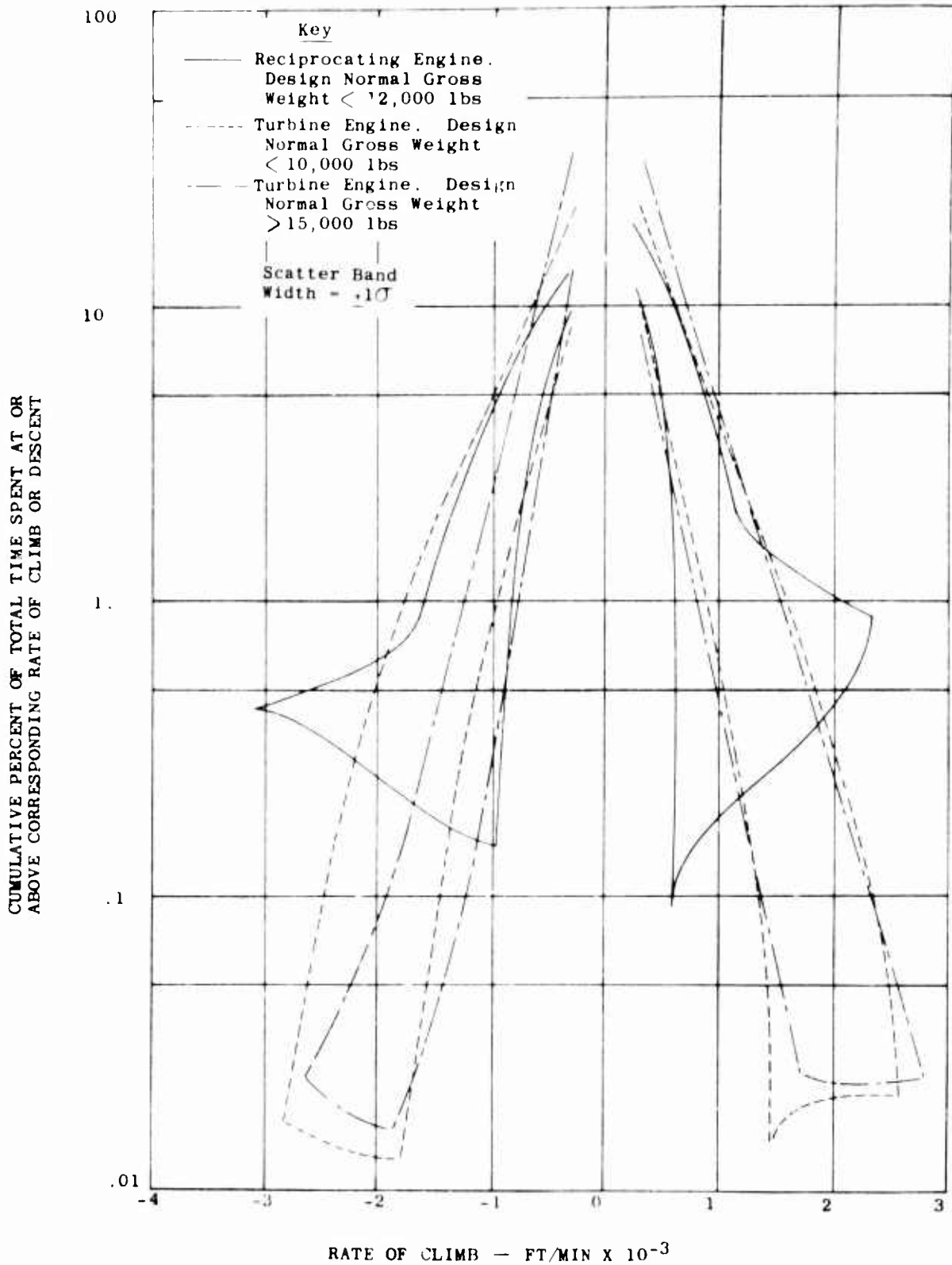


Figure 16. Composite Cumulate Rate-of-Climb Frequency Distributions.

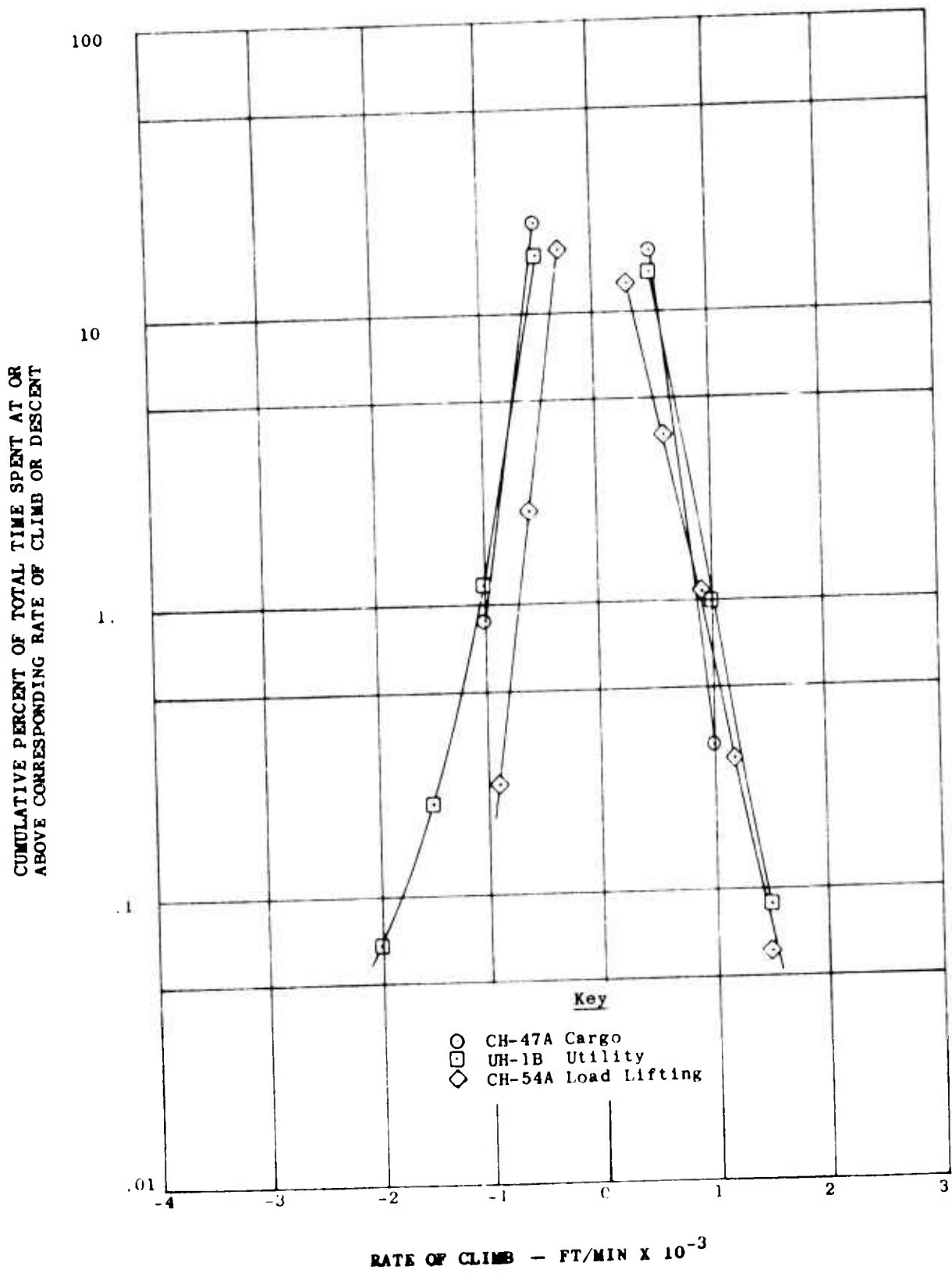
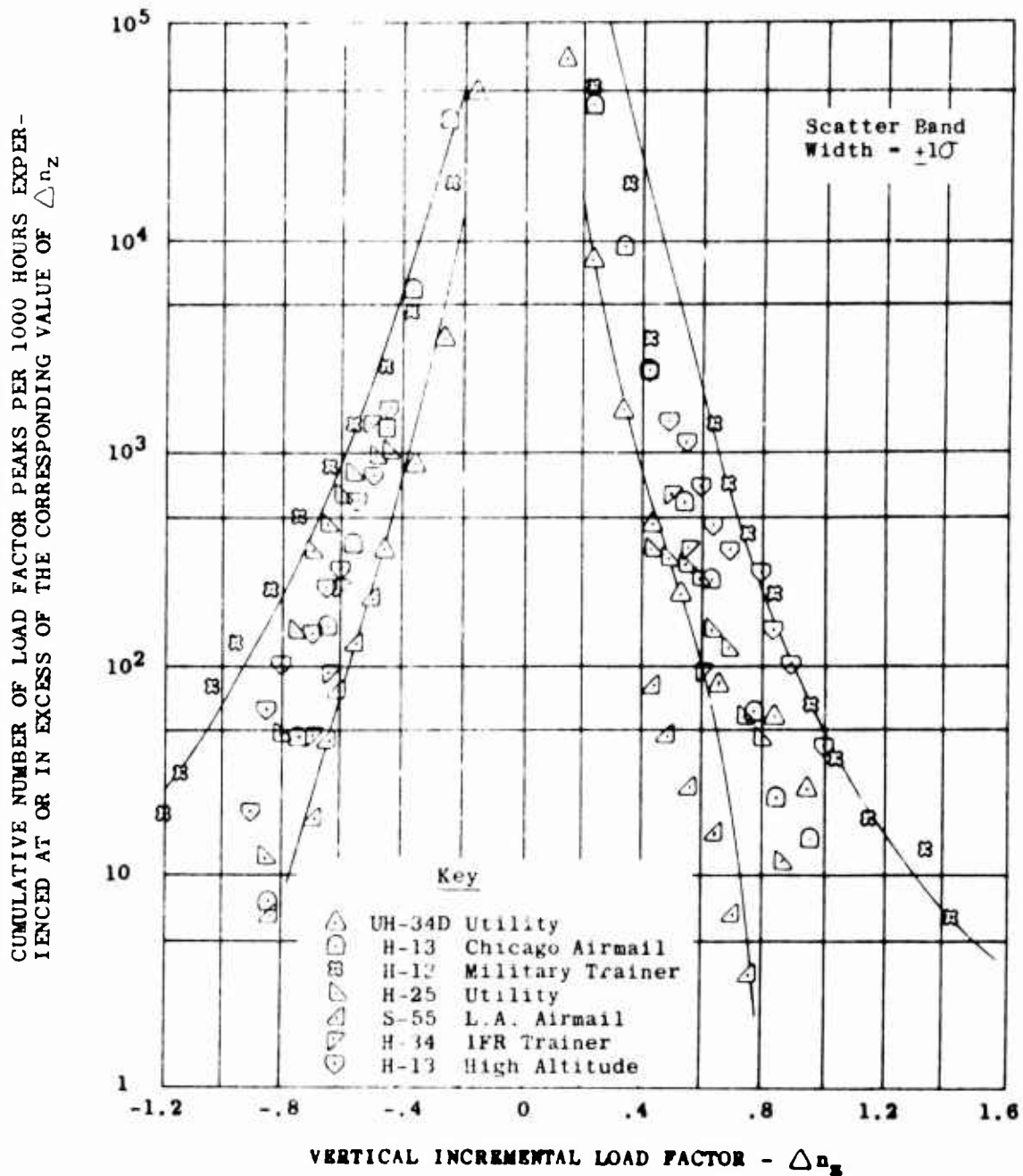


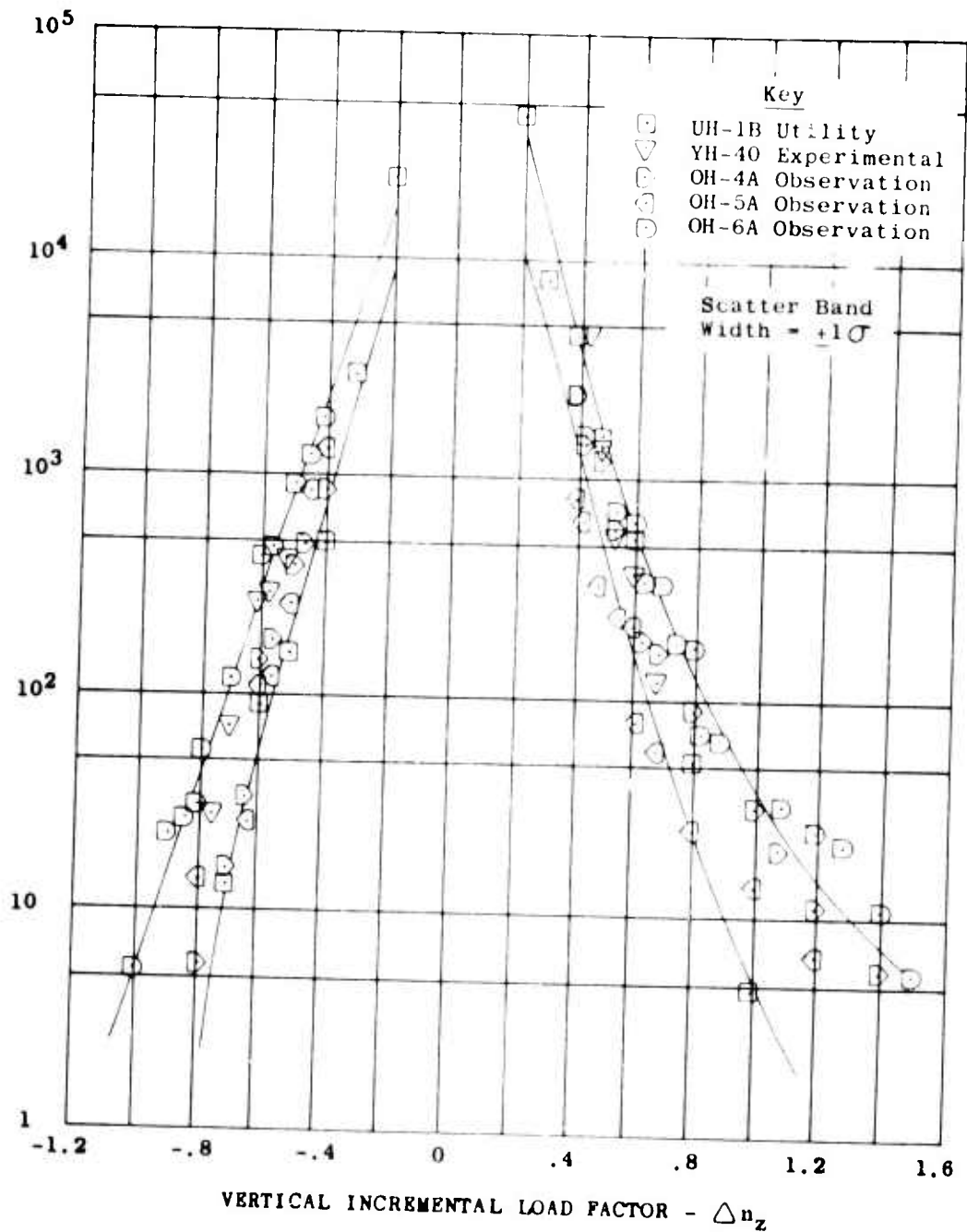
Figure 17. Cumulative Rate-of-Climb Frequency Distributions for the CH-47A, UH-1B, and CH-54A Helicopters.



(a) Reciprocating Engine-Powered Helicopters Having a Design Normal Gross Weight of Less Than 12,000 Pounds.

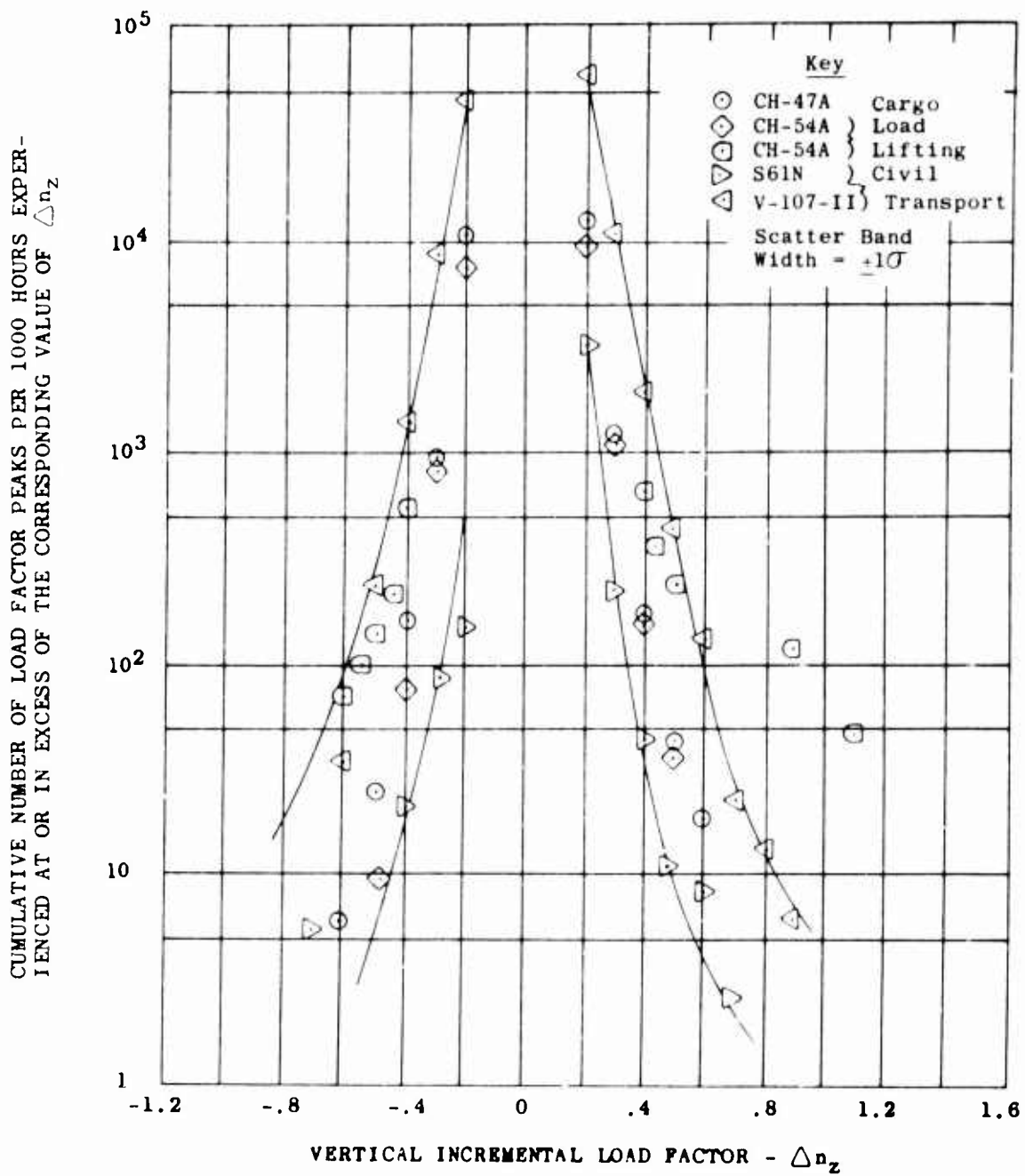
Figure 18. Vertical Load Factor Exceedance Curves.

CUMULATIVE NUMBER OF LOAD FACTOR PEAKS PER 1000 HOURS EXPERIENCED AT OR IN EXCESS OF THE CORRESPONDING VALUE OF  $\Delta n_z$



(b) Turbine-Powered Helicopters Having a Design Normal Gross Weight of Less Than 10,000 Pounds.

Figure 18. Continued.



(c) Turbine-Powered Helicopters Having a Design Normal Gross Weight of Greater Than 15,000 Pounds.

Figure 18. Continued.

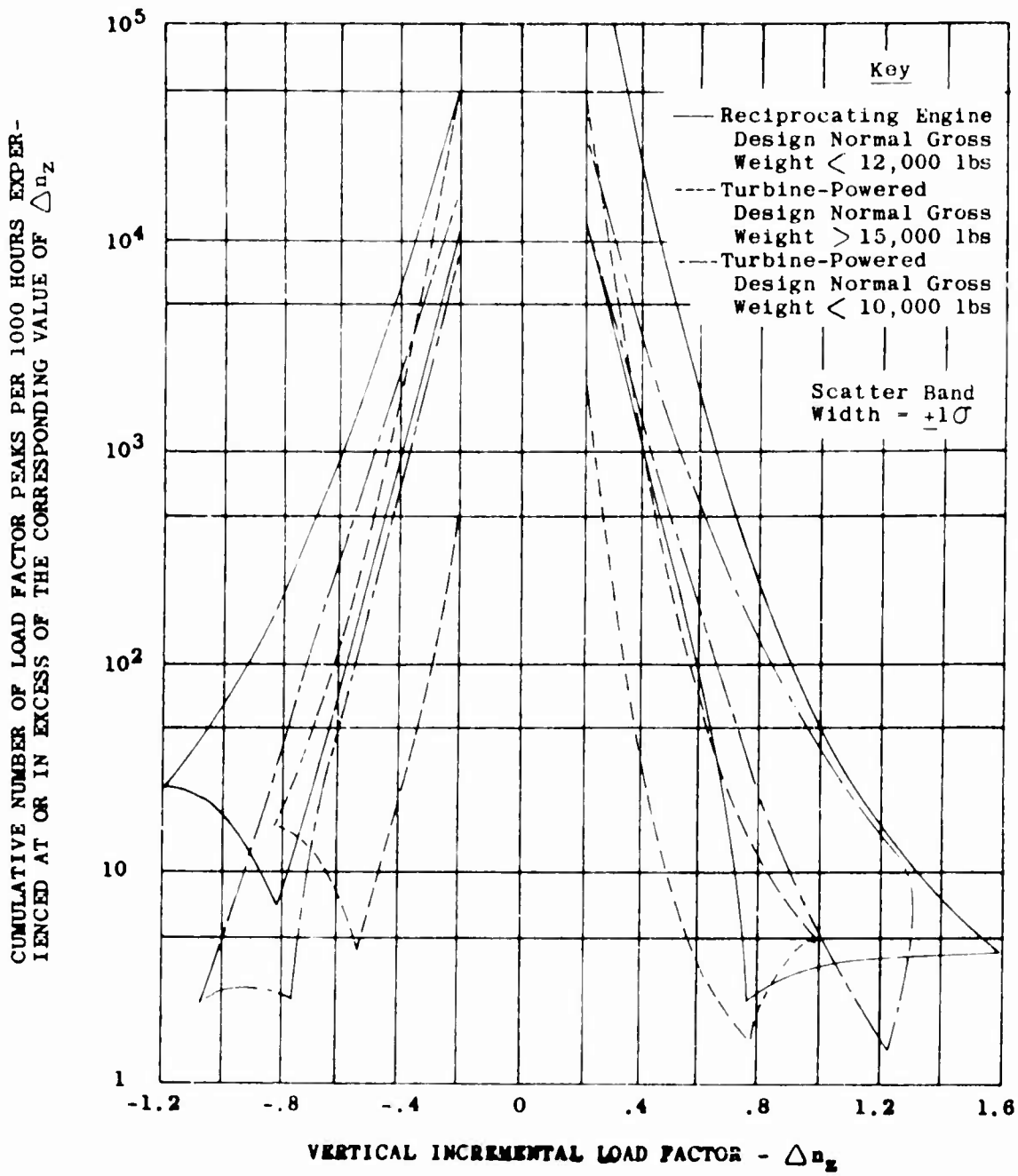
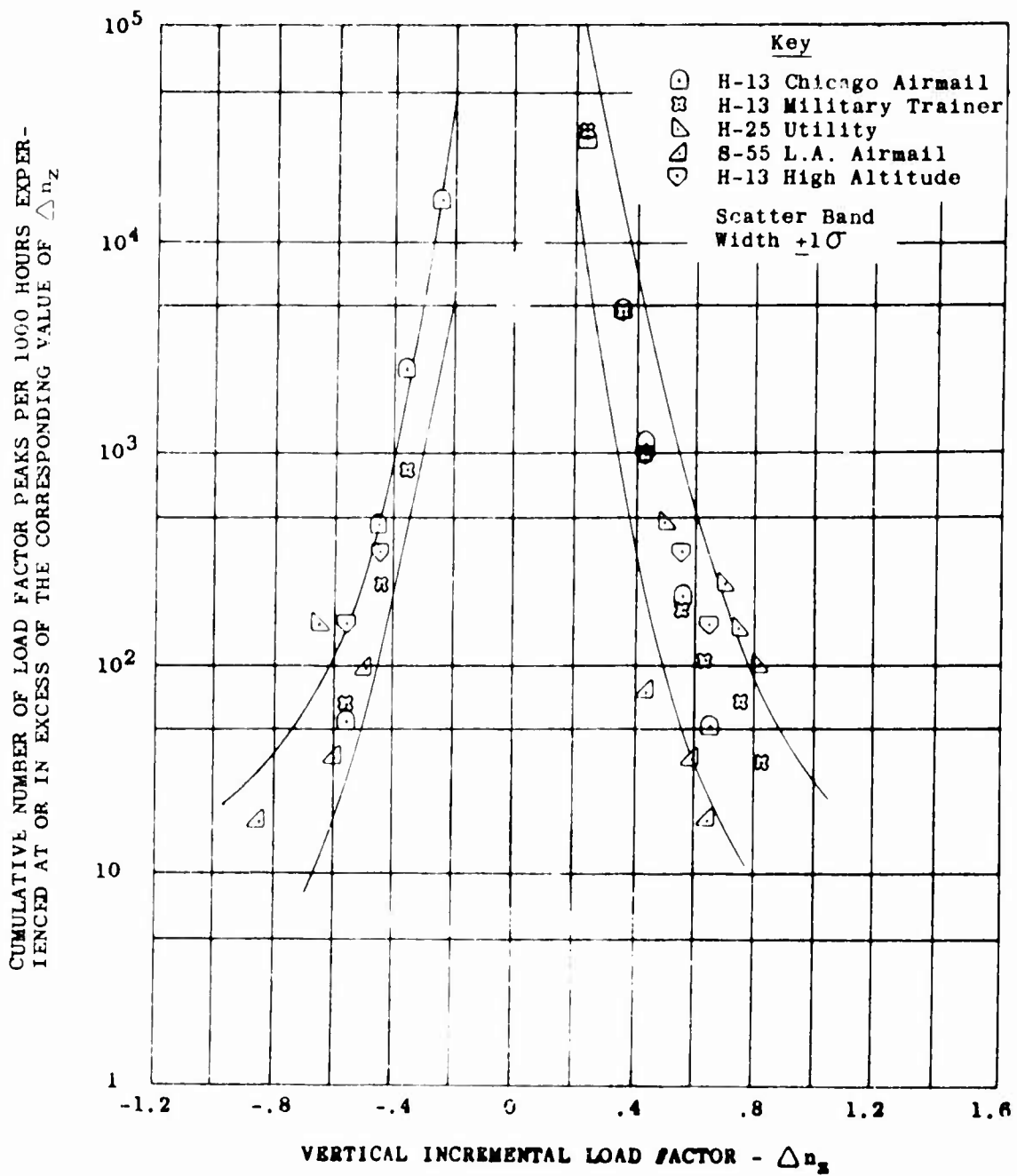
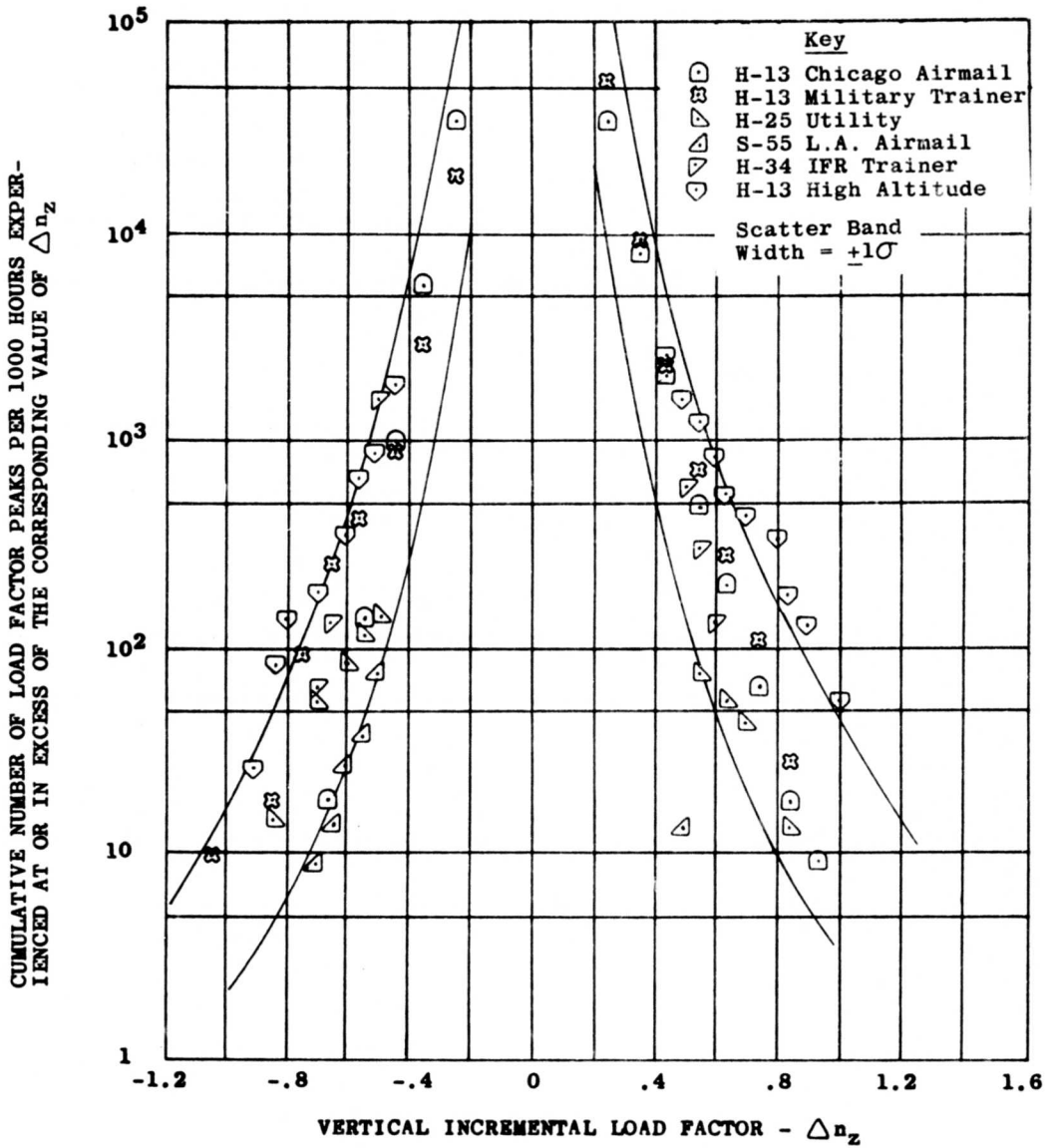


Figure 19. Composite Vertical Load Factor Exceedance Curves.



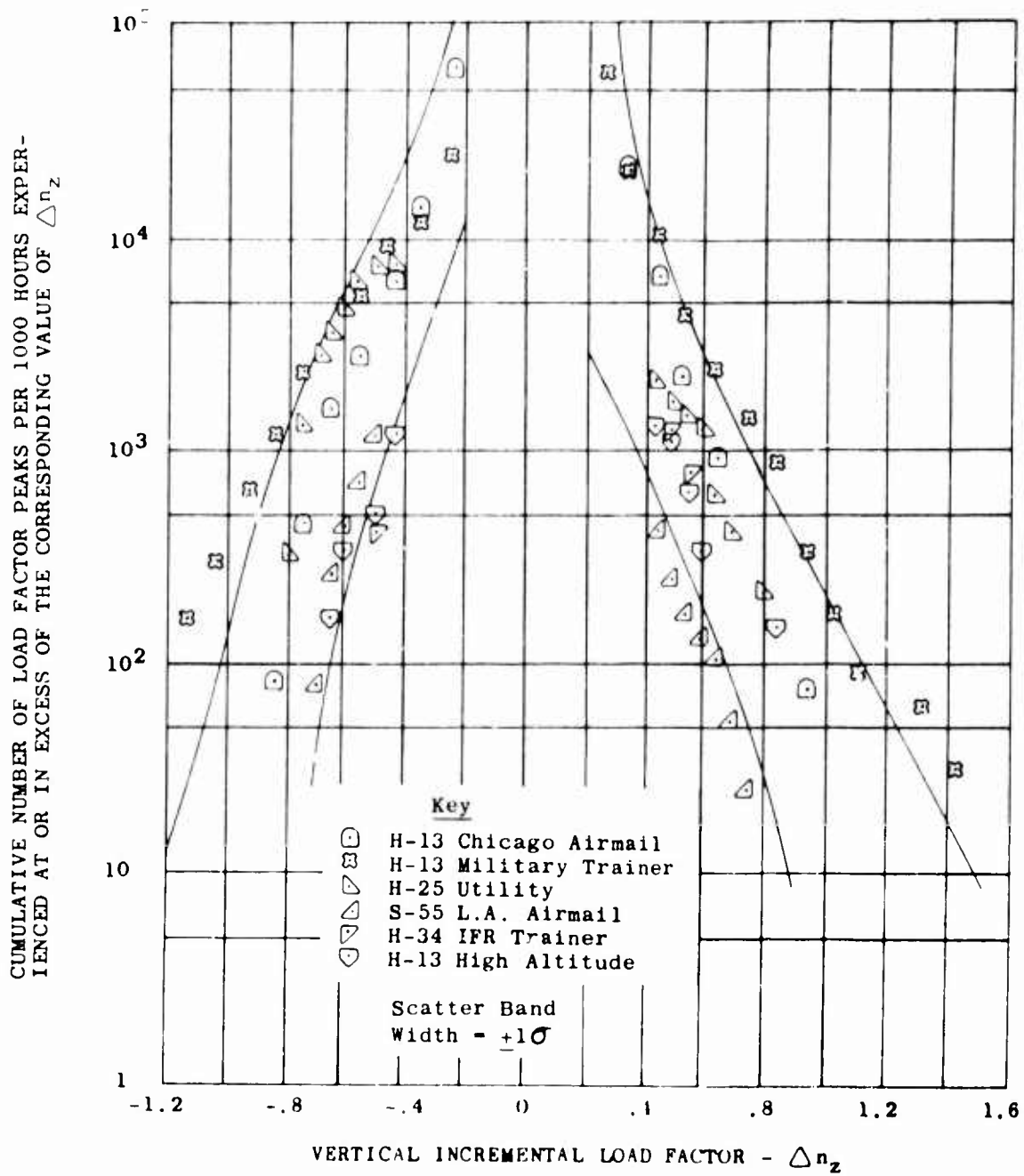
(a) Climb.

Figure 20. Vertical Load Factor Exceedance Curves by Mission Segment for Reciprocating Engine-Powered Helicopters Having a Design Normal Gross Weight of Less Than 12,000 Pounds.



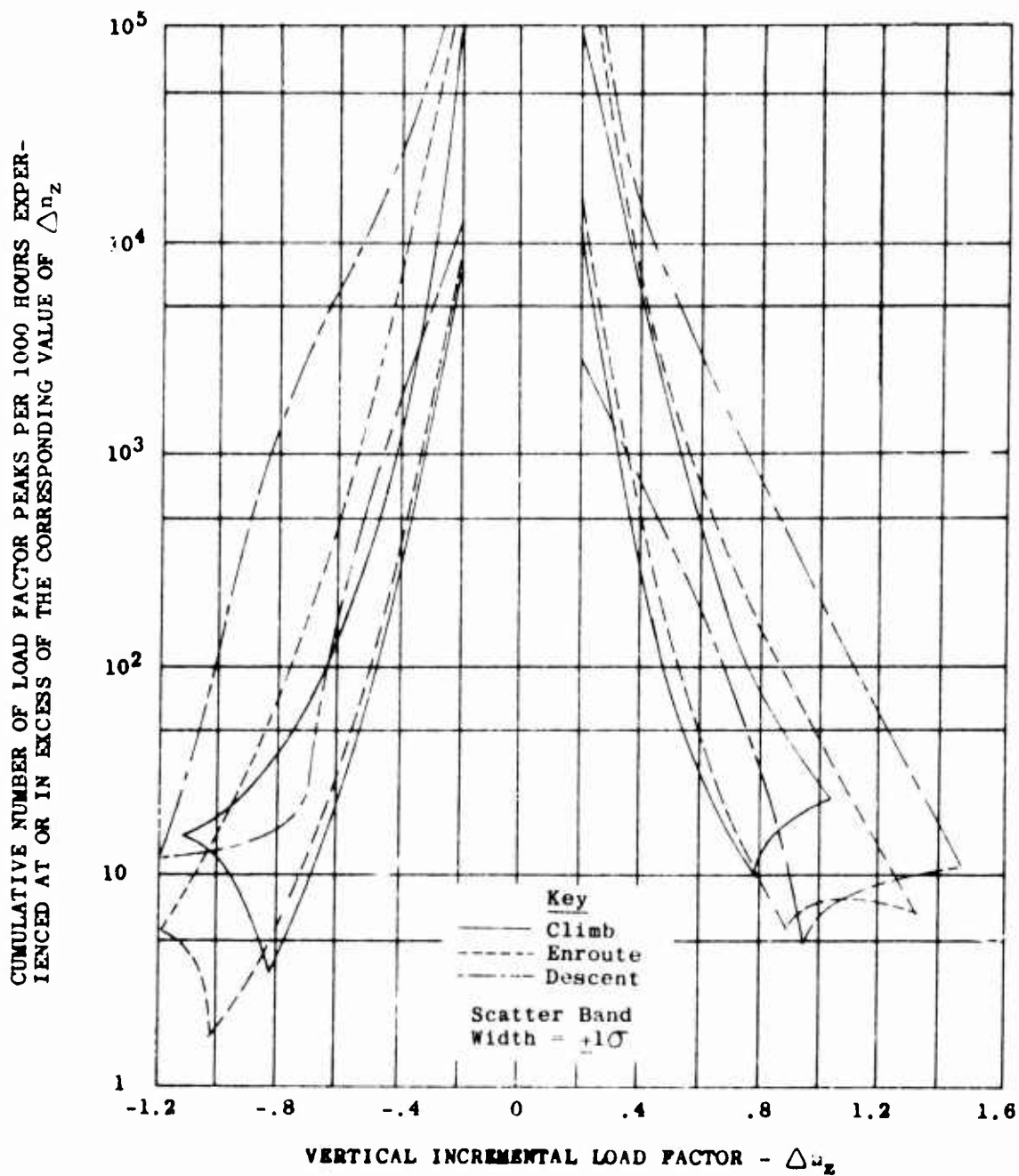
(b) Enroute.

Figure 20. Continued.

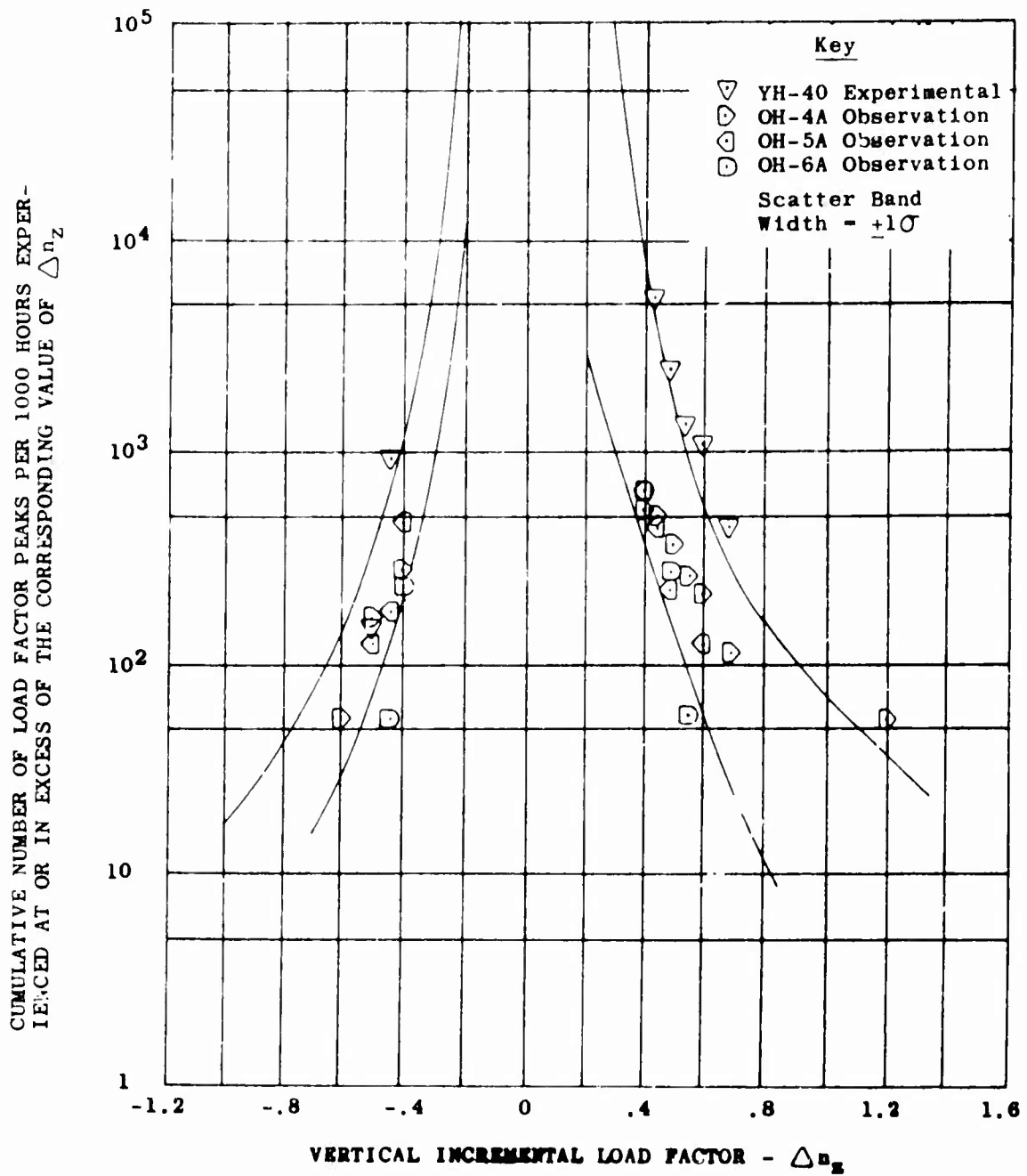


(c) Descent.

Figure 20. Continued.

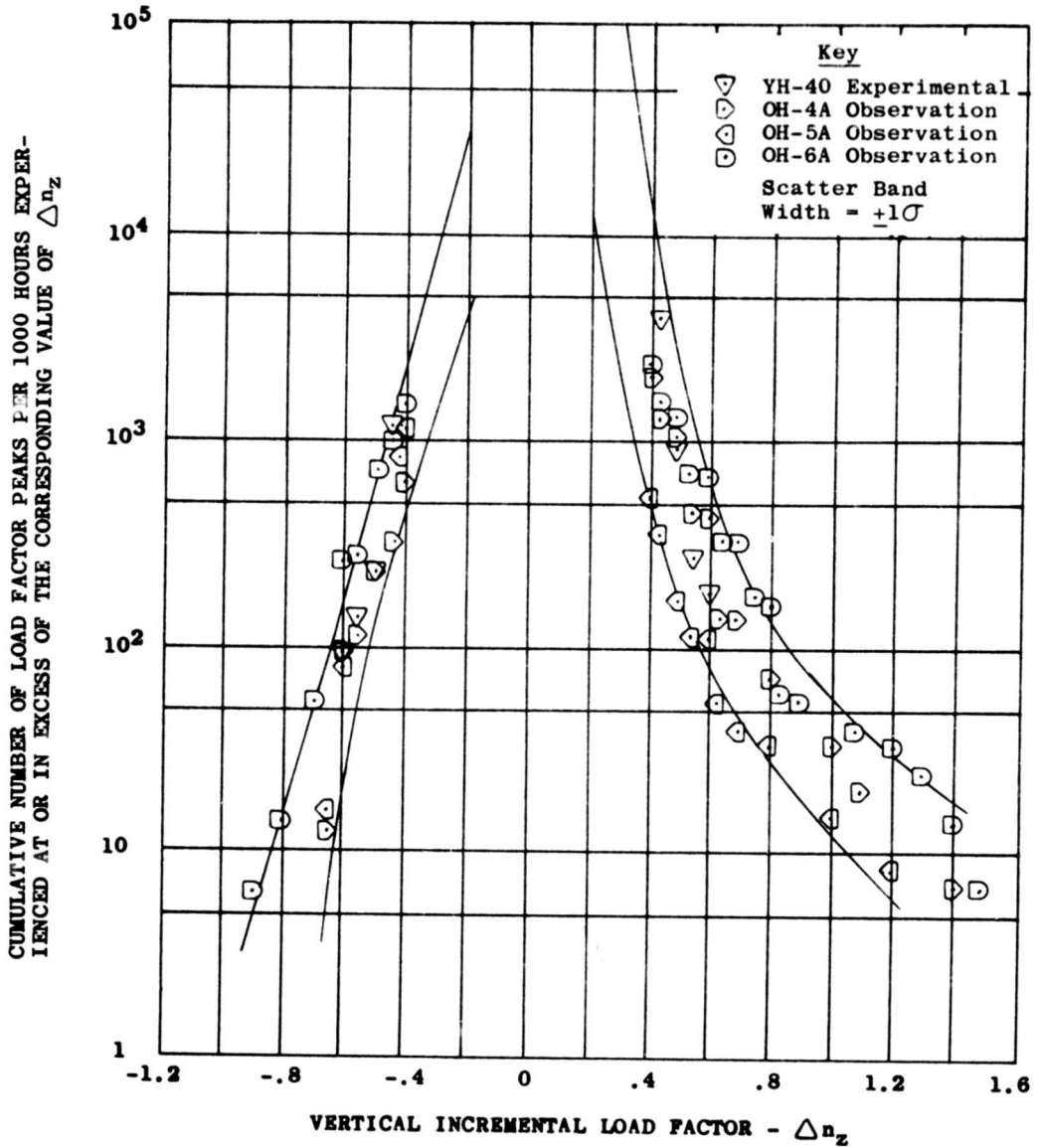


**Figure 21.** Composite Vertical Load Factor Exceedance Curves by Mission Segment for Reciprocating Engine-Powered Helicopters Having a Design Normal Gross Weight of Less Than 12,000 Pounds.



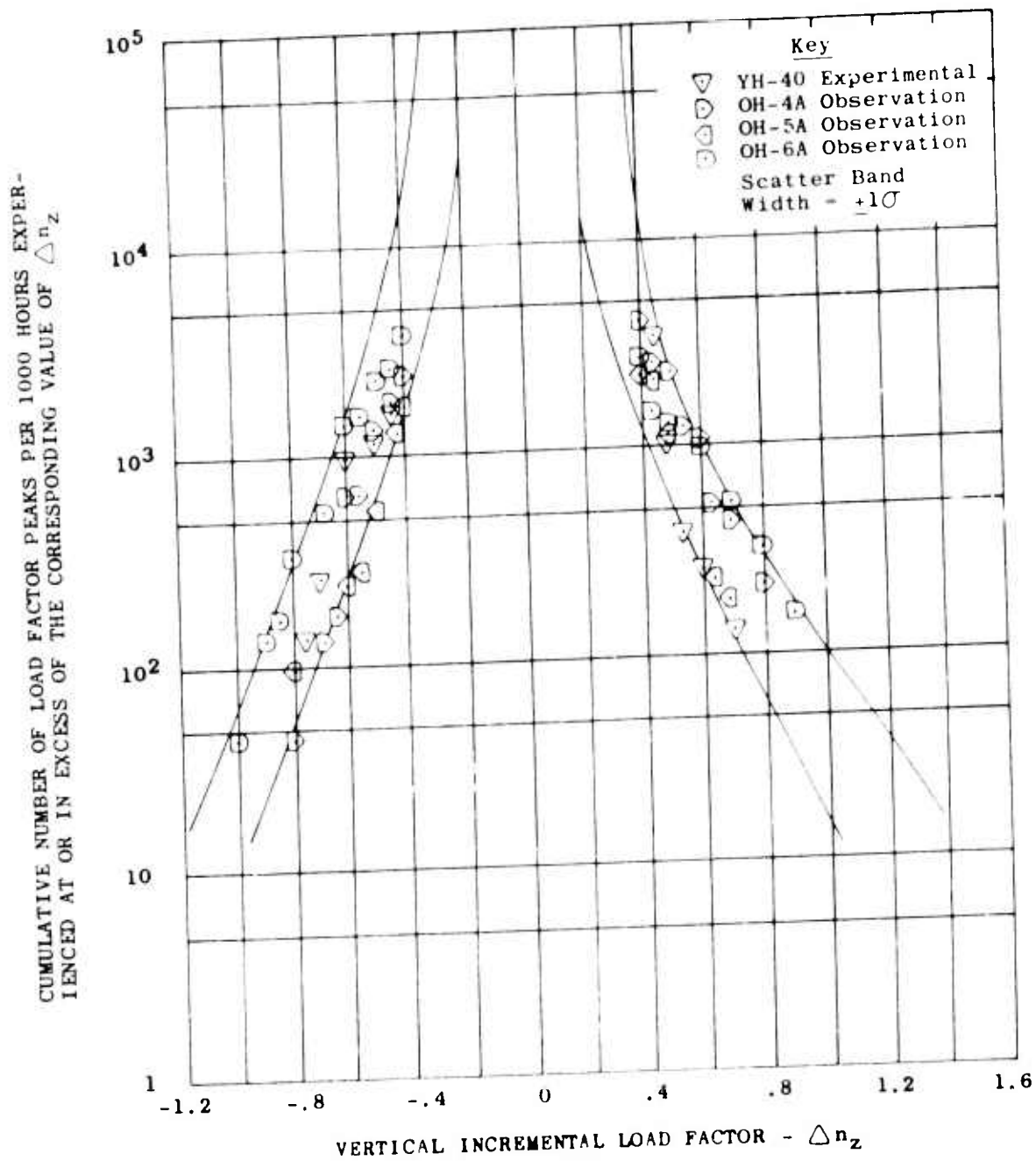
(a) Climb.

Figure 22. Vertical Load Factor Exceedance Curves by Mission Segment for Turbine-Powered Helicopters Having a Design Normal Gross Weight of Less Than 10,000 Pounds.



(b) Enroute.

Figure 22. Continued.



(c) Descent.

Figure 22. Continued.

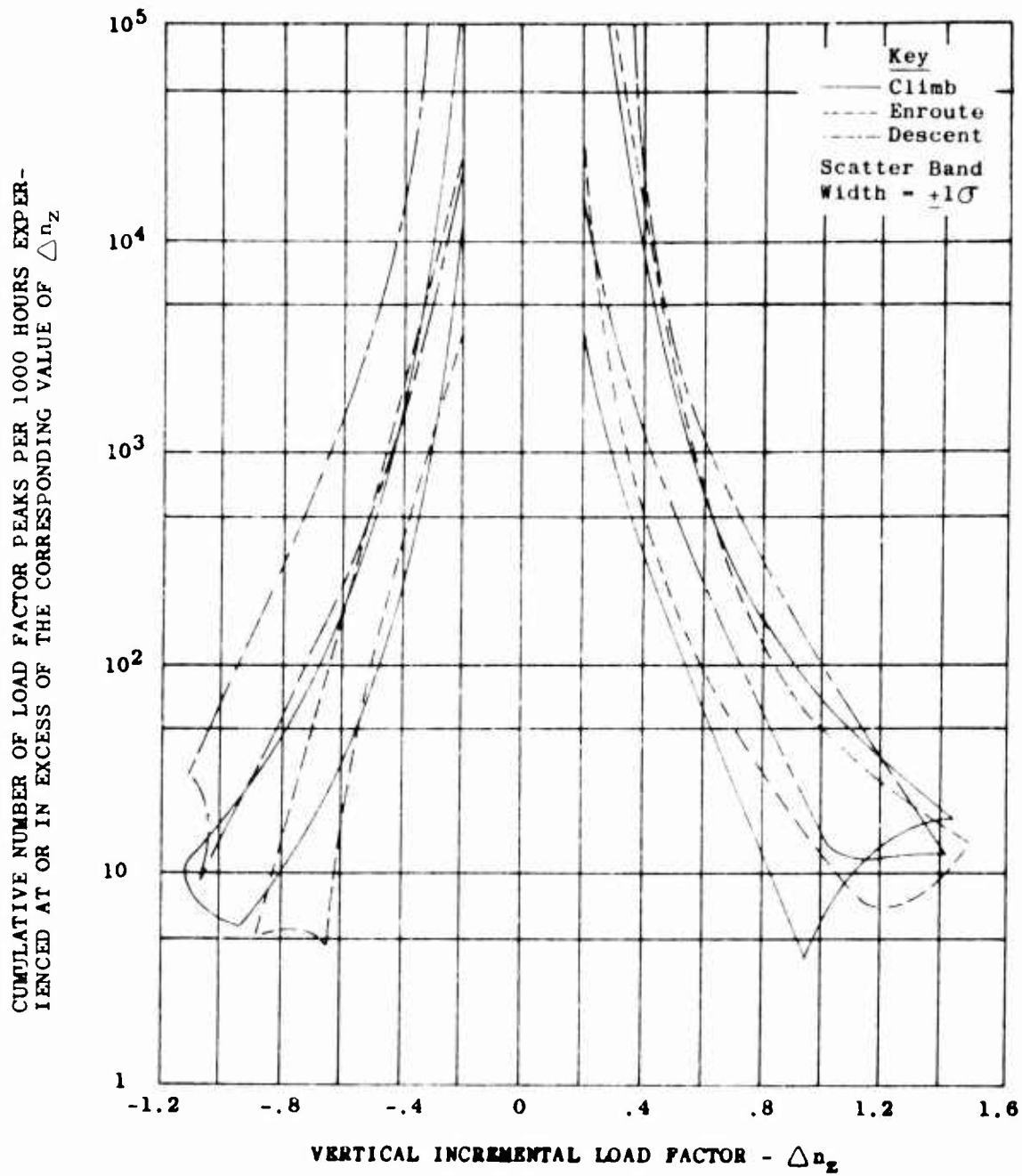


Figure 23. Composite Vertical Load Factor Exceedance Curves by Mission Segment for Turbine-Powered Helicopters Having a Design Normal Gross Weight of Less Than 10,000 Pounds.

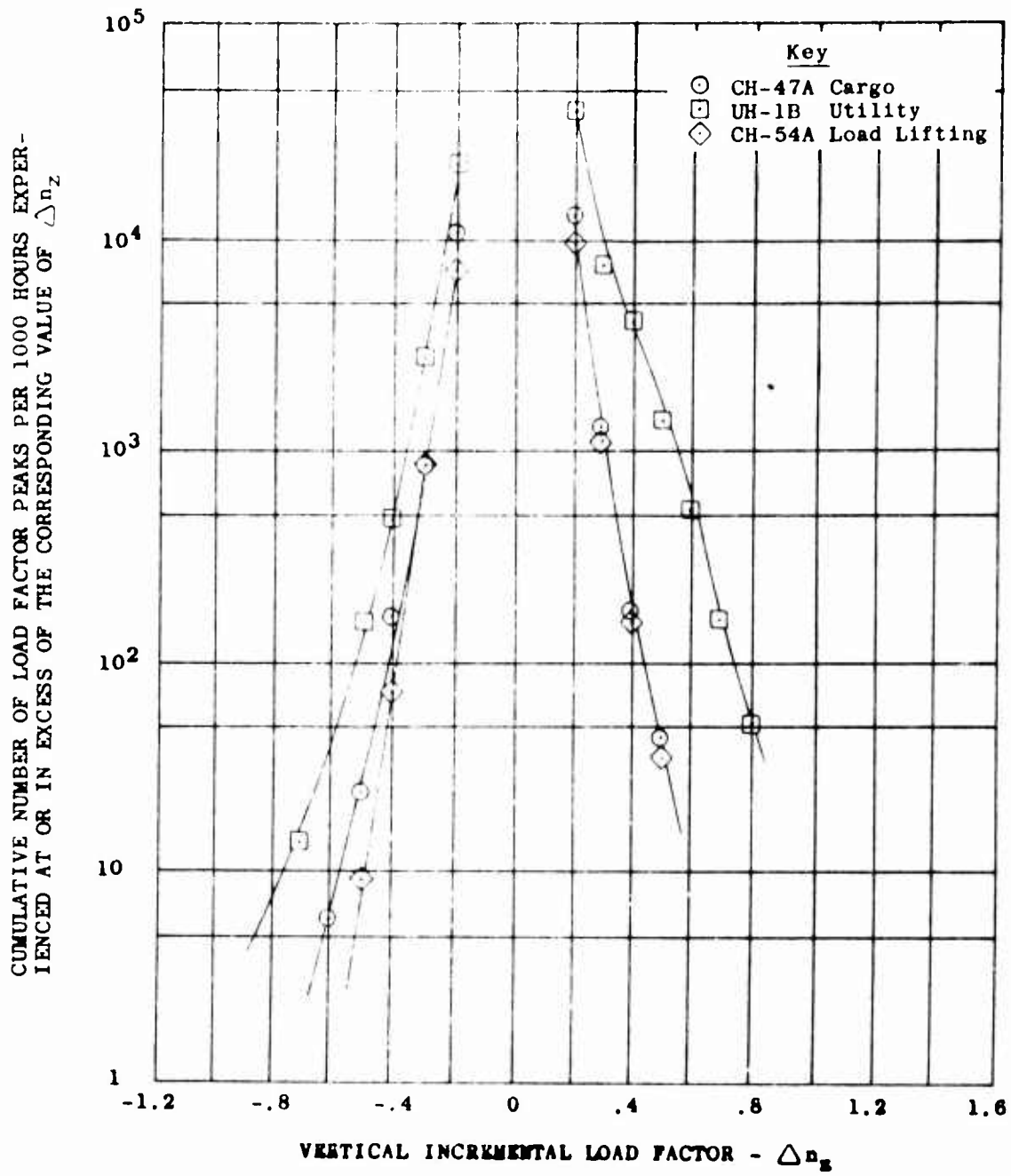
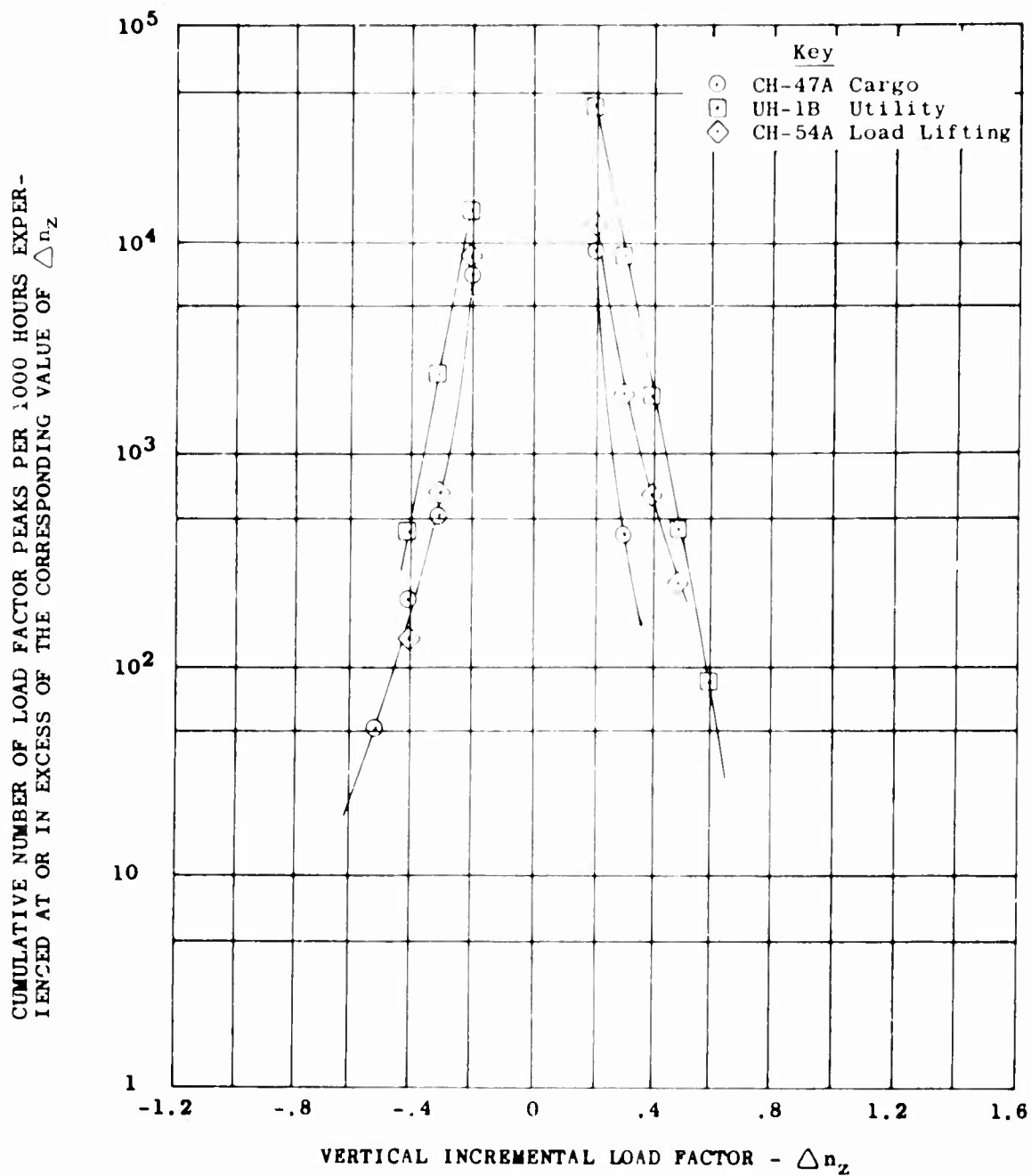
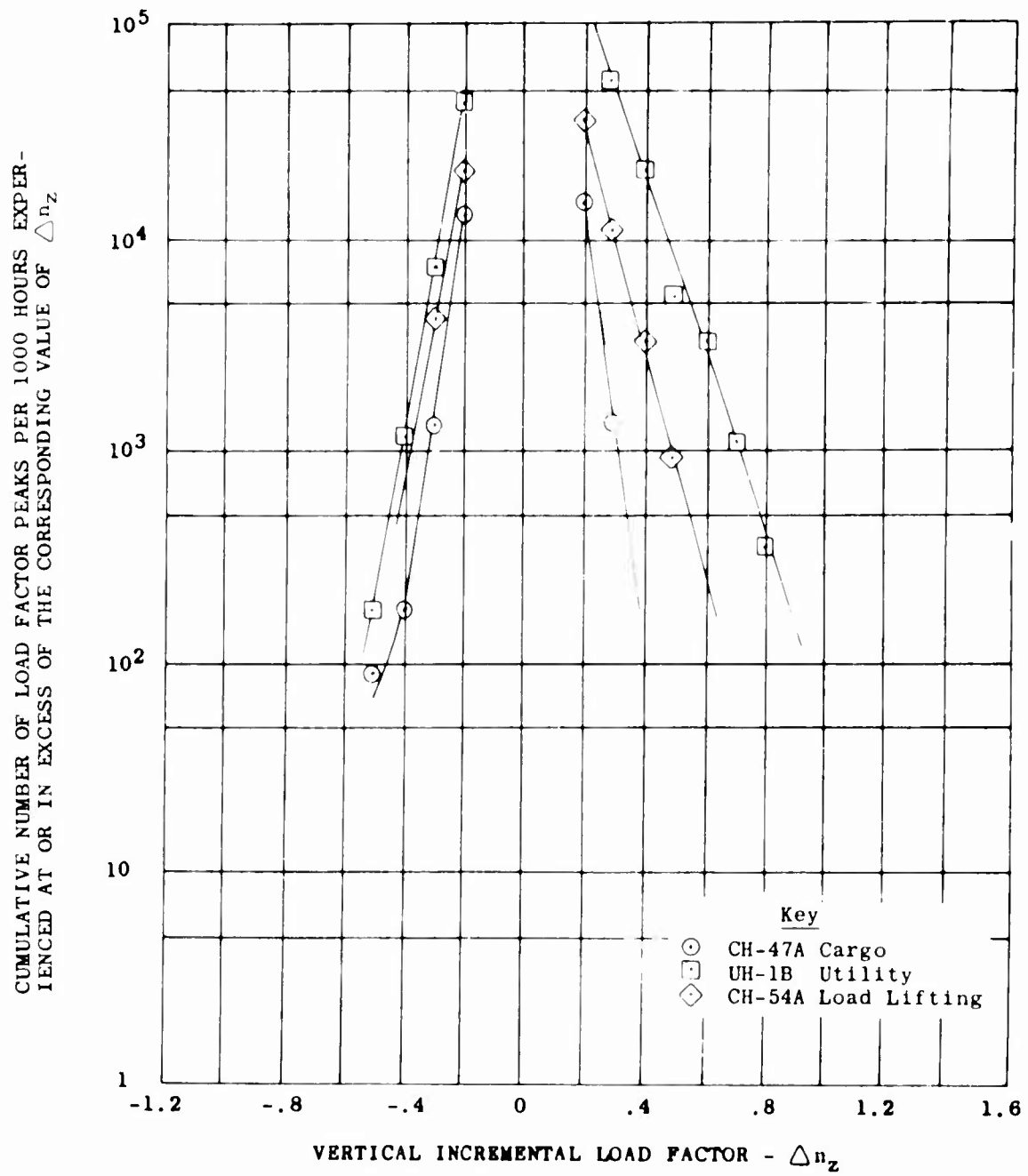


Figure 24. Vertical Load Factor Exceedance Curves for the CH-47A, UH-1B, and CH-54A Helicopters.



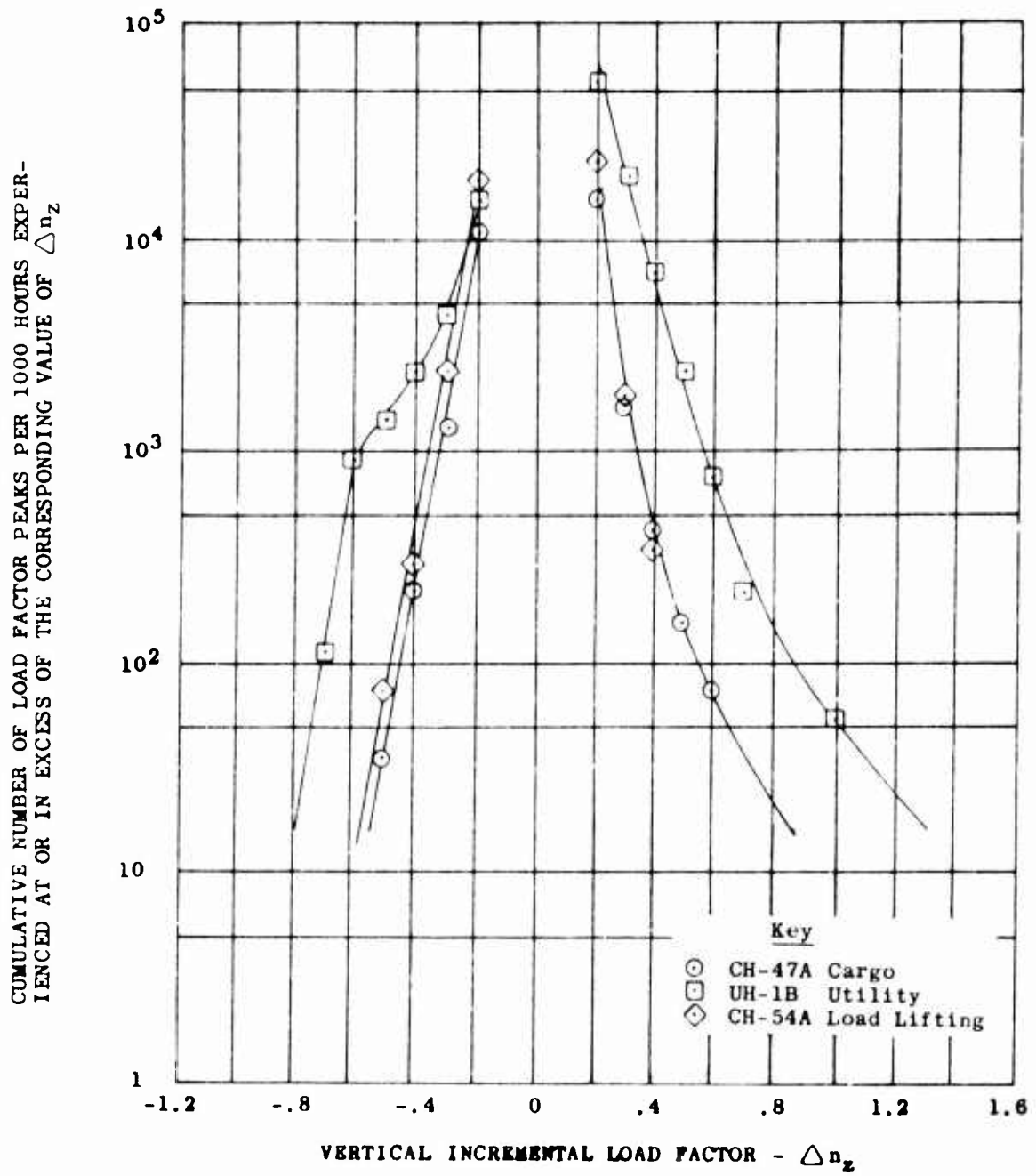
(a) Ascent.

Figure 25. Vertical Load Factor Exceedance Curves for the CH-47A, UH-1B, and CH-54A by Mission Segment.



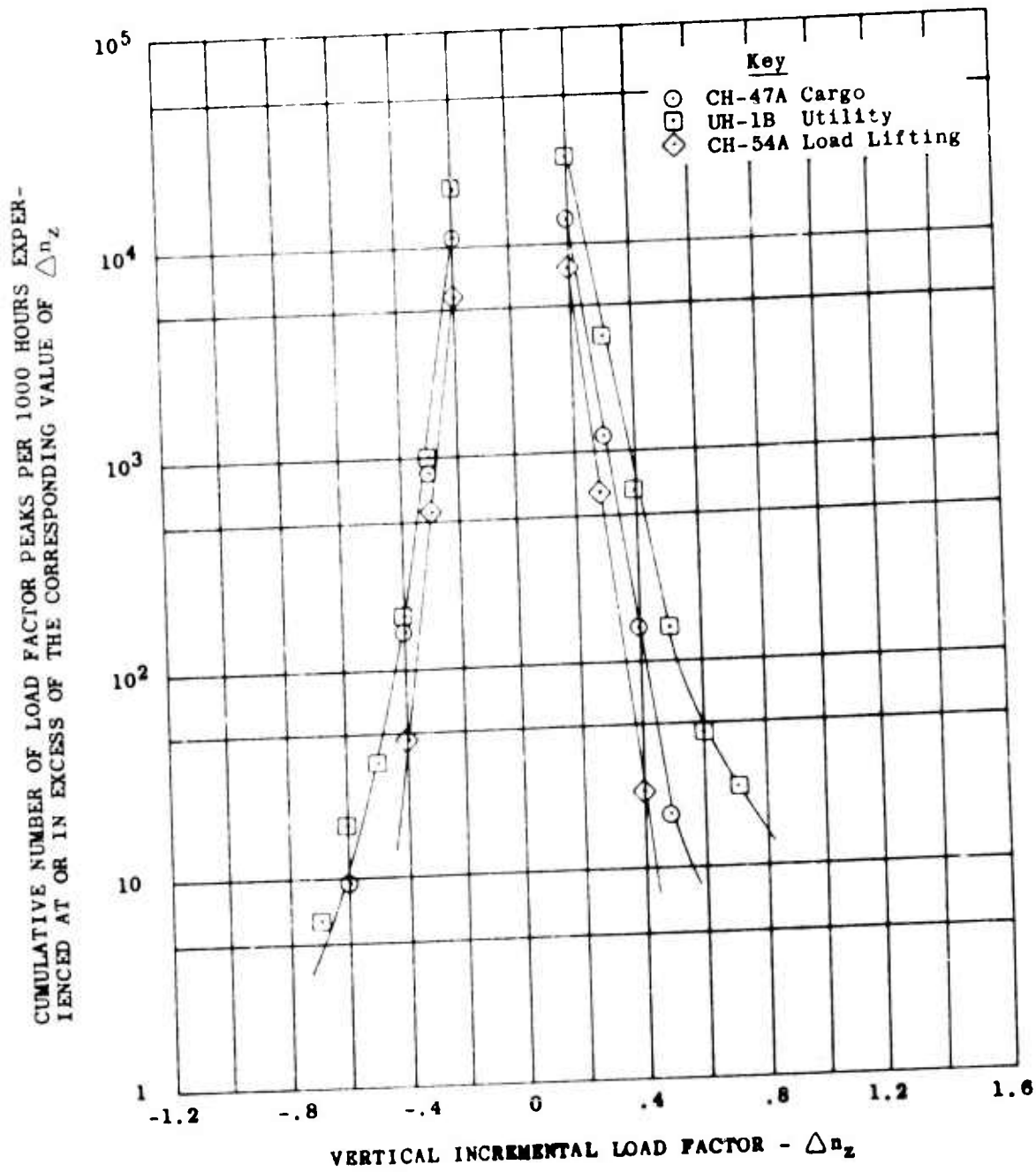
(b) Maneuver.

Figure 25. Continued.



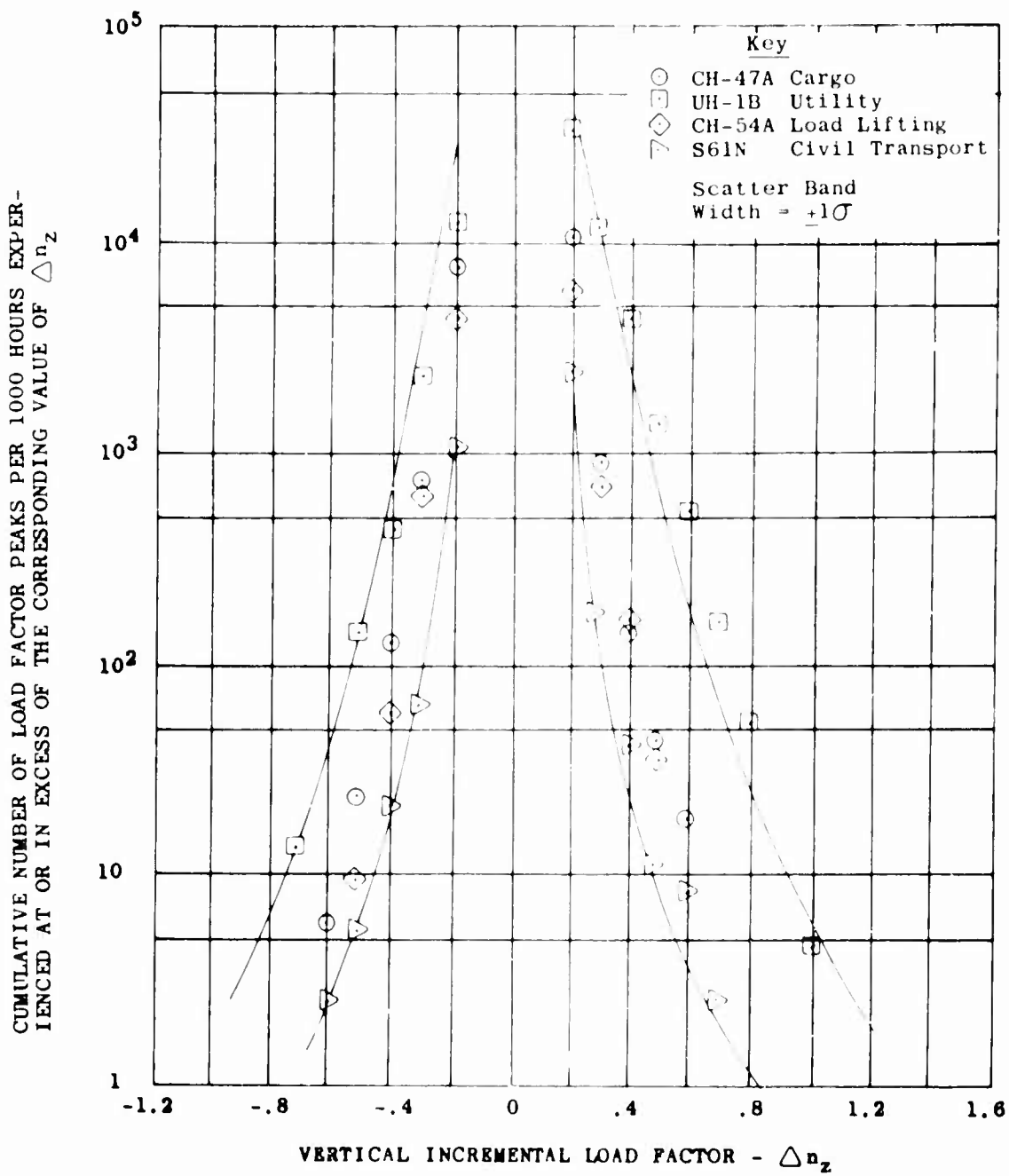
(c) Descent.

Figure 25. Continued.



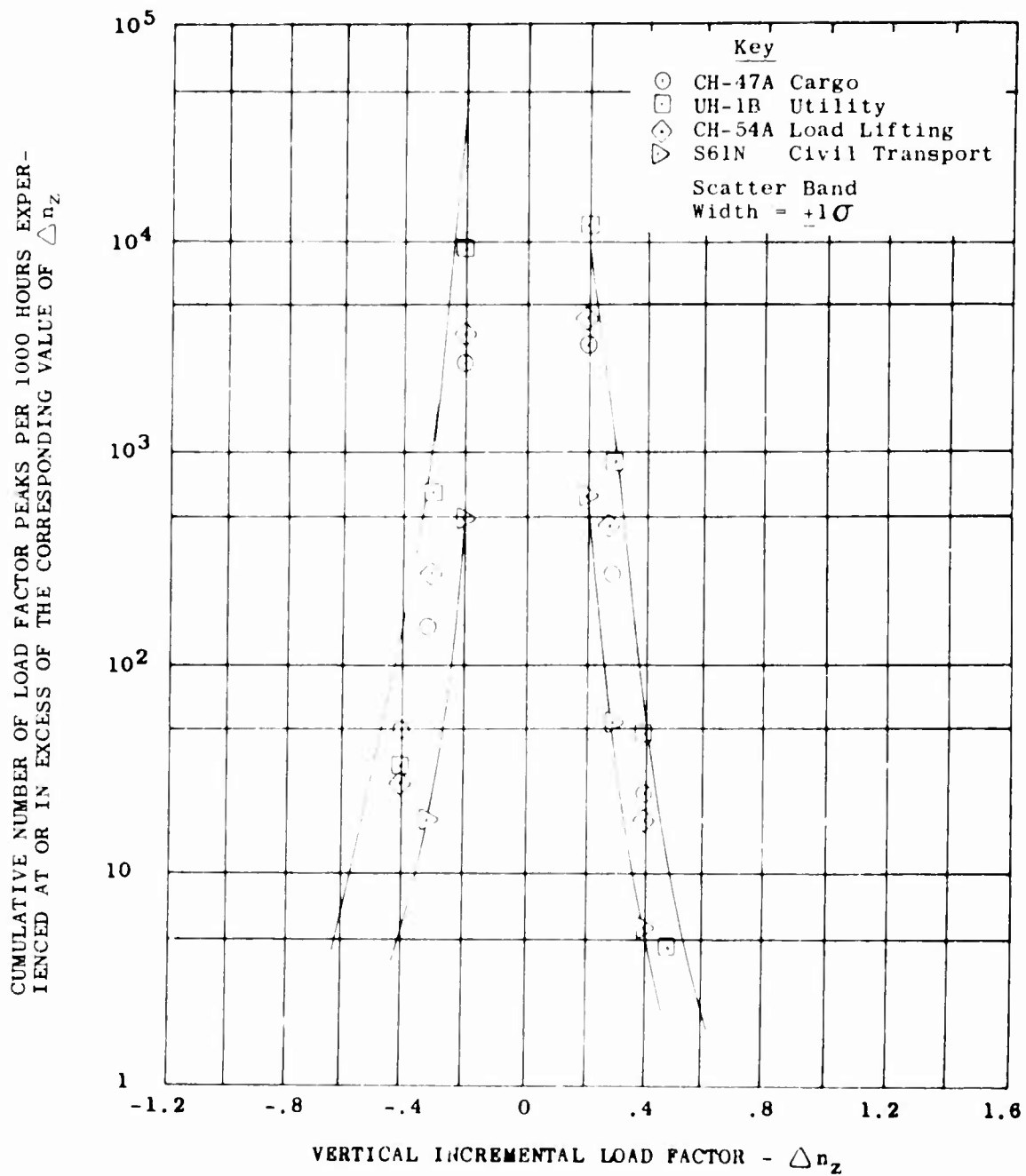
(d) Steady State.

Figure 25. Continued.



(a) Maneuver Induced.

Figure 26. Vertical Load Factor Exceedance Curves by Source.



(b) Gust Induced.

Figure 26. Continued.

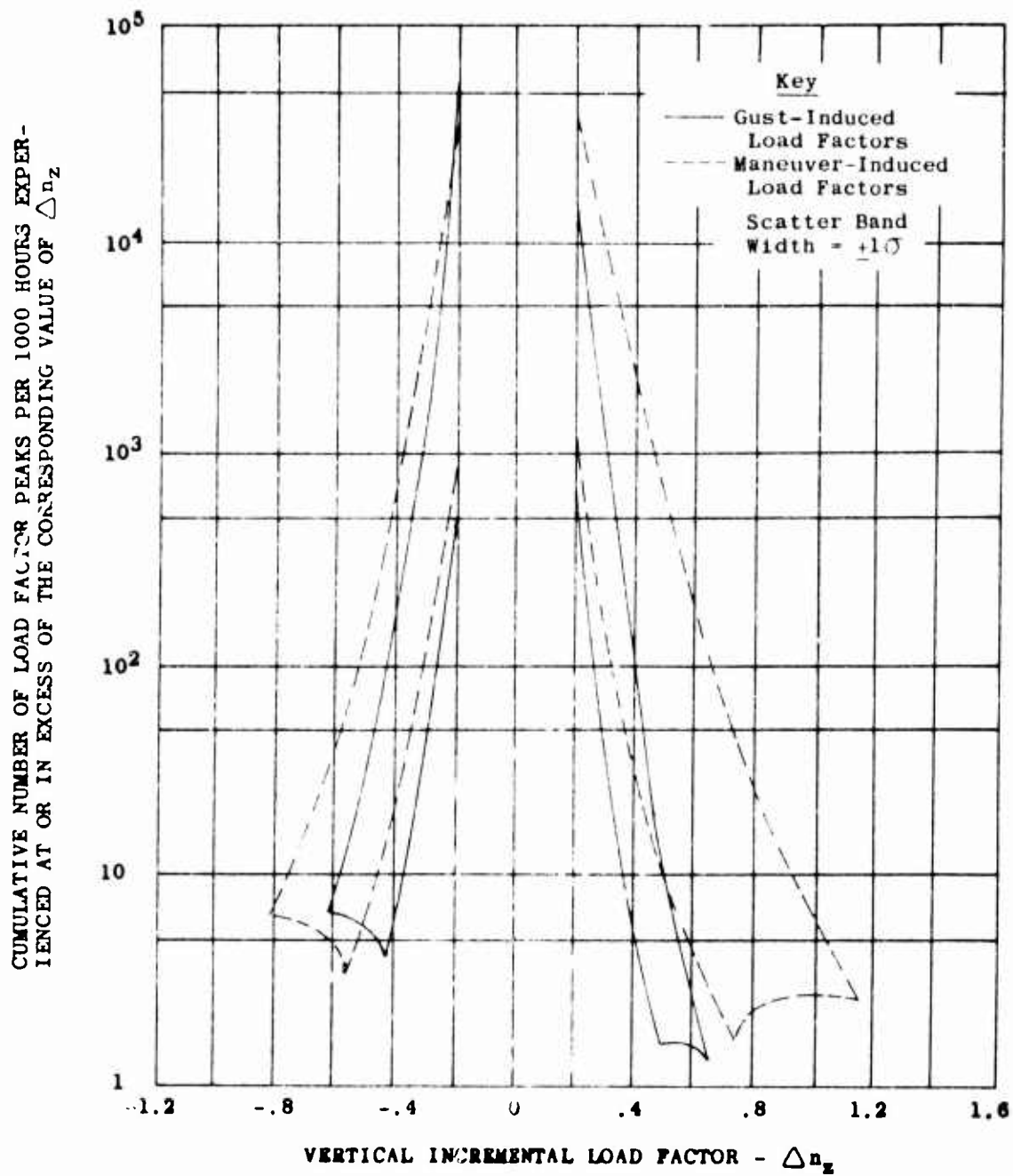


Figure 27. Composite Vertical Load Factor Exceedance Curves by Source.

## REFERENCES CITED

1. Braun, Joseph F., and Giessler, F. Joseph, CH-47 CHINOOK FLIGHT LOADS INVESTIGATION PROGRAM, Technology Inc., Dayton, Ohio; USAAVLABS Technical Report 66-68, Army Aviation Materiel Laboratories, Fort Eustis, Virginia, July 1966, AD 640 142.
2. Clay, Larry E., and Braun, Joseph F., UH-1B HELICOPTER FLIGHT LOADS INVESTIGATION PROGRAM, Technology Inc., Dayton, Ohio; USAAVLABS Technical Report 66-46, U.S. Army Aviation Materiel Laboratories, Fort Eustis, Virginia, May 1966, AD 634 502.
3. Braun, Joseph F., and Giessler, F. Joseph, CH-54A SKYCRANE HELICOPTER FLIGHT LOADS INVESTIGATION PROGRAM, Technology Inc., Dayton, Ohio; USAAVLABS Technical Report 66-58, U.S. Army Aviation Materiel Laboratories, Fort Eustis, Virginia, June 1966, AD 638 364.
4. Roeser, E.P., and Flowers, J.A., SURVEY OF HELICOPTER FLIGHT-LOAD PARAMETERS, WEPTASK Problem Assignment No. 1-22-71; Aeronautical Structures Laboratory Report No. NAEC-ASL-1061, U.S. Naval Air Engineering Center, Philadelphia, Pennsylvania, 27 September 1963.
5. Crim, Almer D., and Hazen, Marlin E., NORMAL ACCELERATIONS AND OPERATING CONDITIONS ENCOUNTERED BY A HELICOPTER IN AIR-MAIL OPERATIONS, Langley Aeronautical Laboratory; NACA TN 2714, National Advisory Committee for Aeronautics, Washington, D.C., June 1952.
6. Hazen, Marlin E., A STUDY OF NORMAL ACCELERATIONS AND OPERATING CONDITIONS EXPERIENCED BY HELICOPTERS IN COMMERCIAL AND MILITARY OPERATIONS, Langley Aeronautical Laboratory; NACA TN 3434, National Advisory Committee for Aeronautics, Washington, D.C., April 1955.
7. Connor, Andrew B., and Ludi, Le Roy H., A SUMMARY OF OPERATING CONDITIONS EXPERIENCED BY TWO HELICOPTERS IN A COMMERCIAL AND A MILITARY OPERATION, Langley Research Center; NASA TN D-251, National Aeronautics and Space Administration, Washington, D.C., April 1960.
8. Connor, Andrew B., A SUMMARY OF OPERATING CONDITIONS EXPERIENCED BY THREE MILITARY HELICOPTERS AND A

**MOUNTAIN-BASED COMMERCIAL HELICOPTER**, Langley Research Center; NASA TN D-432, National Aeronautics and Space Administration, Washington, D.C., October 1960.

9. Truett, Bruce; Back, Stanley; Frickle, Theresa; and Flowers, William; **SURVEY OF STRAINS AND LOADS EXPERIENCED BY THE BELL H-13H, VERTOL H-21C, AND SIKORSKY H-34A HELICOPTERS DURING SERVICE OPERATION**, University of Dayton Research Institute; WADD Technical Report 60-818, Aeronautical Systems Division, Air Force Systems Command, United States Air Force, Wright-Patterson Air Force Base, Ohio, May 1961.
10. DiCarlo, Daniel J., **A SUMMARY OF OPERATIONAL EXPERIENCES OF THREE LIGHT OBSERVATION HELICOPTERS AND TWO LARGE LOAD-LIFTING MILITARY HELICOPTERS**, Langley Research Center; NASA TN D-4120, National Aeronautics and Space Administration, Washington, D.C., September 1967.
11. Giessler, F. Joseph, and Braun, Joseph F., **A HELICOPTER STRUCTURAL FLIGHT LOADS RECORDING PROGRAM**, Technology Inc., Dayton, Ohio; FAA-ADS Technical Report 89, Federal Aviation Agency, Aircraft Development Service, December 1966.
12. Peckham, Cyril G., Giessler, F. Joseph, and Braun, Joseph F., **A STRUCTURAL FLIGHT LOADS RECORDING PROGRAM ON CIVIL TRANSPORT HELICOPTERS**, Technology Inc., Dayton, Ohio; FAA-ADS Technical Report 79, Federal Aviation Agency, Aircraft Development Service, July 1966.
13. Federal Aviation Agency. **ROTORCRAFT AIRWORTHINESS: NORMAL CATEGORY**, Civil Aeronautics Manual 6, Appendix A, June 1962.
14. Johnson, Leonard G., **THE MEDIAN RANKS OF SAMPLE VALUES IN THEIR POPULATION WITH AN APPLICATION TO CERTAIN FATIGUE STUDIES**, Industrial Mathematics, Volume 2, Industrial Mathematics Society, Detroit, Michigan, 1951.

Unclassified

Security Classification

DOCUMENT CONTROL DATA - R & D		
<i>(Security classification of title, body of abstract and indexing annotation must be entered when the overall report is classified)</i>		
1. ORIGINATING ACTIVITY (Corporate author) Kaman Aircraft, Division of Kaman Corporation Bloomfield, Connecticut		2a. REPORT SECURITY CLASSIFICATION <b>Unclassified</b>
		2b. GROUP
3. REPORT TITLE EVALUATION OF HELICOPTER FLIGHT SPECTRUM DATA		
4. DESCRIPTIVE NOTES (Type of report and inclusive dates) FINAL REPORT		
5. AUTHOR(S) (First name, middle initial, last name) John D. Porterfield Paul F. Maloney		
6. REPORT DATE October 1968	7a. TOTAL NO. OF PAGES 117	7b. NO. OF REFS 14
8a. CONTRACT OR GRANT NO. DAAJ02-67-C-0055	8b. ORIGINATOR'S REPORT NUMBER(S) USAAVLABS Technical Report 68-68	
b. PROJECT NO. Task 1F162204A14601	9b. OTHER REPORT NO(S) (Any other numbers that may be assigned this report) Kaman Aircraft Report No. R-739	
c.		
d.		
10. DISTRIBUTION STATEMENT This document has been approved for public release and sale; its distribution is unlimited.		
11. SUPPLEMENTARY NOTES	12. SPONSORING MILITARY ACTIVITY U.S. Army Aviation Materiel Laboratories Fort Eustis, Virginia	
13. ABSTRACT This report evaluates helicopter flight spectrum data previously recorded and published in other reports, with emphasis on the UH-1B utility, CH-47A cargo, and CH-54A load lifting helicopters as used in the Army environment. A limited statistical analysis of the data is presented for those parameters for which sufficient data were available. The report includes a comparison of the flight-measured data with the spectrum appearing in Appendix A of Civil Aeronautics Manual 6, and with the assumed fatigue substantiation spectrum, where this was available. Discussion and evaluation of the spectrum variations that do occur, particularly as they might affect component fatigue lives, are also included.  A method for deriving an operational spectrum for the classes of helicopters evaluated is presented along with discussion of some of the considerations and judgment which play a part in the establishment of a rational, conservative spectrum for the critical components.		

DD FORM 1473

REPLACES DD FORM 1473, 1 JAN 64, WHICH IS OBSOLETE FOR ARMY USE.

Unclassified  
Security Classification

**Unclassified**

**Security Classification**

14. KEY WORDS	LINK A		LINK B		LINK C	
	ROLE	WT	ROLE	WT	ROLE	WT
CH-47A						
UH-1B						
CH-54A						
Flight Spectrum						
Helicopter Operations						
Operational Airloads						
Aircraft Structures						

**Unclassified**

**Security Classification**